Stimuli-Adaptable Materials

Frankær, Sarah Maria Grundahl; Skov, Anne Ladegaard; Kiil, Søren; Daugaard, Anders Egede

Publication date:
2013

Document Version
Publisher's PDF, also known as Version of record

Stimuli-Adaptable Materials

Sarah Maria Grundahl Frankær

Ph.D. Thesis

February 2013

DTU Chemical Engineering
Department of Chemical and Biochemical Engineering

Stimuli-Adaptable Materials

PhD Thesis

Sarah Maria Grundahl Frankær

Department of Chemical and Biochemical Engineering
Technical University of Denmark DTU
February 2013

DTU Chemical Engineering
Department of Chemical and Biochemical Engineering

Address: The Danish Polymer Centre
Department of Chemical and Biochemical Engineering
Technical University of Denmark
Building 227
DK-2800 Kgs. Lyngby
Denmark
Phone: +45 4525 6801
Web: www.dpc.kt.dtu.dk

Print: J&R Frydenberg A/S
København
June 2013

ISBN: 978-87-93054-00-4

Preface and acknowledgements

The work presented here is the result of my PhD study which was carried out at the Danish Polymer Center (DPC), Department of Chemical and Biochemical Engineering, Technical University of Denmark DTU. The work was carried out in the period from May 2009 to February 2013 with Associate Professor Anne Ladegaard Skov as main supervisor and Associate Professor Søren Kiil and Assistant Professor Anders Egede Daugaard as co-supervisors, all at the Department of Chemical and Biochemical Engineering, DTU. The project was financed by the Technical University of Denmark.

First of all I would like to thank Anne Ladegaard Skov for believing in me and for giving me the opportunity to pursue a PhD-degree. I have enjoyed our discussions a lot and I am continually impressed by your ability to come up with plausible explanations for divergent results and to find new ways of solving classical problems. I've been happy to be your student and I'm certain that many others will feel the same way.

To my co-supervisor, Søren Kiil, I would like to say that your help have been invaluable. You have helped keeping the focus on what was important rather than letting the project get lost in details. Your solid experience has been very useful to me.

I would also like to thank my co-supervisor Anders Egede Daugaard whose chemical know-how saved me several times. Even though you were added to the project late you made a difference. Your detail orientation made me reconsider many things many times and this way I found new information. Furthermore, it was nice to have someone to discuss the important chemical details with.

I have been affiliated with DPC since 2008 and I have really enjoyed my time here. It's been a pleasure to come to work and there is always someone to talk to or someone with an encouraging comment. I will miss you all.

I would like to particularly thank some of the people in DPC. First of all I owe a special thank you to Ayelén Luna Helling Di Vaia who carried out a series of time consuming experiments as a part of her master thesis. To Kim Chi Szabo for helping with polymer characterisation and general laboratory practice. To Irakli Javakhishvili and Mads Møller Nielsen for good company in the lab and helpful discussions. And Nicolas Javier Alvarez for helping me with some theory and for always asking good questions. I would also like to thank Vibeke Helle Christiansen for taking such good care of the DPC-staff including myself.

I had the pleasure of sharing an office with a lot of the PhD-students and post

docs at DPC during the last five years and thank you for your company and all the good times.

My family and friends have been invaluable throughout the last years and I thank you for your care and support. A very special thanks to my husband Christian and my daughter Elisabeth. You light up my life.

Kgs. Lygnby, February 2013

Sarah Maria Grundahl Frankær

Abstract

The work presented in this Thesis deals with the development of a stimuli-adaptable polymer material based on the UV-induced dimerisation of cinnamic acid and its derivatives.

It is in the nature of an adhesive to adhere very well to its substrate and therefore problems can arise upon removal of the adhesive. This is also known from skin adhesives where it is very undesirable to cause damage to the skin. The overall idea of this project was to resolve this problem by developing a material which could switch between an adhesive and a non-adhesive state. Switchable adhesion is known in the literature but the presented work has a new approach to the field by basing itself on the idea of developing a network into which a photo-active polymer is mixed and which function as an adhesive. Upon irradiation with UV-light for a short time a non-adhering inter-penetrating network material would be formed.

Two simple models for the extent of reaction for the system are presented and show that the timescale for the reaction is minutes to hours. This was further investigated with IR-spectroscopy and UV-absorbance spectroscopy. UV-spectroscopy confirmed that a change in the material occurs upon irradiation with UV and that the reaction time is in the range of minutes.

A number of polymer derivatives with cinnamic acid or cinnamylidene acetic acid were prepared and the material properties of these were studied before and after irradiation with UV-light. For the cinnamylidene acetic acid derivatised polymers a macroscopic change was observed upon dissolution of the irradiated compound. The irradiated polymers formed threads or fibres when exposed to water while the unexposed polymers dissolved as a hygroscopic powder. Cinnamic acid derivatised poly(ethylene glycol) (PEG) was studied in detail and three different polymers were derivatised, namely a 4-armed star PEG (M_n = 2000 g/mol), a short linear PEG (M_n = 1000 g/mol) and a long linear PEG (M_n = 4000 g/mol). The derivatised polymers were mixed to create three different photo-active materials and these were investigated with rheology before and after irradiation with UV-light for one hour. It was observed that the largest change occurred for the system consisting solely of the cinnamic acid derivatised 4-armed star PEG. The development of the material properties of this material was studied in details by exposing the compound to UV-radiation for up to 120 h and determining the rheological properties after the exposure. It was found that approx. 24 hours was needed to form a manageable film and that approx. 70 hours were needed to obtain stable rheological properties. The exposure

times were larger than expected but it was assumed that this would be resolved by preparation of the inter-penetrating network materials.

A number of inter-penetrating network materials where both the permanent network as well as the switching segment was made up of PEG-polymers were prepared. It was found that for a material with relatively long chains in both permanent network (M_n = 10000 g/mol) and switching segment (M_n = 15000 g/mol) no changes occurred upon exposure to UV-light. It is expected that this is because M_n of polymers is above the molecular entanglement weight. Inter-penetrating network materials with M_n = 4000 g/mol in the permanent network were prepared. Initially a linear photo-active PEG was mixed into the material. This material exhibited a decrease in the values for G' and G'' after irradiation with UV-light for 30 minutes. The reason for the decrease in the two rheological parameters is unclear but the change encouraged further work with this type of systems. Two inter-penetrating network materials with the star-shaped cinnamic acid derivatised PEG as switching segment were prepared and irradiated with UV-light for 72 hours. The network with $r = 0.75$ in the permanent matrix proved the expectations by clearly showing a solvent effect when the photo-active polymer was introduced into the permanent network. In addition a significant increase of G' and G'' was observed after 72 h of irradiation with UV-light proving the formation of a second network consisting of the photo-active polymers. A network with $r = 0.5$ in the permanent matrix was also investigated but gave very different results due to the lower value for r. The applied r-value is significantly closer to the critical r_c-value and thus resulted in problems with the film formation. The data showed that the secondary network dominates the rheological properties of this network. A material with shorter chains in the permanent network (M_n = 1000 g/mol) was also investigated but showed no change after irradiation with UV-light for 15 minutes. This is related to the stiffness of permanent matrix.

First steps to creating an inter-penetrating network with two different polymers were taken by incorporating the cinnamic acid derivatised PEG-stars into a poly(propylene oxide) network. However exposure to UV-light did not result in any changes of the material properties. It was also tested if the photo-active PEG could be incorporated into a poly(dimethyl siloxane) network, but the addition of the photo-active PEG resulted in complete hindrance of the cross-linking of the poly(dimethyl siloxane).

A number of problems were identified throughout the work, primarily concerning the mismatch between the expected exposure time needed to induce changes in the materials and the exposure time observed experimentally. This can partially be explained by mobility of the polymers and concentration of the photo-active cinnamic acid. Studies presented in the literature show that the position of the cinnamic acid groups is important for the dimerisation to occur. The nature of polymers makes encounters between end groups less likely and this affects the dimerisation. Furthermore, an NMR-study showed formation of the *cis*-isomer of cinnamic acid. The isomerisation of cinnamic acid only occurs if dimerisation is hindered. This underlines that the circumstances are not ideal for dimerisation.

Dansk Resumé

Nærværende ph.d.-afhandling beskæftiger sig med udviklingen af stimuli-tilpassende materialer baseret på den UV-aktiverede dimerisering af kanelsyre og kanelsyrederivater.

Det er i en klæbers natur at hæfte godt til sit substrat, og det hænder derfor, at der opstår problemer, når den skal fjernes. Disse problemer opstår også med hudklæbere, hvor skade på den underliggende hud er meget uhensigtsmæssig. Den overordnede ide bag dette projekt var at løse dette problem ved at udvikle et materiale, som kunne skifte mellem en klæbende og en ikke-klæbende tilstand; en "tænd-sluk"-klæber. "Tænd-sluk"-klæbere er kendt i litteraturen, men det udførte arbejde har en ny tilgang til feltet ved at basere sig på udviklingen af en klæber, som består af et netværk iblandet en fotoaktiv polymer. Ved at bestråle klæberen med UV-lys omdannes materialet til et interpenetrerende netværk, hvorved klæbeevnen vil blive slået fra.

Systemets omsættelsesgrad blev beskrevet ved hjælp af to simple modeller, som viste, at fuld omdannelse skete på minutter. Dette blev undersøgt grundigere med IR-spektroskopi og UV-Vis spektroskopi. UV-Vis spektroskopi bekræftede en ændring i materialet efter bestråling med UV-lys, samt at denne ændring skete på minutter.

En række kanelsyrederivatiserede polymerer blev fremstillet, og materialeegenskaberne for disse blev undersøgt før og efter bestråling med UV-lys. For polymerer derivatiseret med (2*E*,4*E*)-5-phenylpenta-2,4-dien syre blev en makroskopisk ændring i materialet observeret efter bestråling med UV-lys. Den bestrålede polymer blev nedsænket i vand, hvor den dannede fibre eller tråde. Den ubestrålede polymer opløstes i vand som et hygroskopisk pulver. Et detaljeret studie af kanelsyrederivatiseret poly(ethylen glycol) (PEG) blev udført. Tre forskellige derivatiserede PEG-polymerer blev fremstillet; en 4-armet stjerne PEG (M_n = 2000 g/mol), en kort lineær PEG (M_n = 1000 g/mol) og en lang lineær PEG (M_n = 4000 g/mol). Ved at blande disse tre polymerer i forskellige forhold blev tre fotoaktive materialer fremstillet. De fotoaktive materialer blev undersøgt med reologi før og efter en times bestråling med UV-lys. Materialet, som bestod udelukkende af den kanelsyrederivatiserede 4-armede stjerne PEG, viste den største ændring i materialeegenskaber. Udviklingen af materialeegenskaberne for dette materiale blev studeret i detaljer ved at bestråle materialet med UV-lys i op til 120 timer og undersøge prøverne med reologi før og efter bestrålingen. Det blev observeret, at efter omkring 24 timer var en håndterbar film blevet dannet, samt at efter omkring 70 timers bestråling stabiliserede de reologiske

egenskaber sig. Den anvendte bestrålingstid var højere end forventet, men det blev antaget at dette ville blive forbedret ved fremstilling af et interpenetrerende netværk.

En række interpenetrerende netværk, hvor både det permanente netværk og "tænd-sluk"-netværket bestod af PEG-polymerer, blev fremstillet. Det blev observeret, at et materiale med relativt lange kæder i både det permanente (M_n = 10000 g/mol) og "tænd-sluk"-netværket (M_n = 15000 g/mol) ikke viste nogen ændring i reologiske egenskaber efter bestråling med UV-lys. Dette skyldes sandsynligvis, at M_n for begge polymerer er større end den molekylvægt over hvilken sammenfiltring af polymerkæderne sker. En række interpenetrerende netværk, hvor M_n = 4000 g/mol i det permanente netværk, blev fremstillet. Først blev en lineær fotoaktiv polymer blandet i materialet, og dette gav et fald i G' og G'' efter en halv times bestråling med UV-lys. Det var ikke forventet at se et fald i G' og G'', og grunden til dette er uklar. Dog blev arbejdet med denne type materialer fortsat, ansporet af den observerede ændring. To interpenetrerende netværk, med den kanelsyrederivatiserede 4-armede PEG-stjerne som "tænd-sluk"-netværk, blev fremstillet og bestrålet med UV-lys i 72 timer. Det ene netværk havde $r = 0.75$ for det permanente netværk, og dette materiale opførte sig præcis som forventet. Ved introduktion af den fotoaktive PEG-stjerne observeredes en solvent effekt i G' og G'', og efter bestråling sås en signifikant ændring i både G' og G''. Ændringen skyldes dannelsen af det sekundære netværk bestående af de fotoaktive polymerer. Det andet netværk havde $r = 0.5$ og opførte sig meget anderledes grundet den lavere r-værdi. Den lavere r-værdi er tættere på den kritiske værdi for r, hvilket gav problemer med filmdannelse. Data viser, at det sekundære netværk dannet af de fotoaktive polymerer dominerer de reologiske egenskaber af dette materiale. Et interpenetrerende netværk, med kortere kæder i det permanente netværk (M_n = 1000 g/mol), blev også studeret, men ingen ændring i G' og G'' blev observeret efter bestråling med UV-lys i 15 minutter. Dette skyldes det permanente netværk, som er hårdere på grund af den kortere kædelængde.

De første skridt mod udviklingen af et interpenetrerende netværk, bestående af to forskellige polymerer, blev taget ved at introducere de fotoaktive PEG-stjerner i et poly(propylen oxid)-netværk. Det blev dog observeret, at bestråling af dette netværk ikke ændrede materialeegenskaberne. Det blev også forsøgt at introducere de fotoaktive PEG-stjerner i et poly(dimethyl siloxan)-netværk, men tilsætning af de fotoaktive polymerer resulterede i fuldstændig hindring af krydsbindingsreaktionen.

En række problemer opstod under arbejdet, og primært handlede disse om den observerede uoverensstemmelse mellem den forventede bestrålingstid og den observerede bestrålingstid. Dette kan til dels forklares med mobiliteten af polymererne samt koncentrationen af den fotoaktive kanelsyregruppe. I litteraturen findes en række studier, som viser, at den relative position af kanelsyregrupperne er vigtig i forhold til dimeriseringen af grupperne. Polymerkædernes natur gør at sandsynligheden for at to endegrupper mødes er lav, og dette besværliggør dimeriseringen. Desuden viste et NMR-studie, at *cis*-isomeren af kanelsyre blev dannet ved bestråling med UV-lys. Isomerisering af kanelsyre sker kun, hvis dimerisering er forhindret. Dette understreger, at betingelserne for dimerisering ikke er optimale.

Contents

1 Introduction **1**
- 1.1 Objective . . . 3
- 1.2 Reading guide and thesis outline . . . 4

2 Stimuli-adaptable polymer materials **7**
- 2.1 Introduction . . . 7
- 2.2 Thermo-responsive materials . . . 8
- 2.3 Photo-responsive materials . . . 10
- 2.4 Electrical field responsive materials . . . 12
- 2.5 Mechano-responsive materials . . . 13
- 2.6 Magneto-responsive materials . . . 15
- 2.7 Chemo-responsive materials . . . 16
- 2.8 Redox-responsive materials . . . 16
- 2.9 Materials responsive to non-covalent interactions . . . 18
- 2.10 Biologically-responsive materials . . . 19
- 2.11 Multi-reponsive materials . . . 20
- 2.12 Perspective and motivation . . . 20

3 Monitoring of reactivity and extent of reaction of CAA and CA **23**
- 3.1 Kinetic models for the dimerisation of CAA . . . 23
  - 3.1.1 The Beer-Lambert law . . . 24
  - 3.1.2 Time-dependent model . . . 25
- 3.2 Monitoring the reaction of CAA and CA with FTIR-spectroscopy . . . 27
- 3.3 Monitoring the reaction of CA with UV-spectroscopy . . . 30
  - 3.3.1 Cinnamic acid . . . 30
  - 3.3.2 PEGCA-S2 . . . 33
- 3.4 Conclusion . . . 34

4 PEGCAA and PEGCA as photo-active materials **35**
- 4.1 General introduction to network and rheology terms . . . 35
- 4.2 PEGCAA as a photo-active material . . . 36
  - 4.2.1 Preparation and initial studies of PEGCAA . . . 36
  - 4.2.2 Synthesis of cinnamylidene acetic acid . . . 38
  - 4.2.3 Changing the photo-active group . . . 38

4.3 PEGCA as a photo-active material . . . 39
4.3.1 Preparation and analysis of CA-derivatised PEG . . . 39
4.3.2 CA-derivatised PEG as a stimuli-responsive material . . . 42
4.3.3 Time-dependence of network properties . . . 44
4.3.4 Reversibility . . . 45
4.3.5 Reproducibility . . . 46
4.4 Conclusion . . . 47

5 IPN materials based on PEG 49
5.1 Introduction to inter-penetrating networks . . . 49
5.2 Preparation of IPN-materials . . . 51
5.2.1 Preparation of PEG/HDI/PEGCA-S2 material . . . 52
5.2.2 Preparation of PEG/Desmodur/PEGCA-S2 material . . . 54
5.3 UV-study of CA-derivatised PEG in a PEG-network . . . 55
5.4 Material properties of IPNs with PEGCA/PEGCAA switching segments 59
5.4.1 IPN with PEG-network and a PEGCAA-switching segment . 59
5.4.2 Initial investigations of PEG/PEGCA IPN-material . . . 62
5.4.3 IPN with HDI cross-linked PEG-chains and PEGCA-S2 . . . 64
5.4.4 IPN with Desmodur cross-linked PEG-chains and PEGCA-S2 68
5.5 Conclusion . . . 70

6 IPN-materials 73
6.1 Preparation of IPN-materials . . . 73
6.1.1 Preparation of PPO/PEGCA material . . . 73
6.1.2 Preparation of PDMS/PEGCAA-S2 material . . . 74
6.2 IPN-materials with a PPO-network and a PEGCA-switching segment 75
6.3 Conclusion . . . 78

7 Mobility and reactivity 79
7.1 Crystals and mobility . . . 79
7.2 NMR-study of PEGCA . . . 80
7.3 SEC-study of PEGCA . . . 83
7.4 Conclusion . . . 84

8 Summary and concluding remarks 87

9 Future work and outlook 91
9.1 Final work with CA-derivatised PEG . . . 91
9.2 Further work with photo-active IPN-materials . . . 91
9.3 Alternative photo-activated chemistry . . . 92

Bibliography 93

A Synthesis i

A.1 Chemicals i
A.2 $SOCl_2$-mediated derivatisation of PEG with CAA and CA ii
A.3 Synthesis of CAA iii
A.4 DCC/DMAP-mediated esterification derivatisation of PEG with CA . iii
A.5 One-pot procedure for PEG/PEGHDI-S2/PEGCA(A) materials . . . v
A.6 Two-step procedure for PEG/PEGHDI-S2/PEGCA(A) materials . . vi
A.7 Preparation of PDMS-networks containing PEGCAA vii
A.8 Preparation of PEG/Desmodur/PEGCA materials viii
A.9 Preparation of PEG/Desmodur/PEGCA materials with DBTDL . . . ix
A.10 Preparation of PPO-networks x
A.11 Procedure for preparation of PPO/PTM/PEGCA materials x

B Methods **xi**
B.1 UV-irradiation methods xi
B.2 Spectroscopy, chromatography and rheology xi
B.3 Film formation xii
B.3.1 General film formation xii
B.3.2 Thin film of PEGCAA-mixture on PE-backing xii
B.4 UV-absorbance of CA and PEGCA-S2 in aqueous solution. xii
B.5 UV-absorbance of PEGCA-S2 and PEG/Desmodur/PEGCA-S2 films xii

C Supporting data **xv**
C.1 SEC-data from mono-functional CA-derivatised PEG xv
C.1.1 m-PEGCA-L0.75 irradiated in solid state xv
C.1.2 m-PEGCA-L5 irradiated in solid state xvi
C.1.3 m-PEGCA-L0.75 irradiated in solution xvii
C.1.4 m-PEGCA-L2 irradiated in solution xviii
C.2 NMR-data from mono-functional CA-derivatised PEG xix
C.2.1 m-PEGCA-L0.75 xix
C.2.2 m-PEGCA-L2 xxi

D Articles **xxiii**
D.1 Article 1: Fremstilling af UV-aktive polymerer xxiii
D.2 Article 2: PEGCA as a UV-Active Bio-Inspired Material xxix
D.3 Article 3: Properties of PDMS-networks and their network fractions . xlv

List of Abbreviations

CA	cinnamic acid
CAA	cinnamylidene acetic acid
DBTDL	dibutyltin dilaurate
DETA	diethylenetriamine
DCC	*N,N'*-dicyclohexylcarbodiimide
DCM	dicholoromethane
DL-HMPMA	poly(n-(DL)-(1-hydroxymethyl) propylmethacrylamide)
DMPA	2,2-dimethoxy-2-phenylacetophenone
dr	drop (in synthesis)
FTIR-spectroscopy	Fourier transformed infrared spectroscopy
G'	storage modulus
G''	loss modulus
HDI	hexamethylene diisocyanate
IPN	inter-penetrating network
IR	infrared
J	coupling constant (in NMR)
LCST	lower critical solution temperature
MMA	methyl methacrylate
M_e	molecular entanglement weight
M_n	number average molecular weight (for polymer)
m-PEG	linear mono-functional PEG
m-PEGCA-L0.75	m-PEG (M_n=750 g/mol) derivatised with CA
m-PEGCA-L2	m-PEG (M_n=2000 g/mol) derivatised with CA
m-PEGCA-L5	m-PEG (M_n=5000 g/mol) derivatised with CA
NMR	nuclear magnetic resonance (spectroscopy)
OD	optical density
P4VP	poly(4-vinyl pyridine)
PAAc	poly(acrylic acid)
PDEAAm	poly(N,N'-diethylacrylamide)
PDMAEMA	poly(N,N'-dimethyl aminoethyl methacrylate)
PDMS	poly(dimethyl siloxane)
PE	polyethylene
PEG	poly(ethylen glycol)
PEG-L4	linear PEG (M_n=4000 g/mol)

PEG-S2	4-arm star PEG (M_n=2000 g/mol)
PEGCA-L1	linear PEG (M_n=1000 g/mol) derivatised with CA
PEGCA-L4	PEG-L4 derivatised with CA
PEGCA-S2	PEG-S2 derivatised with CA
PEGCAA	PEG derivatised with CAA
PEGCAA-L15	linear PEG (M_n=15000 g/mol) derivatised with CAA
PEGCAA-S2	PEG-S2 derivatised with CAA
PEGHDI-S2	PEG-S2 derivatised with HDI
PMAAc	poly(methacrylic acid)
PMDETA	N,N,N',N",N"-pentamethyldiethylenetriamine
PMMA	poly(methyl methacrylate)
PNIPAAm	poly(N-isopropylacrylamide)
PPO	poly(propylene oxide)
PTHF	poly(tetra hydrofuran)
PTM	pentaerythritol tetra(3-mercaptopropionate)
PVCL	poly(N-vinylcaprolactam)
r	stoichiometric imbalance
RI	refractive index
RT	room temperature
SAOS	small amplitude oscillatory shear
SEC	size exclusion chromatography
SMP	shape-memory polymer
TEA	triethyl amine
T_g	glass transistion temperature (for polymer)
T_m	melting temperature (for polymer)
T_s	switching temperature (for SMP)
TTS	time-temperature superposition principle
UDETA	aminoethyl imidazolidone
UPy	2-ureido-4[1H]-pyrimidone
UV	ultraviolet
UV spectroscopy	ultraviolet-visible spectroscopy
w%	weight percent

Chapter 1

Introduction

It seems that nature always knows how to make intelligent or extremely specified materials to make the life of plants and animals easier. Many of these materials serve as desirable goals for numerous scientific studies. A well-known example that has been successfully replicated is the super-hydrophobic surface of the Lotus flower. This has been an inspiration for the development of several polymer based surfaces which e.g. exhibit *self-cleaning* capabilities [1]. Another famous example is *gecko*-inspired adhesive surfaces where materials with very high surface areas inspired by the nano-structures found on the feet of geckos have been developed [2, 3]. Products based on this technology have been commercialised as so-called *gecko-pads*.

The examples mentioned focus primarily on controlling the surface of the material but several other types of materials and processes could be mentioned. Such an example could be mussel-inspired adhesives that function in marine environments [2]. Mussels have received increasing attention in the later years because of their unique possibility of attaching themselves to rocks in seawater. Salinity, movement of waves and tides as well as the microorganisms in the sea water makes this environment very unique and harsh [4]. Despite this environment the mussels have developed an adhesive that will keep them attached to the rocks.

Even with the environment created by the sea water life in the seas displays an impressive diversity. In fact this project was initially inspired by the sea cucumbers which are able to transform their normally soft skin into a hard shell in a few seconds, see Figure 1.1 [5]. The animal uses this as a protection from enemies and can therefore regain its soft skin when the threat has passed.

FIGURE 1.1: *The sea cucumber can go from a relaxed (left) to a stiffened (right) state in a few seconds. Adapted from Reference [5]. Reprinted with permission from The American Association for the Advancement of Science.*

As described nature seems to be an inexhaustible source of inspirational materials and processes but the key question is always how to reconstruct these outstanding possibilities synthetically. An area which is proving very promising for this is the area of so-called stimuli-adaptable materials. Stimuli-adaptable materials are in general materials that have one or more properties which can be significantly altered in a controlled manner upon exposure to stimuli. In other words materials that give a measurable response when activated by an external stimulus. Many types of stimuli have been proposed and they span from physical stimuli, such as electromagnetic radiation or application of stress, over simple chemical stimuli, such as changes in pH, to complex biochemical phenomena, like enzyme or antigen adaptability. The intriguing diversity of this field opens up possibilities for many new and innovative materials and processes.

Novel materials are interesting to develop and explore but it must always be considered where they can be applied. This project is based on the idea of ultimately developing a switchable adhesive. A switchable adhesive comprises the two contradicting properties of strong adhesion and fast detachment [6]. This type of adhesive would offer a way to improve the adhesives used for e.g. wound dressings by offering an innovative way of combining comfort for the wearer as well as fast and easy removal with minimum discomfort. These statements are in contrast since generally a comfortable adhesive is soft, while an easily removable adhesive is rigid.

It is crucial that a skin adhesive can be easily removed since it is highly undesirable to cause damage to the skin. Often the person wearing the adhesive will already have an increased skin sensitivity due to e.g. diabetic ulcers and the skin may be easier to tear than the actual skin-adhesive interface.

Adhesion in itself is a complex phenomena, and when considering adhesion to skin several challenges are added. There is a limited amount of literature on the topic of viscoelastic properties of adhesives, however it was found that according to Kenney *et al.*[7] a good adhesive for human skin would have a storage modulus, G', between 10 and 18 kPa. Research carried out at DTU used networks based on poly(propylene oxide) cross-linked with silicone hybrid cross-linkers as adhesives. These networks have G'-values of app. 5 kPa which is slightly lower than Kenney *et al.* predict, but the research has proved that the adhesives adhere excellently to human skin [8]. Adhesion is also influenced by other circumstances such as the adhesives ability to wet the substrate, the appearance of the surface of the substrate as well as chemical or physical interactions between the adhesive and the substrate [9].

The following set of specifications could be extracted by comparing information from Venkatraman *et al.*[10] and Kenney *et al.*[7]
An adhesive used for skin must:

- adhere to the skin surface skin for 24 h to 7 days depending on the use.
- adhere to the skin during perspiration, showering and physical activity.

- allow removal without excessive trauma to skin.
- leave no residue on skin upon removal.
- be comfortable to wear.
- not lead to itching or unacceptable irritation of any kind.

For the wound care field specifically the system is required to be hydrophilic and breathable for accelerated healing [10].

Often poly(dimethyl siloxane) or poly(propylene oxide) based adhesives are used for skin adhesives since they comprise the majority of the specified abilities.

Switchable adhesives are known in literature and the field was recently reviewed by Kampermann and Synytska [6]. They propose that switchable adhesives generally fall into two groups; switchable adhesion achieved by chemical functionality or by topographical changes. Switchable adhesion by chemical functionality use stimuli-adaptable materials to achieve adhesive materials that have switchable adhesive properties. The adhesive properties are influenced by immersion in solvent, changes in pH- or or as a result of electric or biochemical signals.

Switchable adhesion by topographical changes works in a very different way by exploiting changes in contact area between surfaces to achieve changes in adhesion. As mentioned earlier e.g. geckos use large contact areas to adhere to surfaces and several adhesives based on replicating this have been developed and commercialised. Further development of this principle has led to switchable adhesives. In these systems the contact area and thus the adhesive properties can be controlled. Del Campo *et al.*[11] pioneered this field and developed a thermo-switchable adhesive surface. A shape-memory polymer was used to create an adhesive material with a pattern of fibrils on the surface. Deformation of the fibrils resulted in a non-adhering surface. Due to the nature of the shape-memory polymer the deformed fibrils could be fixed in the non-adhering state yielding switchable adhesion. The adhesive properties could be regained by releasing the deformation of the fibrils. Several systems similar to this have been developed and several different types of stimuli have been used to obtain the switchable nature such as magnetic and electric fields and application of mechanical stress. The principle is outlined in Figure 1.2.

Switchable adhesives have also been commercialised by LuminaAdhesives under the product name *Adhelight*.

1.1 Objective

The overall objective of this project was to develop a switchable adhesive to be used as a skin adhesive. It is our ambition that this adhesive would comprise the outlined specifications for a skin adhesive combined with the ability to switch the adhesion on and off several times by remotely activated chemistry.

FIGURE 1.2: *The principle behind the switchable adhesive prepared by del Campo et al.[11] The patterned surface exhibited adhesion. Upon heating and deformation of the fibrils a non-adhering state was obtained. The non-adhering state could be fixed by cooling. Heating the surface reformed the adhering state.*

As will be motivated in Chapter 2 it was decided to base the research on the UV-activated dimerisation of cinnamic acid (CA) and its derivatives. The project is based on the idea of being able to control the rheological properties of a material, namely an adhesive, with UV-light.

Ultimately it would be preferred to create a good adhesive based on e.g. poly(dimethyl siloxane) or poly(propylene oxide) and incorporate the UV-active polymers into this. In its adhesive state the material should have a G'-value of 5-18 kPa[7, 8] depending on the applied polymer and molecular structure of the adhesive. After activation of the UV-active polymers the adhesive properties of the materials should be switched off yielding a material with a value for G' above approx. 50 kPa.

To better understand the processes and the reaction it was decided to start out with a simple model system to prove that the idea could function. It was decided to work with a poly(ethylene glycol) system to understand the UV-activated chemistry in details and from there proceed to developing a more complex adhesive system.

The project should focus on development of UV-active polymers and the UV-controllable material properties of these. Furthermore, it should focus on development of polymer based inter-penetrating network materials for which the properties can also be controlled with UV-light.

This project is unique because of the approach to producing a switchable adhesive combined with the ambition of making a system where the switchable adhesion can be turned on and off repeatedly.

1.2 Reading guide and thesis outline

In this thesis a number of abbreviations will be made. They can all be found in the List of Abbreviations. And for further clarification a few of them will be explained here.

A number of polymers will be presented. They are abbreviated this way: polymer type and type of active group (if any) - structure and molecular weight (in thousands). As example a 4-armed star shaped poly(ethylene glycol) (PEG) with M_n=2000 g/mol will be PEG-S2 while a linear cinnamic acid derivatised PEG with M_n=1000 g/mol

will be PEGCA-L1. S denotes a star-shaped polymer, while L denotes a linear. This nomenclature will be used throughout the thesis.

The prepared IPN-networks will also be abbreviated in a consistent way. For these the abbreviations are: polymer in permanent network/cross-linker/switching segment (r for permanent network, concentration of switching segment in w%). For example a material consisting of a permanent PEG-network cross-linked with Desmodur and with a r-value of 1.2 in which the switching segment is 19.8 w% PEGCA-S2 will be written in this way: PEG/Desmodur/PEGCA-S2 (r=1.2, 19.8 w% PEGCA-S2).

In Chapter 2 an overview of the field of stimuli-adaptable materials will be given. In the end of Chapter 2 a motivation for the choice of stimuli-adaptable chemistry will be given.

The applications are highly dependent on a fast and reliable development of material properties and it was expected that this was very closely linked to the extent of reaction for the photo-active dimerisation reaction. In Chapter 3 the extent of reaction is examined in a number of ways. Firstly two simple kinetic models will be presented and discussed in order to get an overview of the expected time frame. Secondly results from Fourier-transformed infrared (FTIR) and ultraviolet-visible spectroscopy (UV-spectroscopy) will be given.

In order to understand the materials better a thorough study of the photo-active polymers was carried out. The material properties of samples consisting solely of photo-active polymers are reported in Chapter 4. A study of the dependency of the UV-irradiation time on the development of the material properties in also presented.

In Chapters 5 and 6 the work on IPN-materials is presented. Chapter 5 deals with materials where both the permanent network and the switching segment consist of the same polymer, namely poly(ethylene glycol). Three different routes to obtaining the materials are reported and the materials are characterised by linear rheology. Chapter 6 deals with IPN-materials consisting of different polymers and the characteristics of these materials. The routes to obtaining the materials are described and one of the systems is characterised by linear rheology.

Chapter 7 summarises and discusses some of the challenges the work faced. Data from nuclear magnetic resonance spectroscopy (NMR) and size exclusion chromatography (SEC) are presented along with a discussion of mobility in polymers.

Finally a summary and concluding remarks are given in Chapter 8 along with a discussion of the outlook of the work in Chapter 9.

There are four Appendices to this Thesis. Synthetic details are found in Appendix A while details on the applied methods are in Appendix B. Supporting data are found in Appendix C and Appendix D holds published and submitted articles.

The presented work resulted in an article published in the Danish journal Dansk Kemi and an article submitted to Macromolecular Chemistry and Physics which is currently under review. Both articles present some of the data discussed in Chapter 4.

- S.M.G. Frankær, A.L.H. Di Vaia, A.E. Daugaard, S. Kiil & A.L. Skov. Fremstilling af UV-aktive polymerer. *Dansk Kemi,* **2011** (92):24-27 (Appendix D.1)

- S.M.G. Frankær, A.L.H. Di Vaia, A.E. Daugaard, S. Kiil & A.L. Skov. Cinnamic Acid Derivatised Poly(Ethylene Glycol) as a UV-Active Bio-Inspired Material. *Macromol. Chem. Phys.,* submitted. (Appendix D.2)

Alongside the work with the development of a switchable adhesive a study of poly(dimethyl siloxane) networks and their extracted network fractions was also carried out. This work was initiated before the PhD-work. This study resulted in a full paper published in Rheologica Acta:

- S.M.G Frankær, M.K. Jensen, A.G. Bejenariu & A.L. Skov. Investigation of the properties of fully reacted unstoichiometric polydimethylsiloxane networks and their extracted network fractions. *Rheol. Acta,* **2012** (51):559-567 (Appendix D.3)

Chapter 2

Stimuli-adaptable polymer materials

The following chapter provides an overview of the types of stimuli-adaptable polymer materials reported in the literature. The present review is not meant to be conclusive but to present the diversity, perspective and possibilities of the field.

2.1 Introduction

Over the last decades the amount of research articles published within the field of so-called *smart materials* has increased significantly [12]. The field holds many promises for the future and it is a field that has grown in size and complexity. Many names are used to describe the same type of material; stimuli-adaptable/stimuli-responsive materials, smart materials, active materials and designed materials, to mention a few. In this review the term *stimuli-adaptable* will be used. Furthermore, the type of *material* is also important and must be further specified. The phenomenon of stimuli-adaptation is not restricted to one type of material. Several types of materials, such as metals, polymers and composites, can be stimuli-adaptable, most well-known is probably the shape-memory alloys which are in fact temperature-responsive metal alloys. Here the focus is put on polymers.

In general stimuli-adaptable materials are materials that have one or more properties that can be altered in a controlled manner upon exposure to stimuli. The stimulus can be changes in the chemical environment (e.g. pH, ionic strength, redox/electrochemical properties) as well as changes in the physical environment (e.g. temperature, electric field, electromagnetic radiation, magnetic field, stress).

The field of stimuli-adaptable polymer materials is wide-ranging and filled with exciting new approaches to developing novel materials. The most widely used way to get an overview of the field of stimuli-adaptable polymer materials is to review it by type of stimulus [13, 14], which will also be done here. Besides the type of stimulus it is also important to consider whether adaptation is due to formation or scission of a covalent dynamic bond, e.g. photo-activated dimerisation of cinnamic acid [15], changes in the non-covalent interactions between the species, e.g. molecular recognition between dibenzo[24]crown-8 and dibenzylammonium salt moieties [16] or due to physical adaptation to the environment, e.g. thermo-responsive shape-memory polymers [17]. Some reviews focusing on the type of material, such as solutions, interface/surface material, gels and solids, can also be found [18].

2.2 Thermo-responsive materials

Thermo-responsive, or temperature-responsive, polymers are found as solutions, surface or interface materials, hydrogels and solids. In Figure 2.1 a few examples of the chemical structure of thermo-responsive polymers are shown.

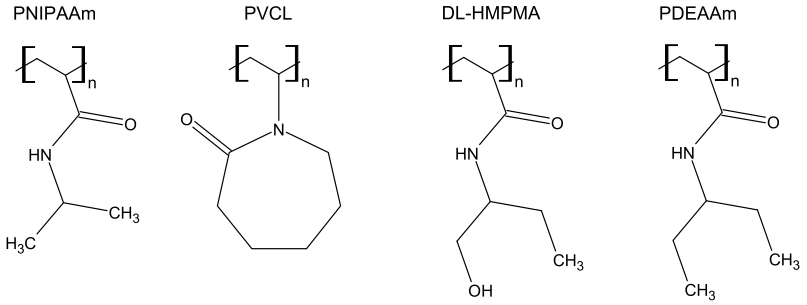

FIGURE 2.1: *A few examples of the chemical structures of thermo-responsive polymers.*

When it comes to thermo-responsive solutions several different transitions caused by external stimuli are known. One such is the lower critical solution temperature (LCST) below which the polymer chains are homogeneously mixed with the solvent. Above LCST a phase separation between the polymer and the solvent occurs. Polymers such as poly(N-isopropylacrylamide) (PNIPAAm) [19], poly(N-vinylcaprolactam) (PVCL) [20], poly(N-(DL)-(1-hydroxymethyl) propylmethacrylamide)(DL-HMPMA)) [21] and poly(N,N'-diethylacrylamide) (PDEAAm) [22] exhibit this behaviour and have LCSTs of approx. 32-35 °C. The LCST behaviour has also been applied to polymers grafted onto surfaces yielding materials with reversible swollen/collapsed properties [23]. In the collapsed state the chains are densely packed giving rise to significant changes in surface morphologies, stiffness, and adhesion properties compared to the swollen state. The changes in the material give a possibility for controlling e.g. cell adhesion and protein absorption on the surface [18].

Solid phase thermo-responsive polymers are often used as so called shape-memory polymers (SMPs). Shape-memory is a technique that exploits the thermo-responsive polymers to create materials that are able to recover their original shape after experiencing deformation, see Figure 2.2. As Figure 2.2 shows the changes in the material are governed by the transition across a switching temperature T_s. T_s is unique for each polymer material and for some systems T_s is equal to the glass transition temperature T_g. The fixation of the deformed material as well as the process of restoring of the original shape is brought on by changing the temperature across T_s. The transition across T_s greatly influences the mobility of the polymer chains thus generating the shape-memory effect. SMPs activated by light have also been reported, see Section 2.3 [15].

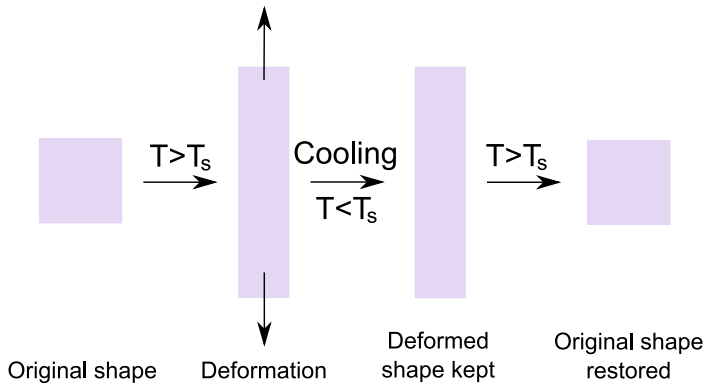

FIGURE 2.2: *Schematic representation of the shape memory effect where T_s is the switching temperature. The material is heated above T_s, deformed, fixed and cooled. After removing the fixture the material retains its deformed shape. Heating the material above T_s restores the original shape of the sample [17].*

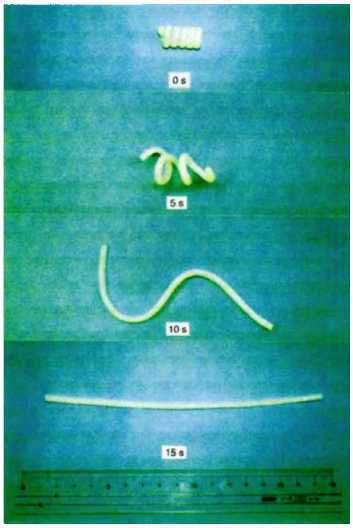

FIGURE 2.3: *An example of shape memory applied to a co-polymer gel consisting of an acrylic acid n-stearyl acrylate co-polymer. The co-polymer was made in a glass tube and swelled in water to form a hydrogel. The hydrogel was then heated to 50 °C, coiled up to a spiral and then cooled to room temperature. The hydrogel maintained its spiral shape. When the deformed hydrogel was heated to 50 °C the original straight shape was recovered in only 15 seconds [24]. (Reprinted by permission from Macmillan Publishers Ltd: Nature 376(6537):219. ©1995.)*

Gels can also be shape-memory materials. As an example Osada and Matsuda [24] reported shape-memory for water-swollen gels of co-polymerized acrylic acid with *n*-stearyl acrylate. The switching temperature of the system is 50 °C. The shape-memory effect is used and the material is deformed (spiral shape) and cooled. Upon heating the deformed material regains its original shape, see Figure 2.3.

Furthermore, other types of thermally induced responses in solids have also been reported. For instance Liu and Urban [21, 25] report contraction in the x-y-plane and expansion in the z-plane of poly(N-(DL)-(1-hydroxymethyl) propylmethacrylamide-co-n-butyl acrylate) films as well as poly(2-(N,N-dimethylamino)ethyl methacrylate-co-n-butyl acrylate) films that shrink in all directions at elevated temperatures.

Thermo-responsive systems have also been used by Lendlein *et al.* [26, 27] to develop so-called triple-shape polymers; polymers with two switching temperatures and thus three possible shapes.

2.3 Photo-responsive materials

Polymer systems responsive to electromagnetic radiation are often referred to as photo-responsive systems [18]. This type of polymer systems change when they are exposed to electromagnetic radiation (light). Many systems responsive to UV-light [15] have been reported, but infrared (IR) [28] and visible light [29] are also possible. It must be noted that exposure to IR-radiation will induce an increase in temperature. In some systems this temperature change is the source of the stimuli-adaptability meaning that the systems are thermo-responsive and not directly photo-responsive [28].

Photo-induced isomerisation of diarylethenes has been studied. Diarylethenes are compounds that have aromatic groups on each side of a carbon-carbon double bond. An example of this type of reaction is the photo-induced isomerisation of stilbene [30]. Furthermore, bispyridine and bispyridinium compounds have been reported in this group of photo-active compounds. These structures have an open and a closed form and the closed form gives the possibility of electron conduction, see Scheme 2.1 [31].

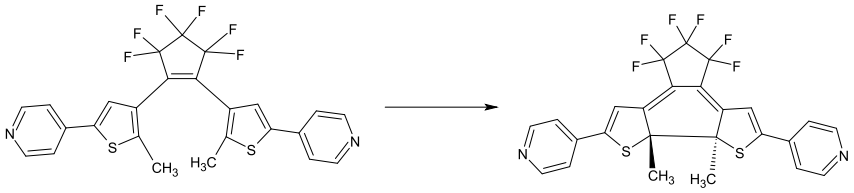

SCHEME 2.1: *Left: The open form of the photo-active bispyridine compound. Right: The structure closes when the compound is exposed to electromagnetic radiation and creates a molecule that has the possibility of electronic communication [31].*

A similar group of compounds is the azobenzenes which can undergo photo-activated *cis-trans*-isomerisation. The isomerisation is shown in Scheme 2.2 where it can be seen that the contracted *cis*-configuration of the molecule takes up much less space than the *trans*-configuration. The *trans*-isomer measures approx. 9 Å in legth while the *cis*-isomer measures 5.5 Å which is significantly less. This molecular level contraction of the molecule can induce macroscopic changes in the material. The formation of the *cis*-isomer is induced by irradiation with light ($\lambda = 330 - 308$ nm), while the *trans*-isomer, which is the more stable isomer, can be restored by irradiation with light with a longer wavelength ($\lambda = 420$ nm) or by heating [32].

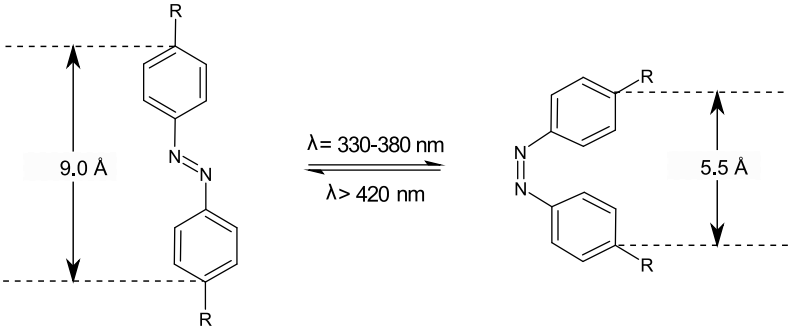

SCHEME 2.2: *Schematic representation of the photo-induced cis-trans-isomerisation of compounds containing azobenzene groups. The trans-isomer measures approx. 9 Å in legth while the cis-isomer measures 5.5 Å [32].*

The ionisation of compounds containing leuco-derivatives, such as bis(4-(dimethylamino)phenyl) (4-vinylphenyl)methyl leucocyanide, can induce expansion and shrinkage of polymers or gels. In Scheme 2.3 the general reaction of a leuco-derivative is shown. The changes in the material arise due to the change in electrostatic repulsion between the charges. The ionisation of the compound is caused by irradiation with UV-light with a wavelength larger than 270 nm. The reversed reaction can be induced thermally [18, 32].

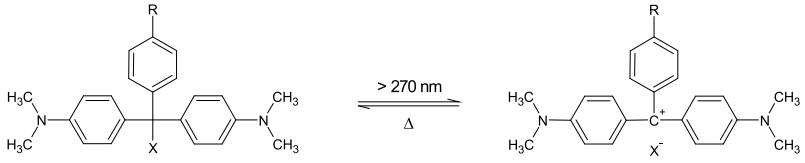

SCHEME 2.3: *The ionisation of a leuco-derivative happens when the compound is irradiated with UV-light [18, 32].*

The formation of cyclobutanes from cinnamic acid (CA) and its derivatives is well-known. Upon irradiation with UV-light with a wavelength of more than 300 nm two

CA-molecules will dimerise and form a cyclobutane, as shown in Scheme 2.4. The reaction can be reversed by irradiation with UV-light with a shorter wavelength ($\lambda =$ 254 nm) [33]. Lendlein *et al.* [15] used this type of photo-active compounds to create a photo-active SMP.

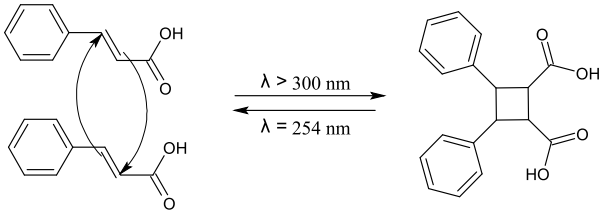

SCHEME 2.4: *When cinnamic acid is irradiated with UV-light with $\lambda > 300$ nm dimerisation occurs. Irradiation with shorter wavelength UV-light ($\lambda =$254nm) reverses the reaction [32].*

This reaction has been applied for many different applications and has shown great versatility. Yamaoka *et al.* [34] have applied the functional group to phenoxy resins, Andreopoulos *et al.* [35, 36] applied the functional group to different poly(ethylene glycol) (PEG) polymers to make hydrogels, Coqueret [37] have applied the chemistry to siloxanes, Lendlein *et al.* [15] have applied the functional group to acrylates and PEGs while Gattás-Asfura *et al.* [38] made functional gelatines.

2.4 Electrical field responsive materials

In Figure 2.4 a number of molecules that act as liquid crystals can be found. The molecules have the ability to align themselves along an applied electrical field, as can be seen in Figure 2.5. The liquid crystal molecules posses a permanent dipole generated by strong electron-withdrawing groups, such as the nitrile and trifluoromethyl groups.

The liquid crystals can be embedded in polymers and thereby create polymers that respond to electrical fields. As the name "liquid crystal" indicates the effect can be observed in solutions and emulsions of polymers [39]. The effect has also been observed in gels; Liu and Zhao [40] report gelatin/alginate semi inter-penetrating networks which show bending upon application of an electrical field.

Another way of using polymers in electrical field responsive materials is the so-called dielectric polymer actuators. In these materials an elastomer film is *sandwiched* between two electrodes. When a voltage is applied across the electrodes the incompressible nature of the elastomer film causes a change in the material. The electrodes attract each other leading to a decrease of the film thickness. Simultaneously the surface area of the material is increased, see Figure 2.6. The materials can be regarded as composite materials rather than polymer materials [41, 42].

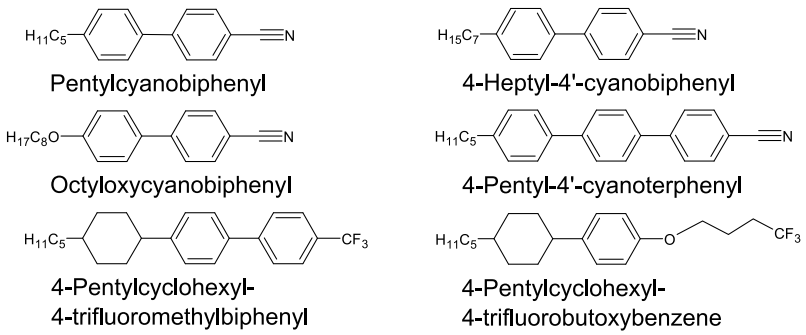

FIGURE 2.4: *Examples of molecular structures of liquid crystals.*

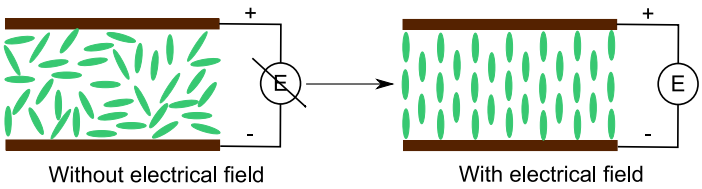

FIGURE 2.5: *The characteristic feature of the liquid crystals is that they arrange themselves in the direction of an applied electrical field.*

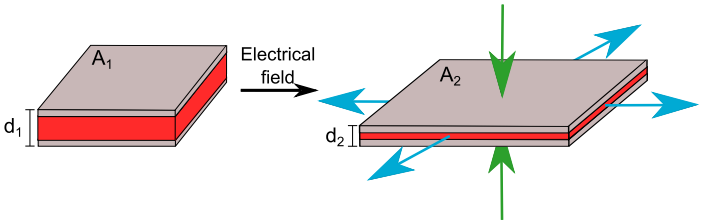

FIGURE 2.6: *The principle of dielectric elastomers. Left: The elastomer (red) is sandwiched between the electrodes (grey). The surface area of the electrode is A_1 and the thickness of the film is d_1. Right: After applying an electrical field the surface area is increased (A_2) and the thickness is reduced (d_2) due to attraction between the two electrodes [41].*

2.5 Mechano-responsive materials

Some research groups have been investigating materials where the inter-molecular interactions could be altered by mechanical stimulus, namely application of force or sonication with ultrasound. Inter-molecular forces rely on the spatial orientation of the molecules which can be distorted by applying stress or ultrasound. The spatial orientation of the molecules will simply be forced to change by application of stress

while ultrasound can *shake* the molecules apart [14].

Kushner *et al.* [43] reported a polymer system that mimics the protein *titin*, a muscle protein. Titin is an interesting material that offers a unique combination of strength, toughness and elasticity [14, 43, 44]. The material reported by Kushner *et al.* utilises the 2-ureido-4[1H]-pyrimidone (UPy) moiety that exhibits quadruple hydrogen bonding, see Figure 2.7. The UPy functional group has been used in several studies [45, 46] and in the case described here it is incorporated as a macrocyclic system along a polymer backbone. The UPy-molecules will dimerise but application of stress can force the hydrogen bonds in the dimer apart, see Figure 2.7. As Figure 2.7 shows stress does not tear the material apart since the polymers are kept together not only by the UPy-dimer but also by a polymer macrocycle. The elasticity of the material will upon time/heating restore the UPy-dimer [43]. The UPy-molecule can homo-dimerise, as described here, but it can also selectively hetero-dimerise with 2,7-diamido-1,8-naphthyridine groups. This reaction have been used to create supramolecular polymers [47].

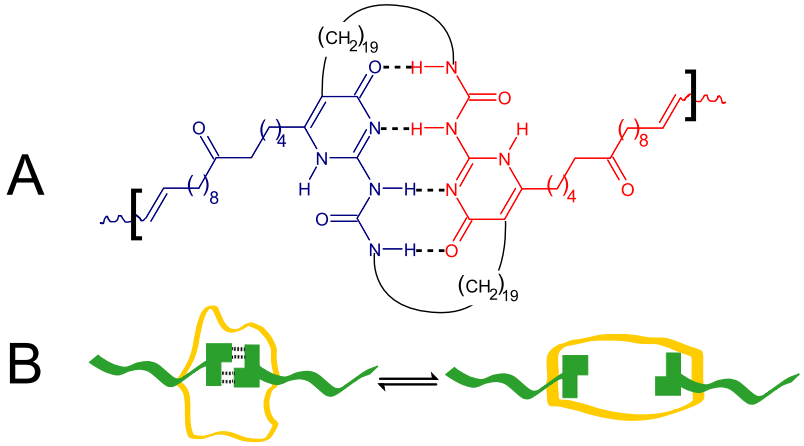

FIGURE 2.7: *A) Two 2-ureido-4[1H]-pyrimidone (UPy) molecules dimerise due to quadruple hydrogen bonds. The two UPy-molecules are furthermore constrained by a macrocycle. B) The UPy-dimer is schematically shown here. The dimer can be ripped apart by application of stress. The polymers (green) are the held together by the macrocyclic system (yellow). The presence of the macrocyclic system ensures that the polymers are kept together by covalent bonds [43, 14].*

Materials that are responsive to ultrasound (sonication) are often also held together by inter-molecular forces. An example is a system reported by Sijbesma *et al.* [48] where the complexation between phosphor and palladium is used to yield a kinetically stable high-molecular weight metallo-polymer. The researchers use low-molecular weight diphenylphosphine-terminated poly(tetra hydrofuran) (PTHF)

which is bound together by complexation with palladium(II)chloride, see Figure 2.8. After treating a solution of the polymer in THF the molecular weight significantly decreases, and the high molecular weight is restored within 23 hours after removal of ultrasound [48].

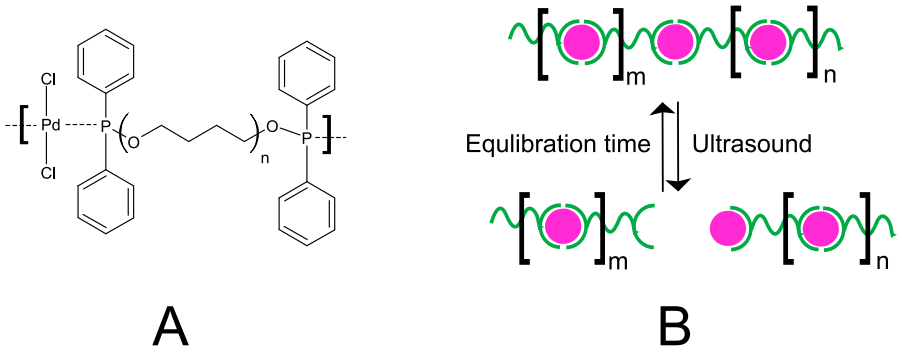

FIGURE 2.8: *A) Low molecular weight diphenylphosphine-terminated poly(tetra hydrofuran) (PTHF) complexed with Pd(II)Cl_2. B) A high molecular weight metallo-polymer is formed by the pTHF complexed with Pd(II)Cl_2. Exposing a solution of the polymer to ultrasound ruptures the complex bonds and yields lower molecular weight complexes. The high molecular weigh polymer is restored after 23 hours [48, 14].*

2.6 Magneto-responsive materials

Systems responsive to the presence or absence of a magnetic field have also been described in the literature. The majority of the systems consists of a polymer network in which magnetic particles are distributed or covalently immobilised. This causes materials that respond to magnetic fields by reversible shape and size distortion [49, 50].

Out of many examples of this type of responsive polymer systems Xulu *et al.* [51] prepared poly(N-isopropylacrylamide) (PNIPAAm) hydrogels with magnetic nanoparticles of Fe_2O_3. As described earlier PNIPAAm is a thermo-responsive polymer so the system presented by Xulu *et al.* is in fact responsive to temperature as well as magnetic fields. The thermo-sensitivity is not influenced by the magnetic nanoparticles. Small beads of the PNIPAAm/Fe_2O_3-hydrogel were prepared and they showed the ability to form a chain-like structure in a uniform magnetic field while a non-uniform magnetic field caused the beads to aggregate [51].

2.7 Chemo-responsive materials

Chemo-responsive materials change as response to variations in the chemistry of their environment, such as changes in pH or ionic strength of the surrounding medium. In Figure 2.9 a number of pH-responsive polymers can be seen. The polymers have ionisable groups and are thus greatly influenced by the pH of the environment.

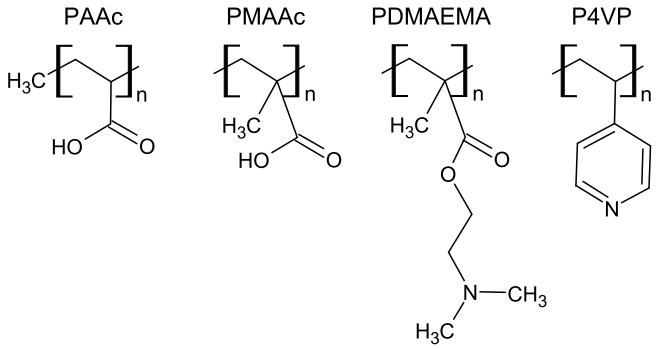

FIGURE 2.9: *Examples of pH-responsive acid/base polymers.*

In solutions acidic polymers, such as poly(acrylic acid) (PAAc) and poly(methacrylic acid) (PMAAc), have pK_a-values in the range of 5. These polymers will release protons in alkaline solution and swelling will occur. pH-responsive basic polymers, such as poly(N,N'-dimethyl aminoethyl methacrylate) (PDMAEMA) and poly(4-vinyl pyridine) (P4VP), accept protons and expand under acidic conditions [18].

pH-responsiveness have also been observed with polymers grafted on surfaces and interfaces [18]. The pH-value of the surrounding solution is essential when preparing so-called layer-by-layer materials. This type of materials often depend strongly on the electrostatic interactions between the layers and the electrostatic interactions depend of pH [52].

pH-responsive gels have also been fabricated. Orlov *et al.* [53] manufactured ultra thin hydrogel membranes controlled by pH. The swelling degree and thereby also the pore size of the material is controlled by pH. This way the flow through the membrane can be controlled, as illustrated in Figure 2.10.

2.8 Redox-responsive materials

Some materials show their responsiveness as a reaction to oxidative or reductive changes in their environment. The changes can be induced either by addition of chemicals or by electrolysis (electrochemical responsiveness) [14, 13]. There are advantages to using redox-responsiveness induced electrochemically; in fact Yan *et al.* stated that the *green* electrochemically controlled redox switching is more interesting than redox-responsiveness controlled by the addition of chemical reagents [13].

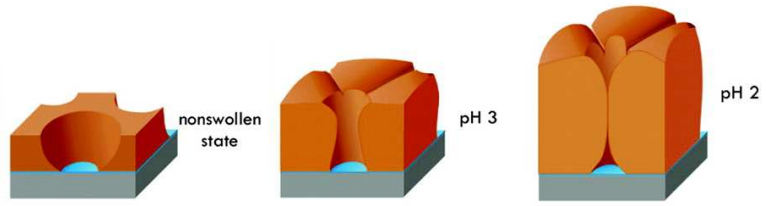

FIGURE 2.10: *A thin film of cross-linked poly(2-vinylpyridine) partially reacted with 1,4-diiodobutane acts a a membrane which can open and close due to the acidity of the environment. This sketch shows the cross-sectional profile of membrane in its non-swollen state and at pH=2 and 3. As can be seen the membrane gradually swells and ultimately the pores are closed (pH=3) [53].(Adapted and reprinted with permission from Macromolecules, 40(6):2086–2091, 2007. Copyright (2007) American Chemical Society.)*

As an example Royal *et al.* [54] made a system that exploits the metal coordination of terpyridine and a cyclam (1,4,8,11-tetraazocyclotetradecane) macrocycle in a system where metallo-supramolecular polymers are formed upon addition and complexation with cobalt ($Co(ClO_4)_2$). Stepwise oxidation from Co^{2+} to Co^{3+} which can be achieved by electrolysis gives a gel-sol transition as well as a vivid colour change, see Figure 2.11 [13, 54].

FIGURE 2.11: *a) Two terpyridine groups linked with a cyclam (1,4,8,11-tetraazocyclotetradecane) macrocycle. b) Addition and complexation with Co^{+2} yields a red redox-responsive metallo-supramolecular polymer gel. The gel can be oxidized to a green sol. The red gel is restored by reduction. The redox-effect can be controlled electrochemically [54].(Adapted and reprinted with permission from Langmuir, 25(15):8751–8762, 2009. Copyright (2009) American Chemical Society.)*

2.9 Materials responsive to non-covalent interactions

Systems where the change of properties is controlled by hydrogen bonding and other non-covalent interactions are also available. The systems are controlled by supramolecular interactions rather than dynamic covalent bonds, which is the case for some of the reactions reviewed earlier. In this type of stimuli-adaptable polymer materials external stimulus, such as temperature, light or pH, significantly influences the specific and selective interaction between chemical groups and/or molecules, such as van der Waals forces, hydrogen bonding, hydrophobic interactions, metal coordination, electrostatic effects, electromagnetic effects and π-π-stacking [13]. Systems of this type are also sometimes referred to as systems with *molecular recognition* [55]. The systems described earlier as mechano-responsive, Figures 2.7 and 2.8 are also examples of materials controlled by non-covalent interactions.

As an example Leibler *et al.* [56] have developed a material based on fatty acids derivatised with aminoethyl imidazolidone (UDETA), diethylenetriamine (DETA) and and urea, see Scheme 2.5. The properties of the material can be changed depending on the ratio between the different constituents. When the amount of UDETA is large the material is dominated by physical cross-links due to hydrogen bonding. When the amount of DETA in the system is increased the amount of chemical cross-links is increased as well. This induces a change in the material [56].

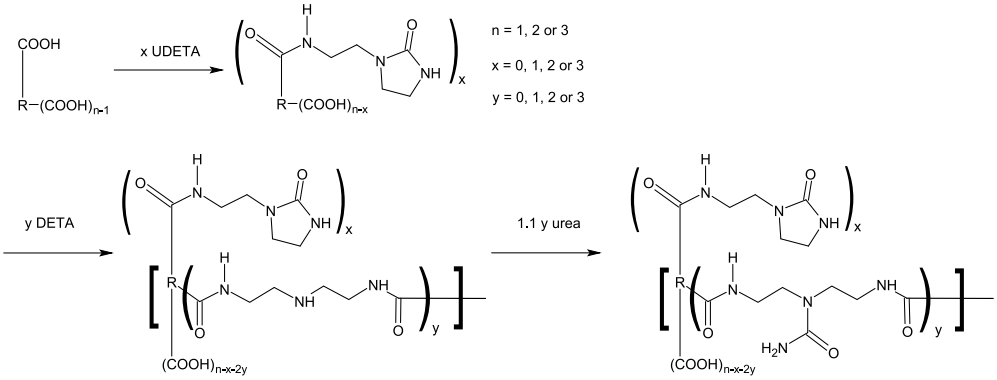

SCHEME 2.5: *The formation of the materials described by Leibler et al. [56] Fatty acids are reacted with aminoethyl imidazolidone (UDETA), diethylenetriamine (DETA) and urea. Depending of the values for n, x and y different materials result.*

Another example is the formation of responsive supra-molecular gels as reported by Ge *et al.* [16] Supra-molecular gels were made by molecular recognition between the crown ether group in dibenzo[24]crown-8-terminated four-arm star poly(ε-caprolactone) and the ammonium ion in dibenzylammonium-salt-terminated two-arm poly(ε-caprolactone), see Figure 2.12. The molecular recognition between the groups took

place in a 20 g/L solution and disruption of the formed gel was observed by heating (to above 60 °C) or by adding base [16].

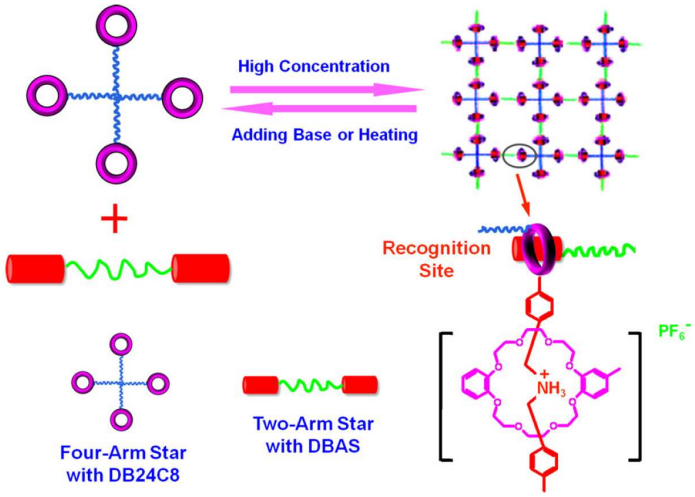

FIGURE 2.12: *Schematic representation for the fabrication of responsive supramolecular networks from dibenzo[24]crown-8-terminated four-arm star poly(ε-caprolactone) and dibenzylammonium-salt-terminated two-arm poly(ε-caprolactone as a result of molecular recognition between dibenzo[24]crown-8 and dibenzylammonium salt moieties. (Reproduced with permission of John Wiley & Sons, Inc. from ref. [16]).*

2.10 Biologically-responsive materials

Another area where stimuli-adaptable polymers have large application potential is within biomedicine. Polymers responsive to stimuli readily available in biological systems are especially interesting. There are four general types of biologically-responsive polymers; glucose-responsive, enzyme-responsive, antigen-responsive and redox/thiol-responsive polymers [12].

Glucose-responsive polymers are receiving attention primarily because of their potential as both glucose sensing systems and for insulin delivery applications. Polymers responsive to glucose are normally based on either oxidation of glucose with glucose oxidase [57], binding of glucose with concanavalin A [58] or reversible bond formation between glucose and boronic acid [12, 59].

Enzyme-responsive systems are a relatively new area within stimuli-adaptable polymers. The area is of great interest mainly because the nature of the enzymatic reactions is highly selective and because the reactions work under mild conditions (aqueous, pH 5–8, 37°C). Furthermore, enzymes play key roles in healthy and diseased biological pathways [60].

Systems with antigen-responsiveness utilise the highly specific antigen-antibody interactions to create responsive polymers. The responsiveness is induced by entrapping antibodies or antigens in networks, connecting the antibody or antigen to a network or using antigen-antibody pairs as cross-linkers in a network [61].

As an example of a biologically active system the reversible conversion of disulfide bonds have been used to create redox/thiol-responsive polymers. The disulfide bond can be reduced to thiols (thiol response) which can then be oxidized back to a disulfide in the presence of other thiols (redox response), see Scheme 2.6 [12, 62].

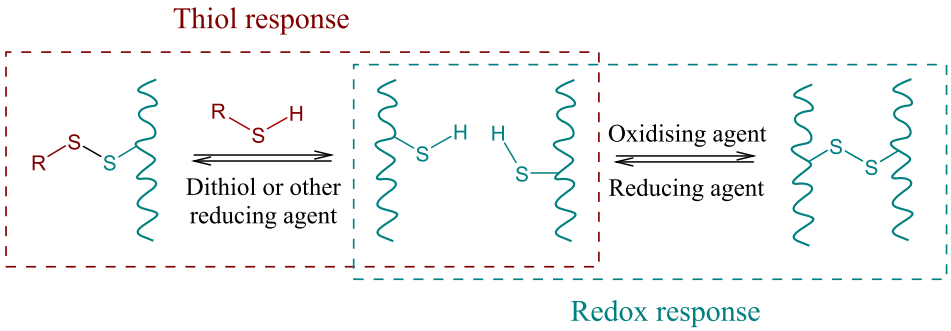

SCHEME 2.6: *The redox/thiol-response can be applied in responsive polymer systems [12].*

2.11 Multi-reponsive materials

A growing trend in stimuli-adaptable materials is multi-responsive systems, meaning systems that have several components that each responds to different stimuli. An example is functional copolymers of PNIPAAm with spirobenzopyran as reported by Sumaru [63]. The functional copolymer has a temperature sensitive segment (PNIPAAm) as well as a pH- and photo-responsive segment (spirobenzopyran). The researchers showed that a solution of the described copolymer shows responsiveness determined by temperature, pH or electromagnetic radiation.

2.12 Perspective and motivation

As this chapter outlines the field of stimuli-adaptable materials is broad and holds many promises for the future. Stimuli-adaptable materials can most likely be used in many innovative solutions and products. As mentioned earlier light-switchable adhesives have already been commercialised by LuminaAdhesives [64, 6]. Several other types of applications for stimuli-adaptable polymers have been proposed such as microfluidic devices [65], drug release systems [36, 66], and fouling release systems [67, 68].

The purpose of the literature survey presented was partly to get an overview of this vast and complex field but also to review possible materials and reactions to be used in the project. In Chapter 1 a discussion of the ideal properties of the material are made along with a number of specifications for the used chemistry. Some of the specifications can now be discussed relatively to the findings in literature.

First of all a type of stimuli-adaptable chemistry was needed which could be controlled remotely. A decision was therefore made to focus on the physical types of stimuli, such as photo-active reactions and thermo-responsive systems. The physical types of stimuli have the advantage that they can be switched on and off quickly and on demand. Further possible applications, besides the idea of creating a switchable adhesive, were discussed and the majority of these related somehow to implants which should be placed inside the human body. The tissue in the body might be damaged by increased temperatures and therefore thermo-responsive systems were discarded. The focus was instead put on the photo-active systems. Another reason to focus on photo-active systems was that many of these are reversible which would allow a system where the properties could be changed several times.

There are a number of photo-active reactions and the ones presented in Section 2.3 are just a small selection. The overall goal was to prepare a very stable inter-penetrating network material and therefore a system with controllable covalent bonds was needed. Of the reviewed reactive groups cinnamic acid (CA) and bispyridine/bispyridinium have this ability. Another candidate, which has not been included in this review, is the reaction of coumarine [69]. There are a number of reasons why it was decided to focus on CA rather than other candidates. The primary reason is the many published studies that utilise this type of chemistry in a convincing and inspiring way. Many types of polymers have been successfully derivatised with CA or CA-derivatives. This encouraged us to believe that this type of chemistry was right for the project. It is also very appealing that the synthetic pathways to the active polymers are very straight forward. This allows for the focus of the work to be on the material properties and the stimuli-adaptability.

Furthermore, it became evident that only a few research groups had focused on the material properties, namely the rheological properties, in their studies. The present work deals exactly with the development of the rheological properties of stimuli-adaptable materials.

During the project it was decided to study CA-derivatised poly(ethylene glycol) (PEG) as a photo-active material. This has been done before by Lendlein *et al.* [15] and Andreopoulos *et al.* [35, 36] Lendlein *et al.* propose an inter-penetrating network (IPN) system where the permanent network is a butyl acrylate while the switching segment is made up of a PEG-polymer. The purpose of the work was to create light-switchable SMP materials, as mentioned earlier. The researchers furthermore report an increase in Young's modulus of 26% for the IPN-material [15] which was a great inspiration for the work conducted. The present research is different from the work by Lendlein *et al.* in a number of ways but first and foremost the focus is on the development of the material properties rather than achieving shape-memory.

Furthermore, the properties of the photo-active polymers are studied before an IPN is constructed. Last but not least the majority of the materials studied have the same polymer type in both the permanent network as well as the switching segment which is not the case for the materials reported by Lendlein *et al.*[15] Regarding the studies done by Andreopoulos *et al.*, who worked with CA-derivatised PEG for controlled release [35, 36], the work in this thesis focuses on the properties of the photo-active material and not the process of controlled release.

Chapter 3

Monitoring of reactivity and extent of reaction of cinnamylidene acetic acid and cinnamic acid

The findings in literature gave reason to believe that the photo-activated dimerisation of cinnamic acid (CA) and its derivatives would be a good starting point for preparing a photo-active material. The dimerisation of CA is activated by irradiation with UV-light and since it is well-known that exposure to UV-light can be harmful it was important to get an idea about the needed exposure time. This would give an indication of how long the material should be exposed to UV-light before a significant change in material properties could be expected.

In the following Chapter, light will be shed on this issue from several angles in order to obtain a better fundamental knowledge of the dimerisation reaction. Two simple kinetic models for the dimerisation of CA-derivatives will be shown and evaluated, and the results from studies with Fourier transformed infrared spectroscopy (FTIR-spectroscopy) and ultraviolet-visible spectroscopy (UV-spectroscopy) will be presented.

3.1 Kinetic models for the dimerisation of cinnamylidene acetic acid

The present work is highly inspired by the work presented by Lendlein *et al.* [15] who reported an inter-penetrating network where the switching segment consisted of cinnamylidene acetic acid derivatised 4-armed star poly(ethylene glycol). The initial approach for the present work was to make a system very similar to the one presented by Lendlein *et al.* In this Section the focus is therefore put on the active group applied by these authors, namely cinnamylidene acetic acid (CAA). In Scheme 3.1 the molecular structure of CAA as well as the UV-activated dimerisation of the compound is shown. As Scheme 3.1 shows the photo-active group is attached to a polymer (R). For clarification, the system presented by Tanaka *et al.* [33], where R is a polyethylene chain, is prepared by esterification of a poly(vinyl alcohol). In other words the polymer contains polyethylene chains with pendant CAA-groups on every second C-atom. In this Section the results from two independent models will be presented. The Beer-Lambert law was used to get an overview of the system and a kinetic equation from Tanaka *et al.* [33] was used to develop a time-dependent model.

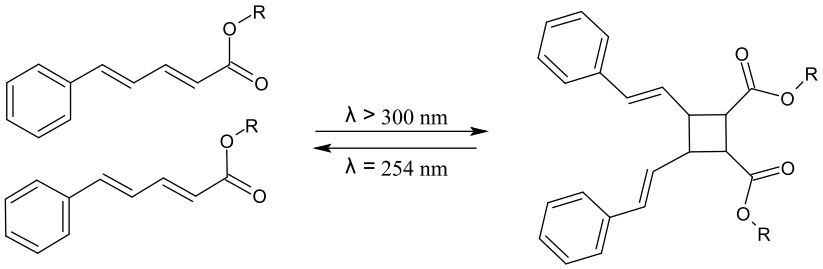

SCHEME 3.1: *Irradiation of compounds containing CAA-groups with UV-light will result in dimerisation of the CAA-group. The dimerisation can be reversed. R can be different groups, in the systems presented here it is either poly(ethylene glycol) [15] or polyethylene [33].*

3.1.1 The Beer-Lambert law

The Beer-Lambert law, Equation 3.1, is a simple and effective way of understanding how UV-light is absorbed in the medium through which it is travelling. It is assumed that no reflection or scattering of the incoming UV-light occurs.

$$A = -log\frac{I}{I_0} = \varepsilon lc \tag{3.1}$$

In Equation 3.1 A is the absorbance, I_0 is the intensity of the incoming light, I is the intensity of the light that passes through the sample and l is the thickness of the sample. ε is the extinction coefficient and c is the concentration, both related directly to the absorbing species (CAA). ε is a constant, for a given wavelength, and is specific for the absorbing compound and for CAA it has a value of 37390 L/(mol·cm) [35]. It is assumed that attaching CAA to a poly(ethylene glycol)-polymer does not influence the value for ε significantly.

A number of different situations were examined using Equation 3.1 by varying I/I_0, l and c. For a system like the one described by Lendlein *et al.* [15] Equation 3.1 very briefly showed that practically all UV-radiation would be absorbed in the first few micrometers of the material. This is an advantage in applications since practically all UV-light is absorbed into the material and thus no risk of harmful irradiation to substrates or the like is expected. The results also show that due to the very high ε-value, the change in the material will only take place in a very thin layer of the material. It is unlikely that a very stiff top layer of approx. 1 μm thickness will influence the overall properties of the materials as is the aim of the work presented here. It however may lead to bending as illustrated by Lendlein *et al.* [15]

The Beer-Lambert law showed that CAA absorbs a lot of UV-light. It is expected that the absorption of UV-light in the compound is closely related to the dimerisation reaction which then should occur rapidly and to a large extent. Using the Beer-Lambert law for this type of system is most probably not all-encompassing since the

law does not take a time-dependence into account. There must be a time-dependent change of both c and ε. Whenever two molecules dimerise the concentration of CAA is reduced. Furthermore, ε depends highly on the molecular structure of the absorbing compound which is altered after dimerisation occurs, see Scheme 3.1. ε for the CAA-dimer is expected to be different than for CAA. The combination of these factors gives a system where the situation changes significantly with time.

3.1.2 Time-dependent model

A literature survey showed that Tanaka *et al.* [33] had published a study dealing with the time-dependency of the dimerisation of two CAA-groups. The study showed that if the two CAA-groups were maintained in a pairing position in a rigid medium at 77 K the photo-dimerisation of the molecules would follow the first order kinetic equation:

$$ln(e^{2.303D} - 1) - ln(e^{2.303D_0} - 1) = -2.303\phi I_0 t \tag{3.2}$$

In Equation 3.2 D is the absorbance at time t while D_0 is the absorbance at zero time. ϕ is the quantum yield of the dimerisation reaction and I_0 is the intensity of the incoming UV-light. ϕ is a measure for how much reaction each incoming UV-photon will give. In this case ϕ is 0.5 [33] meaning that two photons are needed to make a dimerisation between two CAA-molecules. D is equal to the absorbance A and can be expressed as shown in Equation 3.3.

$$D = A = \varepsilon l c \tag{3.3}$$

In Equation 3.3 c is time-dependent, and will be denoted $c(t)$. For D_0 the concentration is the initial concentration c_0. ε is the molar absorptivity and l is the thickness of the sample. This gives the possibility of rewriting Equation 3.2 to Equation 3.4.

$$c(t) = \frac{1}{2.303\varepsilon l} ln(e^{c_1 - c_2 t} + 1) \tag{3.4}$$

$$c_1 = ln(e^{2.303\varepsilon l c_0} - 1)$$

$$c_2 = -2.303\phi I_0$$

In Table 3.1.2 the applied values for ε, l, c_0, I_0 and ϕ can be found. ε and ϕ have been found in literature [35, 33]. The value used for c_0 corresponds to 20 w% of the CAA-functional 4-armed star poly(ethylene glycol) which is the concentration used by Lendlein *et al.* [15] The value for l was set to 100 μm which correpsonds to the order of magnitude of the thickness of adhesive layers in commercial products. I_0 was

TABLE 3.1: *The parameters and values used in Figure 3.1 [33].*

Parameter	Value
ε	37390 L/(mol cm)[1]
l	100 µm (0.01 cm)
c_0	0.0743 mol/L
I_0	0.0012 W/cm^2
ϕ	0.55

[1] It is assumed that attaching CAA to a poly-(ethylene glycol)-polymer does not influence the value for ε significantly.

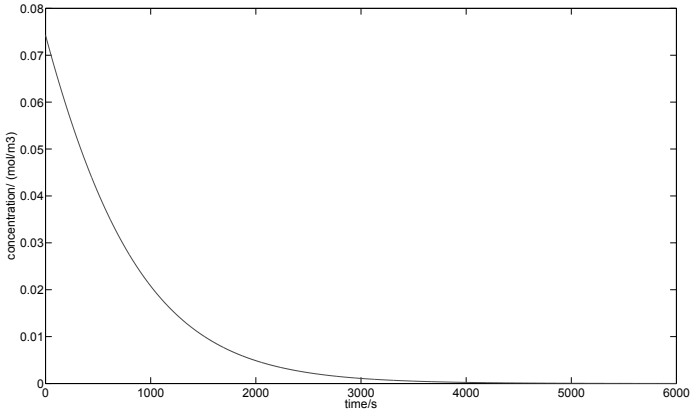

FIGURE 3.1: *The concentration, $c(t)$, of the photo-active CAA plotted as a function of time, t, for t between 0 and 6000 s. $c(t)$ decreases with t and after approx. 3600 s the reaction has run to completion.*

set to 0.0012 W/cm^2 which is the order of magnitude of the available UV-lamps. In Figure 3.1 a plot of *c(t)* can be seen. The plot shows that after 1 hour (3600 s) the conversion is practically 100 %. This value corresponds well with values reported in the literature, where an exposure time of 10 minutes to 1 hour [15, 35] is needed to obtain changes in the materials.

The model proposed by Tanaka *et al.* [33] is valid at 77 K which is significantly lower than the expected working temperature of the materials presented in this thesis. They should preferably function around room temperature. Larger exposure times could thus be needed to obtain full conversion since the higher temperature influence the relative position of the functional end groups. In the model the groups are kept in pairing position, this is not necessarily the case when the temperature is raised and position of the end groups is controlled by the diffusion of the polymers. This should

not be a problem since it is expected that the developed system can be optimized so the extent of reaction, exposure time, concentration of photo-active polymer and development of material properties will all come together.

3.2 Monitoring the reaction of cinnamylidene acetic acid and cinnamic acid with Fourier transformed infrared spectroscopy

FTIR-spectroscopy is well-known, easy to do and it would be a very convenient method to follow the dimerisation of the cinnamic acid (CA) and cinnamylidene acetic acid (CAA) groups on photo-active polymers. The dimerisation of CA, shown in Scheme 3.2, is very similar to the dimerisation of CAA, shown in Scheme 3.1.

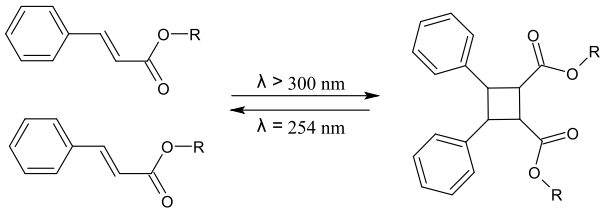

SCHEME 3.2: *Irradiation of compounds containing CA-groups with UV-light will result in dimerisation of the CA-group. The dimerisation can be reversed. R is a poly(ethylene glycol).*

Two photo-active polymers were prepared based on a 4-armed star poly(ethylene glycol) (M_n=2000 g/mol) (PEG-S2). The procedure for synthesising this compound is described in Chapter 4 and the details can be found in Appendices A.2 and A.4. The photo-active polymers were made by derivatising PEG-S2 with CAA (PEGCAA-S2) and CA (PEGCA-S2), respectively. In Figure 3.2 the structures of the photo-active polymers are shown. Upon irradiation with UV-light with the appropriate wavelength the photo-active groups will dimerise and the 4-armed polymers should form a network, see Figure 3.3.

The FTIR-spectra of PEGCAA-S2 and PEGCA-S2 before and after irradiation with UV-light were recorded to clarify if the dimerisation reaction could be monitored with this type of spectroscopy.

In Figure 3.4 the the FTIR-data obtained on PEGCAA-S2 before and after exposure to UV-light ($\lambda = 300 - 400$nm for 4 hours) can be seen. The data show that the treatment with UV-light gives rise to distinct changes in the region around 1900-1500 cm^{-1}. In this region the carbonyl-compounds are known to absorb strongly. Before irradiation three strong absorptions are observed at 1770, 1705 and 1616 cm^{-1} and after irradiation one strong band is observed in the region at 1722 cm^{-1}. The changes arise as a consequence of the break-up of the highly conjugated system of the carbonyl, the two double bonds and the benzene ring. The observed changes in the

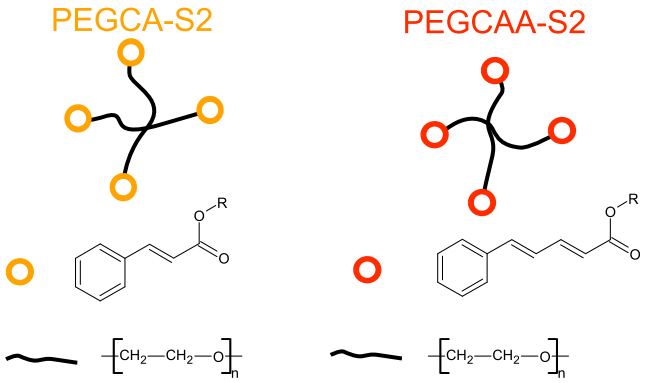

FIGURE 3.2: *The structures of the photo-active polymers PEGCA-S2 (left) and PEGCAA-S2 (right).*

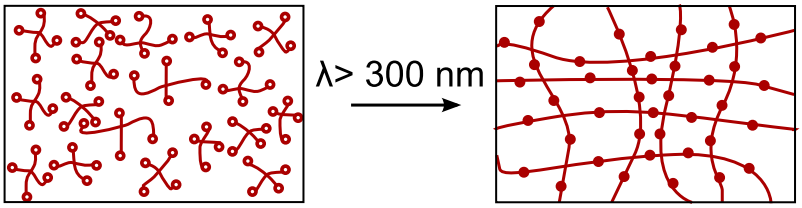

FIGURE 3.3: *The photo-active star-shaped molecules will form a network upon irradiation with UV-light. The photo-active groups are marked as open circles and the formed dimers are full circles.*

IR-spectrum are very pronounced making it clear that a reaction has occurred in the irradiated polymer.

In Figure 3.5 the FTIR-spectra of PEGCA-S2 before and after UV-irradiation for (λ =315-400 nm) for 1 hour are shown. Two strong absorption bands are observed prior to irradiation with UV-light. The two absorption bands show the stretches of the conjugated C=O in the ester (1716 cm^{-1}) and of the C=C (1636 cm^{-1}), respectively. It was expected that the break-up of the conjugation of the carbonyl groups would induce a very clear change in the region from approx. 1800-1500 cm^{-1} similar to the observations described above for CAA-derivatised PEG. This however proved not to be the case and only a small shift from 1709 cm^{-1} to 1716 cm^{-1} of the peak related to the carbonyl group in the ester was observed. The observed shift was discussed and it was concluded that the change was not sufficiently large to conclude regarding the extent of reaction. The presented IR-spectra of PEGCA-S2 before and after UV-irradiation show some other differences that deserve consideration. A change in the absorptions between approx. 3200-2400 cm^{-1} is observed and specifically the absorption at approx. 2500 cm^{-1} increases significantly after UV-irradiation. A

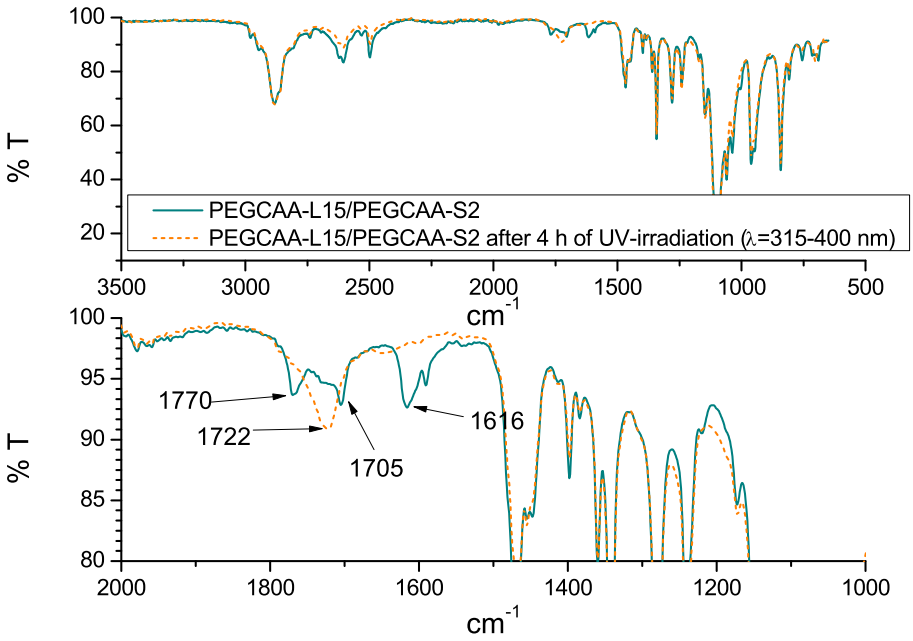

FIGURE 3.4: *The FTIR-spectrum of PEGCAA-S2 before (—) and after (- - -) irradiation with UV-light* $\lambda = 300 - 400$*nm) for 4 hours .*

possible explanation for the observed change is that this absorption arises due to the protons in the cyclo-butane formed when two CA-molecules dimerise. Another explanation could be that this absorption shows the *cis*-isomer of CA. The increase is very evident in the presented spectrum, but it is important to note that the change was not consistently present in all FTIR-spectra of PEGCA-S2 after UV-irradiation. It was therefore not possible to use this as a marker for the extent of reaction and it was not determined precisely why the difference appeared.

IR-spectroscopy is a very useful tool and as can be deduced from the previous section it is helpful in determining the presence of the photo-active CA and CAA-groups. However, as the discussion in this Section showed it is not the right tool to follow and quantify the extent of reaction for the dimerisation of CA. It should be possible to follow and quantify the dimerisation of CAA but this has not been done since it was beyond the scope of the project.

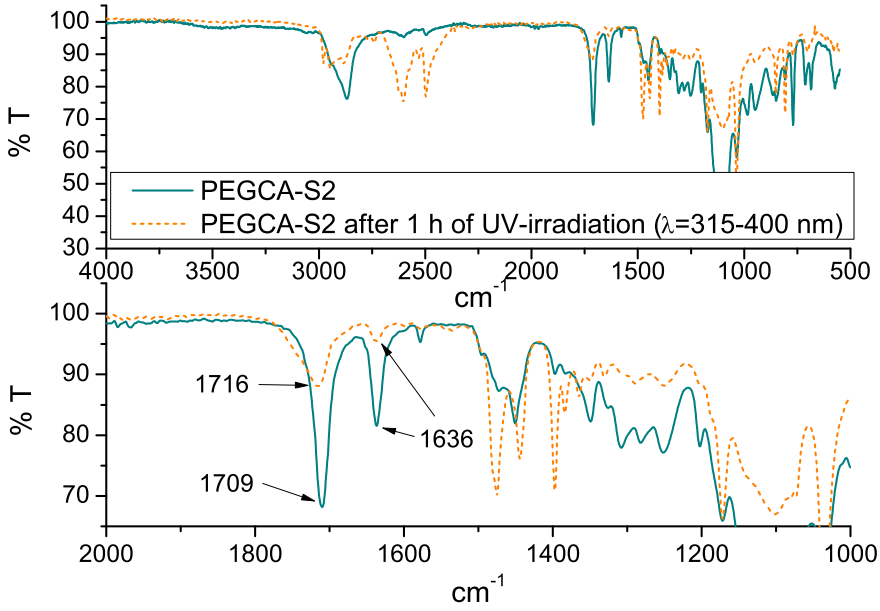

FIGURE 3.5: *The FTIR-spectrum of PEGCA-S2 before (—) and after (- - -) irradiation with UV-light (λ =315-400 nm) for 1 h.*

3.3 Monitoring the reaction of cinnamic acid with ultraviolet-visible spectroscopy

Ultraviolet-visible spectroscopy (UV-spectroscopy) is an obvious choice to use to follow the cross-linking of CA-derivatives since the break-up of the conjugated system is thought to decrease the absorbance of UV-light in the compound significantly. It is also well-known that the UV-absorbance spectrum is very sensitive to changes in the molecular structure of the absorbing species.

3.3.1 Cinnamic acid

Initially the cross-linking of CA was studied. It was expected that a tendency similar to the one predicted in Figure 3.6 would be observed. Figure 3.6 shows the expected development of the UV-absorbance spectrum of CA and not experimental data. In Figure 3.6 A a schematic drawing of the expected UV-absorbance spectrum of CA can be found. It is unclear whether CA is fully dissociated when it is purchased but to ensure full dissociation the compound could be treated with short wavelength UV-light ($\lambda = 254$ nm), see Figure 3.6 B. Upon irradiation with UV-light with $\lambda > 300$ nm the dimerisation of CA will occur and thus decrease the main absorption peak

dramatically, see Figure 3.6 C. Finally it is expected that the molecules will fully dissociate upon irradiation with short wavelength UV-light restoring the *trans*-CA-molecule, see Figure 3.6 D.

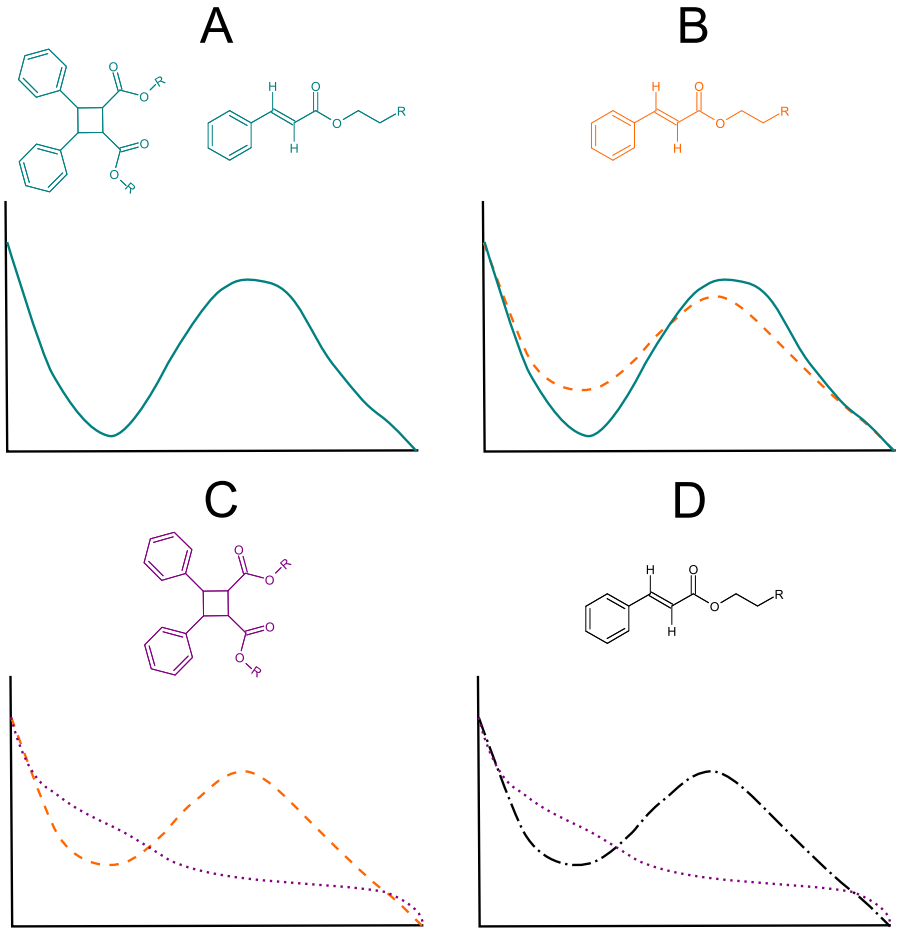

FIGURE 3.6: *Schematic representation of expected UV-traces. For CA the R-group is H. A) UV-absorbance spectrum of untreated CA. B) Irradiation with short wavelength UV-light ($\lambda = 254$ nm) ensures full dissociation to CA. C) Upon irradiation with UV-light with $\lambda > 300$ nm the dimerisation of CA occurs. The primary absorption peak decreases dramatically. D) CA is recovered by irradiation with short wavelength UV-light.*

This expectation was tested experimentally. The cross-linking reaction was followed by examining aqueous solutions of CA which had been irradiated with UV-light ($\lambda = 302$ nm) for up to 30 minutes with UV-absorbance spectroscopy. The concentration of CA was 0.365 mmol/L. Figure 3.7 shows that the primary absorption for

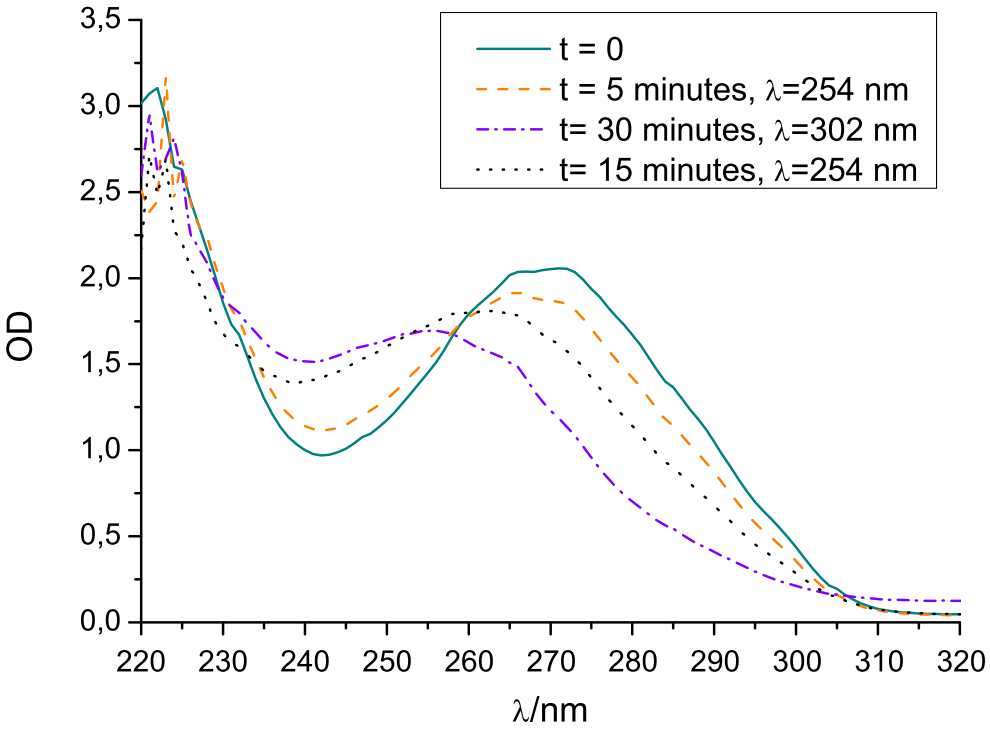

FIGURE 3.7: *Experimental UV-absorbance spectra of CA. (—) CA (aq) before UV-irradiation. The primary absorption is at 274 nm. (- - -) CA (aq) after irradiation with UV-light (λ = 254 nm) for 5 minutes. (– · –·) CA after irradiation with λ=302 nm UV-light for 30 minutes. (· · ·)CA after irradiation with λ = 254 nm for 15 minutes. The concentration of CA was 0.365 mmol/L.*

an untreated aqueous solution of CA is at 274 nm. Upon irradiation with UV-light ($\lambda = 254$ nm) for 5 minutes a small blue shift of the main peak occurs as expected and it is now at approx. 265 nm. Furthermore, the absorbance at the short wavelengths ($\lambda = 230-255$ nm) have inreased. After this step no CA-dimers should be present. As expected irradiation with UV-light (λ=302 nm) for 30 minutes results in significant changes in the spectrum as a consequence of the dimerisation of CA. The primary absorbance peak is blue shifted and the absorbance increases at low wavelengths. The main absorbance peak does not diminish as much as expected but a change is observed. Finally irradiation with $\lambda = 254$ nm again changes the spectrum, but the original spectrum is not fully recovered indicating that the reversible reaction and reformation of the CA-molecule are not completed.

The cross-linking of CA can be traced by following the reaction with UV-spectro-

scopy and a significant change is seen. It was observed that no further change in the UV-spectrum occurred after approximately 30 minutes of irradiation with UV-light for the dimerisation of CA (λ = 302 nm) while 5-10 minutes was enough for the dissociation (λ = 254 nm).

3.3.2 Cinnamic acid derivatised 4-armed star poly(ethylene glycol)

After examining CA a similar study was carried out on PEGCA-S2. The molecular structure of PEGCA-S2 is shown in Figure 3.2. It was expected that this study would give results very similar to those obtained on CA. Thin films of PEGCA-S2 (approx. 20 μm) were made and the UV-absorbance spectra of these were recorded before and after irradiation with UV-light. In Figure 3.8 the results are shown.

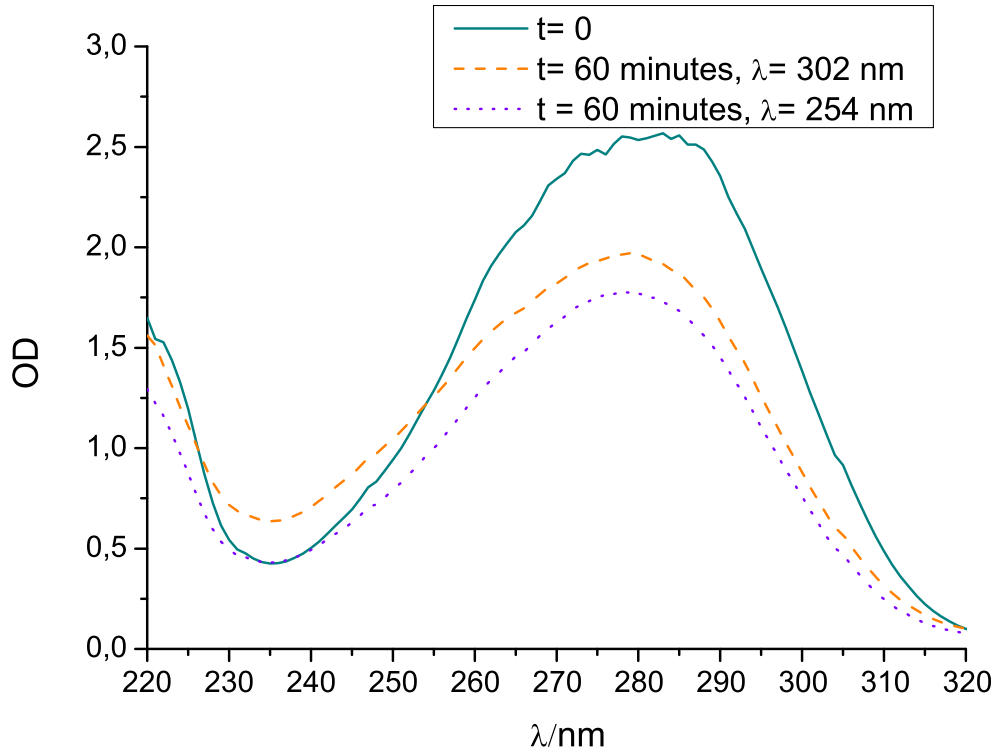

FIGURE 3.8: *UV-spectra of PEGCA-S2. (—) PEGCA-S2 before irradiation. (- - -) PEGCA-S2 after irradiation with UV-light (λ=302 nm) for 60 minutes. (···) PEGCA-S2 after irradiation with UV-light (λ =254 nm) for 60 minutes.*

The spectrum of PEGCA-S2 before irradiation is dominated by a main absorption peak at approx. 280 nm. After subjecting the film to irradiation with UV-light (λ = 302 nm) for 60 minutes the main peak is significantly decreased and the absorbance

at short wavelengths (λ = 230-240 nm) is increased. The observed changes were as expected and correlate well with the findings for CA. Finally irradiation of the film with UV-light of shorter wavelength (λ = 254 nm) resulted in a decrease in the absorption at λ = 230-240 nm and also a small decrease in the main peak. It was expected that the break-up of the dimerised CA-end groups would give an increase and a shift of the main peak, as was observed for CA. But it can easily be seen that this is not what the data show.

3.4 Conclusion

In this Chapter it was shown that the Beer-Lambert law and the time-dependent model based on Tanaka *et al.* could be used to describe the photo-reaction. The Beer-Lambert law gave results that indicated that the majority on the UV-light would be absorbed in the material and that the dimerisation of CAA would primarily take place in a very thin layer of the material. The Beer-Lambert law does not take the time-dependent changes in the material into account and is thus too limited to fully describe the system. A time-dependent kinetic model for the system was developed based on the model presented by Tanaka *et al.* [33] This model showed that full conversion to the dimer could be obtained in approx. 1 hour. It must be noted that the model presented by Tanaka *et al.* operates at low temperatures. The materials prepared in this thesis will be working around room temperature. It must therefore be expected that a larger exposure time could be needed to obtain full conversion. This should not be a problem since the properties of the system that will be prepared should be fine tuned for the application. Therefore, it is not necessarily needed to obtain full conversion to the dimer.

IR proved to be a useful tool in determining the presence of CA- and CAA-groups. It was observed that exposure to UV-light induced changes in the IR-spectra of both PEGCA-S2 and PEGCAA-S2. The change was most profound and stable for the polymer derivatised with CAA. It was not possible to follow the dimerisation of PEGCA-S2 with IR in the same way as for PEGCAA-S2. It was decided that IR could not be used to follow and quantify the extent of reaction for CA.

An extensive study of the UV-spectra of CA and PEGCA-S2 was carried out and it was observed that exposure to UV-light gave distinct changes in the UV-spectrum of both CA and PEGCA-S2. UV-spectra obtained on an aqueous solution of CA showed a significant change upon irradiation with UV-light. For the dimerisation of CA it was determined that after approx. 30 minutes of irradiation with UV-light (λ = 302 nm) no further changes were observed in the UV-spectrum. 5-10 minutes were enough for the dissociation (λ = 254 nm). A similar study of PEGCA-S2 also showed changes occurring in the IR-spectrum as a result of exposure to UV-light. For PEGCA-S2 it was observed that approx. 60 minutes of irradiation with UV-light (λ = 302 nm) was enough for the dimerisation. A change in the UV-spectrum after irradiation with UV-light (λ = 254 nm) was also observed.

Chapter 4

Cinnamylidene acetic acid and cinnaminc acid derivatised poly(ethylene glycol) as photo-active materials

As shown in Chapter 3 spectroscopic methods as well as two simple models showed that the timescale for the dimerisation of cinnamic acid (CA) and cinnamylidene acetic acid (CAA) was in the range of minutes to hours. This makes the reaction suitable for the applications outlined in Chapter 1 and the work with these photo-active compounds was proceeded.

The following chapter concerns the study of CAA and CA derivatised poly(ethylene glycol) (PEG) as photoactive materials. The preparation of the derivatised PEGs will be described along with studies of the rheological properties of the material before and after exposure to UV-light.

It was decided to focus on CA-derivatised PEG rather than CAA-derivatised PEG due to economical and experimental considerations. This choice will be discussed in details.

Sections 4.3.1 to 4.3.3 have been prepared for publication, see Appendix D.2, and is currently under review.

4.1 General introduction to network and rheology terms

Throughout the following Chapters a couple of network and rheology terms will be used, namely namely G', G'' and r. The terms will be briefly presented in this Section.

The networks were made by end-linking polymer chains with a cross-linker. During the process of cross-linking the material changes from consisting of a large number of individual and finite polymer chains into, in theory, one large infinite molecule [70]. This transition is denoted the gel point.

In order to control the samples it is useful to apply the stoichiometric imbalance, r. r expresses the relationship between the functional groups. For a general cross-linking between a f_p-functional polymer, P, and a f_x-functional cross-liker, X, r is defined as the molar ratio between the cross-linking groups, $f_x[X]$, and the end groups on the polymer chains, $f_p[P]$.

$$r = \frac{f_x[X]}{f_p[P]} \tag{4.1}$$

For $r < 1$, there is excess of the polymer chains, and some chains will not be part of the cross-linking process. For $r > 1$ there is excess cross-linker and all polymer chains should be linked to a cross-linker molecule.

The value of r greatly influence the network. In general the higher r is the stronger and more stable the formed network will be. However, r needs to be within the gelation regime.

The prepared materials will be investigated by linear rheology which is one way to understand the formed network better. In general the networks will be characterised by the storage and loss moduli, G' and G'', respectively. Very briefly G' is related to the elastic part of the network while G'' is related to the viscous part. The elastic part will store energy upon deformation and this energy can be regained when the deformation is released. The energy used to deform the viscous part of the network will simply dissipate.

4.2 Cinnamylidene acetic acid derivatised poly(ethylene glycol) as a photo-active material

In this section the work carried out with CAA-derivatised PEG will be presented.

4.2.1 Preparation and initial studies of cinnamylidene acetic acid derivatised poly(ethylene glycol)

PEG-polymers derivatised with CAA were prepared via the synthetic route used by Lendlein *et al.*[15] and Andreopoulos *et al.*[35]. The synthesis is shown in Scheme 4.1, for details see Appendix A.2. A long linear PEG (M_n=15000 g/mol) (PEG-L15) and a 4-armed star PEG (M_n=2000 g/mol) (PEG-S2) were derivatised with CAA resulting in a long linear CAA-derivatised PEG (PEGCAA-L15) and a CAA-derivatised 4-armed star PEG (PEGCAA-S2). In Figure 4.1 the structure of the polymers are shown.

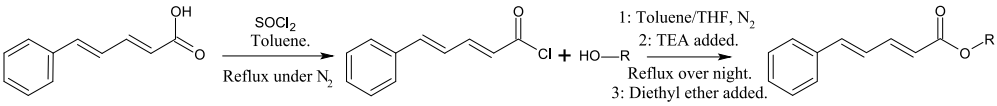

SCHEME 4.1: *The preparation of PEGCAA. R-OH denotes the chosen polymer.*

A thin film (app. 100 μm) of a mixture of PEGCAA-L15 and PEGCAA-S2 (10 w% PEGCAA-S2) was made and irradiated with UV-light ($\lambda = 300-400$ nm for 4 hours). It was assumed that PEGCAA-S2 would act as a cross-linker and that PEGCAA-L15 would be the spacer between the cross-linking points, as shown in Figure 4.2. The reason for using end-group functionalised polymers was that this would allow usage of network theory on the formed networks. As described in Chapter 3 the IR-spectra

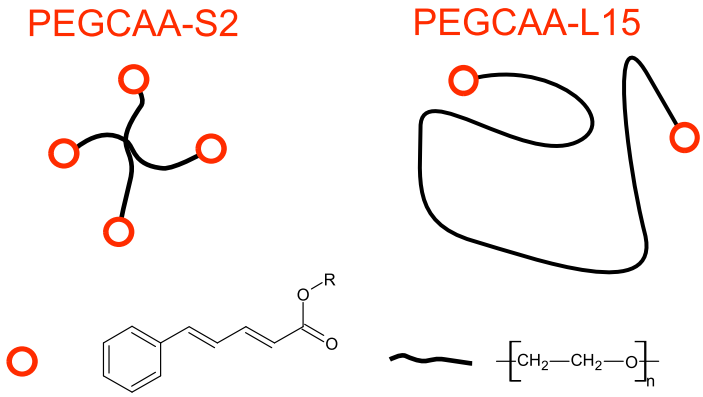

FIGURE 4.1: *The structure of PEGCAA-S2 and PEGCAA-L15.*

of PEGCAA-S2 before and after irradiation with UV-light showed a distinct change related to the formation of the CAA-dimer. The spectroscopically confirmed change in the material could also be observed on the macroscopic scale. The film was placed on a poly(ethylene)-backing, irradiated and afterward submerged in water. In Figure 4.3 a schematic drawing of the film can be seen. It was observed that the pristine film disintegrated quickly into a hygroscopic powder while the irradiated film behaved very differently in the water; threads/fibres were formed slowly and over time the film completely dissolved. This underlined that a reaction had indeed taken place in the material.

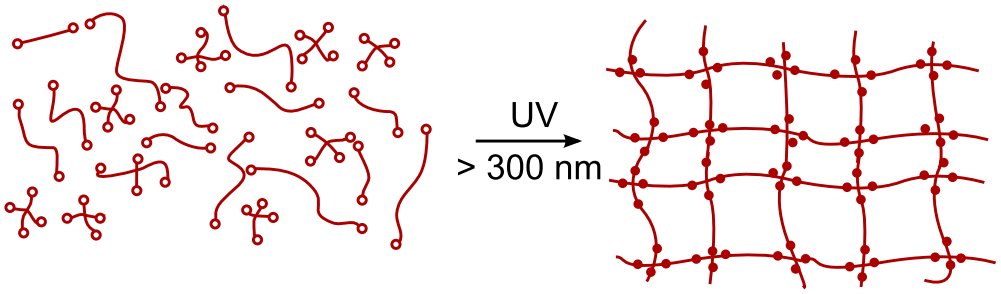

FIGURE 4.2: *A mixture of PEGCAA-S2 and PEGCAA-L15 forms a network upon irradiation with UV-light.*

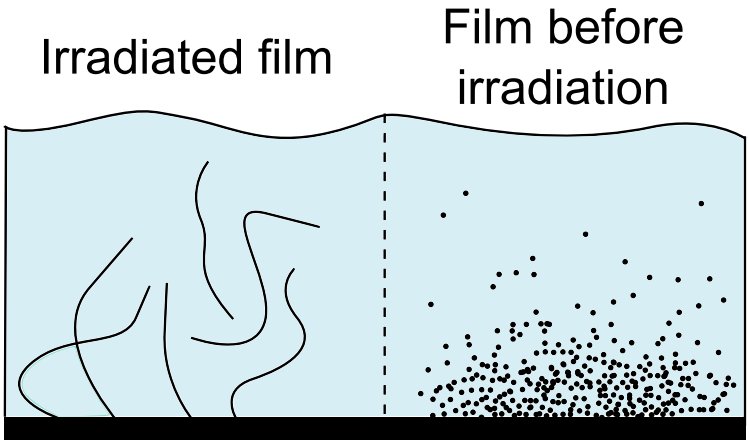

FIGURE 4.3: *Schematic drawing of (PEGCAA-L15/PEGCAA-S2)-film submerged in water. A piece of PEGCAA-L15/PEGCAA-S2 film of PE backing was exposed to UV-light ($\lambda = 300 - 400$ nm for 4 hours). The exposed film acted very differently from the unexposed film when submerged in water. Right) The unexposed film rapidly dissolved into a hygroscopic powder. Left) The irradiated film formed threads/fibres visible to the naked eye and slowly dissolved.*

4.2.2 Synthesis of cinnamylidene acetic acid

For the derivatisation of PEG with CAA a large excess of CAA was needed (100 times) and still the yields were low ($7 - 47\%$). The CAA is quite costly to buy[1] which gave concerns regarding the overall price for a resulting material in case of commercialisation. It was therefore attempted to synthesise CAA in house by using the Knoevenagel reaction, as shown in Scheme 4.2. The Knoevenagel reaction is an aldol reaction that takes place in two steps; first the aldol step where a stable delocalized anion, formed on the malonic acid after addition of base, reacts with cinnamic acid. This step is followed by a decarboxylation and the *E*-diene (CAA) is formed [71]. The reaction was carried out as described by Venkatasamy [72] and synthetic details can be found in Appendix A.3. The reaction were performed a number of times but the product yield remained low and therefore it was decided to pursue other possibilities.

4.2.3 Changing the photo-active group

After working with CAA and conducting the mentioned experiments it became clear that continuing to focus on this photo-active group would be problematic. Especially the cost combined with the large excess needed in the derivatisation of the polymer

[1] In 2009 the price was 185 £ for 25 g CAA when purchased from Apollo Scientific, UK.

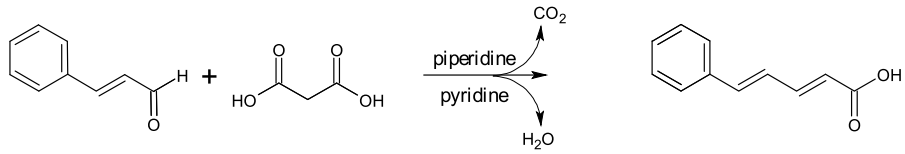

SCHEME 4.2: *The Knoevenagel reaction between cinnamaldehyde and malonic acid.*

became a concern. A possible application of the resulting material would be very expensive and the majority of the price would be due to the photo-active compound.

Looking into the literature on the field showed that many groups reported studies on cinnamic acid (CA) [73, 74, 75, 76] in polymer systems similar to the one described in this section and to the system presented by Lendlein *et al.*[15]. In fact the graft polymer presented by Lendlein *et al.* also has cinnamic acid functional groups. It was therefore decided to continue the work with cinnamic acid.

4.3 Cinnamic acid derivatised poly(ethylene glycol) as a photo-active material

In this section the work done on CA-derivatised PEG will be presented.

4.3.1 Preparation and analysis of cinnamic acid derivatised poly(ethylene glycol)

Three different CA-derivatised PEG-polymers were prepared by *N,N'*-dicyclohexylcarbodiimide/4-dimethylaminopyridine (DCC/DMAP) mediated esterification of commercially available PEG-polymers, see Scheme 4.3. To the best of our knowledge this is the first report of applying this classic esterification route to producing cinnamic acid derivatised PEG. Synthetic details can be found in Appendix A.4. The structure and M_n for the derivatised PEGs are shown in Figure 4.4 and summarised in Table 4.1.

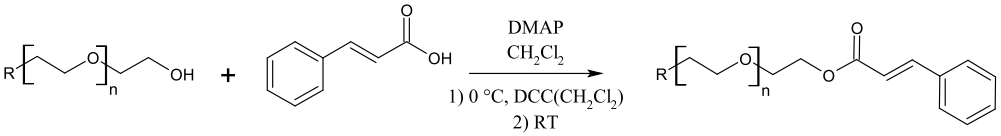

SCHEME 4.3: *Derivatisation of PEG-polymers with CA was carried out with DCC/-DMAP-mediated esterification.*

The structure was confirmed by NMR, SEC and IR. In Figure 4.5 the NMR-spectrum of PEG-S2 and PEGCA-S2 can be found. The differences in the spectra are primarily observed in the regions 3.5-4.5 ppm and 6.0-8.0 ppm. The pattern observed at 6.0-8.0 ppm for PEGCA-S2 shows the characteristic pattern for CA: The

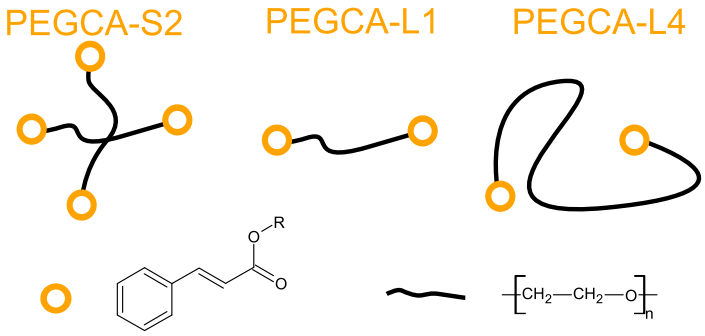

FIGURE 4.4: *The structure of PEGCA-S2, PEGCA-L1 and PEGCA-L4.*

TABLE 4.1: *The CA-derivatised PEG-polymers used in the initial experiments.*

ID	Molecular structure of PEG	M_n g/mol
PEGCA-L1	Linear	1000
PEGCA-L4	Linear	4000
PEGCA-S2	4-arm star	2000

multiplets at 7.51 and 7.37 ppm occur due to the protons on the benzene ring and the doublets at 7.69 and 6.46 shows the vinyl protons in *trans*-position. The *trans*-position is verified by the value for the coupling constant J, which is 16 Hz. The attachment of the CA-group to the polymer is confirmed by the occurrence of the two multiplets at 4.35 and 3.76 ppm. These multiplets arise due to the protons in the first ethylene glycol group on the polymer chain, namely protons H_8 and H_9 in Figure 4.5. The chemical shift for these protons is shifted upfield and can thus be distinguished from the rest of the protons on the polymer chain.

In Figure 4.6 SEC-traces of PEG-S2 and PEGCA-S2 are shown. SEC is often used to estimate the molecular weight of polymers, but the used multi-detector setup of the used SEC enables coupling of M_n-data with e.g. data from UV-absorption spectroscopy. This is very useful for the conducted work since the attachment of an end group to a polymer will not alter the overall M_n to a large extent since the chain lengths are maintained. The used SEC-setup is connected to a UV-detector which can track the UV-active CA-group. In Figure 4.6 the refractive index (RI) and the UV-trace is plotted for PEG-S2 and PEGCA-S2. For PEG-S2 a strong peak is seen at a retention time of 17 mL. For PEGCA-S2 a strong UV-absorption peak at a retention time of 15 mL is observed. The RI-data for PEGCA-S2 also show a strong peak at 15 mL proving that the UV-response is from the polymer. This proves that CA is in fact chemically bound to the PEG-polymer. In case there were free CA-molecules in the sample the low molecular weight of these would assure separation from the polymers

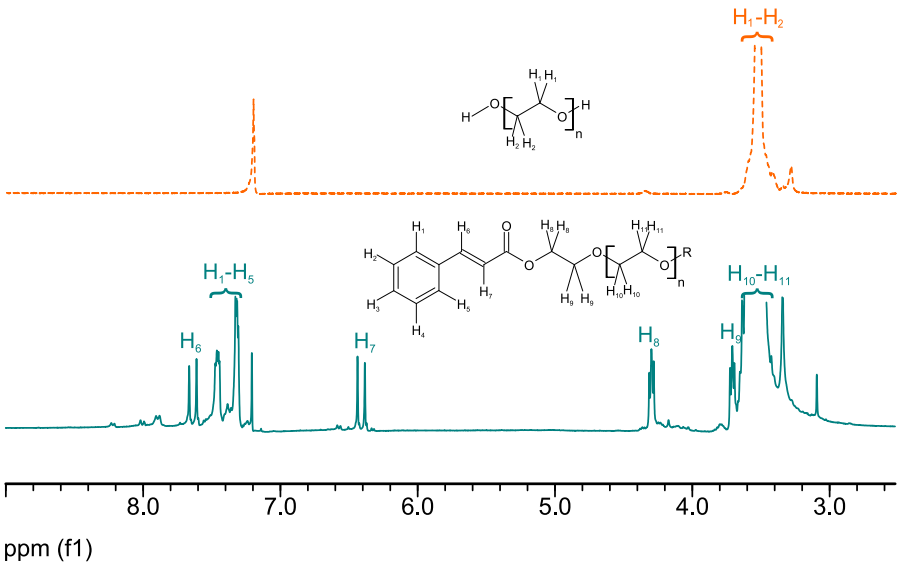

FIGURE 4.5: ^{1}*H-NMR of PEG-S2 (- - -) and PEGCA-S2 (—).*

after passing the SEC-column. The small shift in retention time from PEG-S2 to PEGCA-S2 is due to the increase in molecular weight.

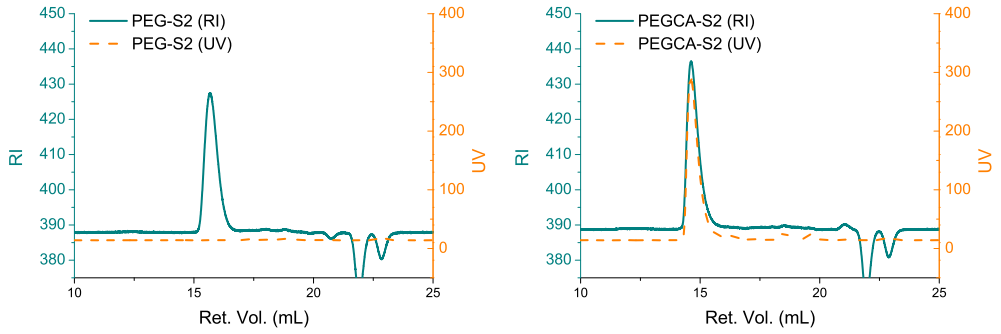

FIGURE 4.6: *SEC-traces of PEG-S2 (left) and PEGCA-S2 (right). Refractive index (RI) (—) and UV-trace (- - -) are shown.*

The IR-spectrum of PEGCA-S2 is presented in Chapter 3. The attachment of CA can be verified with IR by observing the disappearance of the peak from the OH-end group on the PEG-polymer.

4.3.2 Investigation of cinnamic acid derivatised poly(ethylene glycol) as a stimuli-responsive material

Three stimuli-responsive materials, **A**, **B** and **C**, were made by mixing PEGCA-S2, PEGCA-L1 and PEGCA-L4 in different ratios, see Table 4.2 for details. The molar ratio between active groups on PEGCA-S2 and on PEGCA-L1 and PEGCA-L4, respectively, is kept constant in all samples (χ(relationship between end groups)≈ 1). Irradiating the sample with UV-light will form a four functional network similar to the one shown earlier for CAA-derivatised polymers, see Figure 4.2.

TABLE 4.2: *Composition of the stimuli-responsive materials; **A**, **B** and **C**.*

Sample	PEGCA-S2 (M_n=2520 g/mole)	PEGCA-L1/g (M_n=1260 g/mole)	PEGCA-L4/g (M_n=4260 g/mole)
A	100 %	-	-
B	50 %	50 %	-
C	23 %	-	77%

The change in rheological properties (storage modulus, G', and the loss modulus, G'') of the stimuli-responsive materials (**A**, **B** and **C**) after UV-irradiation ($\lambda = 315 - 400$ nm) for one hour was investigated. The results are shown in Figure 4.7.

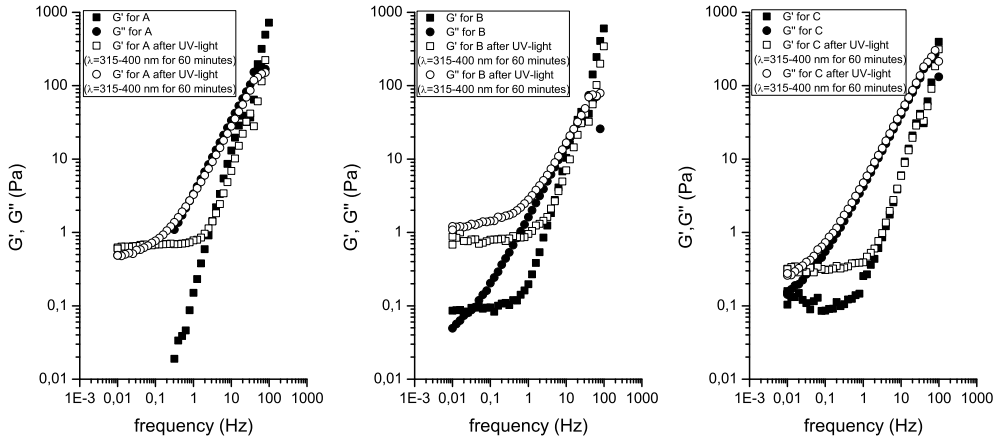

FIGURE 4.7: *Rheological properties of **A**, **B** and **C** before (full symbols) and after (open symbols) irradiation with UV-light for 1 hour (λ=315-400 nm). The measurements were carried out at 50°C with a strain value of 10 %.*

All data sets showed terminal relaxation before irradiation with UV-light indicating that the materials are liquids. The terminal relaxation is seen at frequencies (ν) below 50 Hz, where $G' > G''$ and G'' is proportional to ν and G' is proportional to ν^2. For sample **B** and **C** a plateau was observed for G' at low frequencies. This was

ascribed to the detection limit of the rheometer. After irradiation all data sets showed a plateau at low frequencies. For **A** the observed elastic modulus is low ($G_0 \approx 0.8$ Pa) but the presence of the plateau still clearly shows that a significant change in material properties has taken place. Similarly $G_0 \approx 0.8$ Pa for **B** and $G_0 \approx 0.3$ Pa for **C**. All samples show changes in rheological properties after irradiation with UV-light, but the change is most pronounced for **A**.

It is expected that this observation is closely connected to the concentration of the photo-active CA-group (sample **A** and **B**: 1.59 mol CA/g sample; sample **C**: 0.727 mol CA/g sample) and the structure of the network formed. The concentration of CA-groups in **C** is significantly smaller than in **A** and **B**. For the reaction between two CA-groups to happen it is needed that the CA-groups are in close proximity and when the concentration is lowered the possibility for one CA-group to encounter another CA-group is decreased. The difference between **A** and **B** is not explained by this, since the concentration of CA-groups is the same in both materials. It is expected that the differences between these materials occur because the distance between the cross-linking points is shorter in **A** than in **B** forming a stronger network and thus inducing a bigger change in rheological properties.

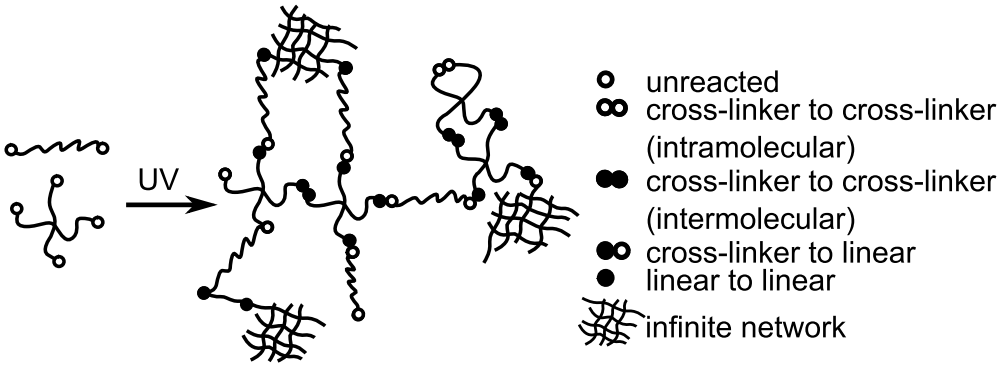

FIGURE 4.8: *Schematic representation of the structures formed during network formation between PEGCA-S2 (star, cross-linker) and PEGCA-L1/PEGCA-L4 (linear chain). The CA-groups react with each other either star to star (intramolecular), star to star (intermolecular), star to linear or linear to linear. There is also a possibility for that the group remains unreacted. Star-star-reactions give the possibility of loop formation, star-linear reaction gives the desired network structure while linear-linear combinations act as chain extenders.*

It was assumed that PEGCA-S2 would act as a cross-linker for the linear polymers (PEGCA-L1 and PEGCA-L4) in **B** and **C**, this is, however, not fully comprehensive. This would require that the reaction between the active groups on the cross-linker and on the linear chain should be very specific compared to reactions occurring *cross-linker to cross-linker* or *linear chain to linear chain*. This is not the case for the dimerisation

of CA where any two CA-groups in close proximity should be able to cross-link. For the described system PEGCA-S2 could be regarded as a branched structure capable of creating complex branched structures. Figure 4.8 shows a drawing of the possible structures formed in the described system. Ideally all reactions would occur *cross-linker* to *linear chain* and form a network where each cross-linking point is connected to four chains, as seen in Figure 4.9. However when the cross-linkers as well as the linear chains can react as well as several other possibilities for resulting structures are present. Inter- and intramolecular cross-linking of the active groups on the cross-linker can form loops in the network. And the coupling of the linear chains will make longer chains and possibly increase the distance between the cross-linking points.

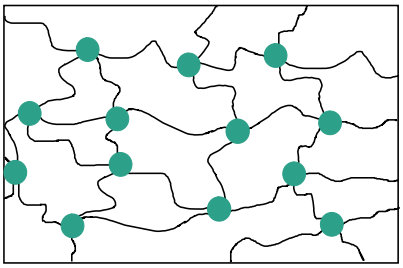

FIGURE 4.9: *Ideal structure of a network formed with a four functional cross-linker and end-functional linear polymer chains.*

4.3.3 Time-dependence of network properties

The data presented in the previous section showed that the sample consisting solely of PEGCA-S2 gave the most profound change in rheological properties after irradiation with UV-light for one hour. Based on this result it was decided to continue the work with this material. A time-dependence study was carried out with samples consisting solely of PEGCA-S2. The development of the mechanical properties of this material is very dependent on the irradiation time and this was studied closely.

A number of samples consisting only of PEGCA-S2 were made and irradiated with UV-light for 0, 1, 2, 4, 8, 10, 15, 24, 31, 50, 65, 80, 95 and 120 hours ($\lambda = 315 - 400$ nm, $I = 2.36 - 4.70$ mW/cm^2, $d = 2$ cm, T=60°)C. Rheological data were collected for all the irradiated samples and in Figure 4.10 a plot of G' and G'' at 0.01, 1 and 10 Hz as a function of the irradiation time (t) is shown.

The data in Figure 4.10 show the structural development of a network which is normally observed during network formation (curing). At low times the curve is steep because the limiting factor here is the collision of the relatively free-moving polymer chains not yet hindered by the network. After approx. 15 hours of irradiation the gel point is observed ($G' > G''$). At longer timescales the curve flattens out because the limiting factor at this point is the spatial orientation of the active groups. If the

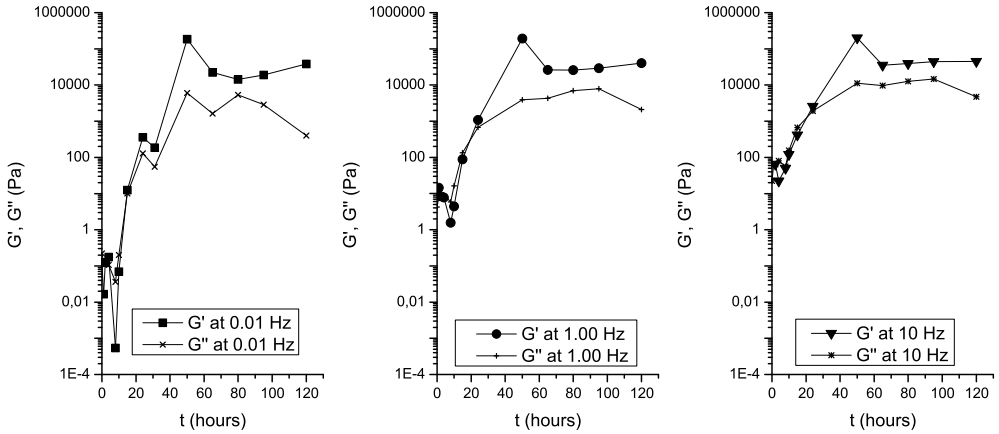

FIGURE 4.10: *Development of G' and G'' over time. The plot shows G' and G'' at ν=0.01, 1.00 and 10 Hz for the PEGCA-S2-samples as a function of the UV-irradiation time (t). The gel point is observed at approx. 15 h irradiation time, where $G' > G''$. After approx. 70 hours a plateau is reached at approx. 0.01 MPa.*

active groups are far from each other and the network is reacted to an extent where the flexibility has decreased significantly the likelihood of remaining active groups to get in close proximity and react is low.

The time-dependence of the reaction could also be observed simply by looking at the differences between the samples. In Figure 4.11 photographs of the material before and after UV-irradiation are shown. For short irradiation times the samples are liquids, while for long irradiation times (more than 24 hours) they are solid films. It was observed that the sample which was irradiated for 120 hours was brittle and broke very easily. A plateau is reached with $G' \approx 35000$ Pa and $G' \approx 10000$ Pa after approx. 70 hours and at larger timescales no profound change is expected.

4.3.4 Reversibility

The scope of the project was to develop a material where bulk changes could be achieved rapidly in a solid material. The primary focus was the cross-linking reaction of CA and by using a UV-lamp with wavelengths above 315 nm it was ensured that the cross-linking reaction is favoured. The results presented show that bulk changes are possible and that irradiation with UV-light induced detectable macroscopic changes in the samples, see Figure 4.11. However, a long exposure time proved to be needed and therefore the samples presented in this study have been subjected to a large amount of UV-radiation. For commercial products such as paints the UV-radiation from the sun can give unwanted reactions. The long exposure times combined with the knowledge that UV-radiation can cause damages led to a discussion of whether it

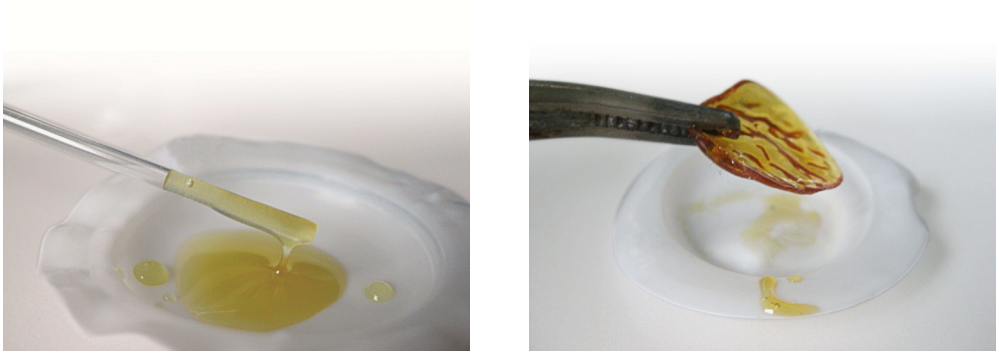

FIGURE 4.11: *Left) Photograph of sample prior to UV-irradiation. Right) Photograph of sample after 90 h of UV-irradiation ($\lambda = 365$ nm).*

was certain that the reaction that was happening was in fact the dimerisation of CA. Research groups applying the dimerisation of CA in materials use irradiation times of approx. 30 minutes to two hours [15, 77, 75, 78, 79, 74] to obtain traceable changes. Which is significantly less than used here.

A qualitative test was done to get a deeper understanding of the problem. The conducted control experiment showed that the PEG-S2 did not cross-link upon UV-irradiation for up to 96 h at 60°C. Furthermore, it was determined that PEGCA-S2 did not spontaneously cross-link after being heated to 60°C for up to 96 h. This verifies that it is the combination of derivatisation with CA and irradiation with UV-light that induce the changes in the material.

The reversibility of the reaction was tested qualitatively by placing a piece of the film that had been subjected to irradiation with UV-light for 120 hours under a UV-lamp with a wavelength of 254 nm. This wavelength should force the reaction backwards and therefore disintegration of the film should occur. However, up to 79 hours of UV-irradiation ($\lambda = 254$ nm) gave no visible change in the film. Furthermore, it was observed that the film did not swell or dissolve when placed in neither water nor acetone. Another sample of PEGCA-S2 irradiated for 120 hour ($\lambda = 315 - 400$ nm) was immersed in water and irradiated with UV-light ($\lambda = 254$ nm). This treatment did not result in dissolution of the film upon irradiation with shorter wavelength UV-light ($\lambda = 254$ nm).

4.3.5 Reproducibility

The presented study shows some clear tendencies toward that a high concentration of the photo-active group combined with long UV-irradiation times gives the best results. And an important point in this is also that problems occurred when attempting to reproduce the data obtained after one hour of UV-irradiation, described in Section 4.3.2. The experiment was repeated several times with various results, but the presen-

ted data were only obtained once and the changes, if any, were significantly smaller in the other experiments. The experiment was also carried out by different people which did not improve the reproducibility. The time-dependence study was repeated as well and here it was found that the reproducibility was significantly better.

As Figure 4.10 shows the data for the first approx. 15 hours of irradiation show no clear tendency. The data at 0.01 Hz show no profound change in the first 15 hours. The data at 1.00 Hz for the first 15 hours also show little change and in fact a slight decrease of G' and G'' is observed. At 10 Hz a small increase is seen in the first 15 hours. This could indicate that it takes some time before the cross-linking reaction is occurring. The reason for this could be the spatial orientation of the groups, as discussed earlier.

The results from this study exhibit issues regarding the expected reversibility of the reaction and the reproducibility of the data. Despite of this it was decided to continue the work with the system since we were convinced that the majority of these issues would be resolved upon development of an inter-penetrating network (IPN) system. As will be discussed in Chapter 5 it is expected that the photo-active polymers will act as a solvent inside the permanent network when the IPN-system is prepared. This will give a very different type of material which is expected to be more sensitive to the changes in the structure of the polymers induced by the dimerisation reaction.

4.4 Conclusion

CAA-derivatised PEG-polymers of different structures were successfully prepared. It was found that irradiating a thin film consisting of a mixture of the linear and the star shaped CAA-derivatised polymers resulted in a material that behaved differently when submerged in water than prior to irradiation. This confirmed that a reaction was taking place in the polymer, just as expected from the findings reported in Chapter 3. Large amounts of the relatively expensive CAA was needed in the preparation of the photo-active polymers and this gave a concern regarding the overall cost of the resulting material in case of commercialisation. CAA was synthesised in house with low yields. It was therefore decided to focus on cinnamic acid derivatised polymers instead.

Preparation of PEGCAs were conducted by DCC-esterification of a number of PEG-polymers. The attachment of CA to the PEG-chain was verified by NMR, SEC and IR.

Stimuli-responsive materials with different concentration of CA-groups and different molecular structures of the PEG-polymers were made and investigated with rheology before and after irradiation with UV-light for one hour. It was found that the sample consisting solely of PEGCA-S2 gave the most pronounced change after one hour of UV-irradiation wherefore it was decided to continue the work with this type of material.

A thorough investigation of the time-dependency of the reaction was conducted. The development of the network structure and thus the rheological properties of the material were found to depend heavily on the UV-irradiation time as expected. After approx. 24 hours of exposure to UV-light the material forms a solid film and after approx. 70 hours the values for G' and G'' reach a plateau at 35000 Pa and 10000 Pa, respectively.

A number of problems were experienced namely difficulties with ensuring full reproducibility of the data as well as loss of the reversible nature after long exposure times.

Since it was not possible to follow the cross-linking reaction with conventional spectroscopy, as discussed earlier, the extent the reaction was unclear. The data presented in this section do not give the exact extent of reaction but it shows that the development of the network takes a long time.

Chapter 5

Inter-penetrating network materials based on poly(ethylene glycol)

A study of samples consisting solely of cinnamic acid or cinnamylidene acetic acid derivatised polymers showed that exposure times larger than those predicted by the physical model as well as by the times predicted spectroscopically was needed to obtain a significant change in rheological properties of the material. It was expected that this issue would be resolved by preparing an inter-penetrating network (IPN).

The IPNs prepared here will consist of a permanent cross-linked poly(ethylene glycol) matrix and a switching segment made up of UV-active polymers. This creates a material that has two states;

1. Permanent cross-linked polymer polymer matrix in which (short) UV-active polymer chains are distributed.
2. IPN-material occurring after irradiation and cross-linking of the UV-active polymer chains.

In the first state the distributed UV-active polymer chains should act as a solvent in the network, if the chain length of the polymers is short. The material properties of a network with a solvent inside are often significantly different from the properties of the network itself. This effect arises since the solvent allows the chains to move more freely making the dynamics of the overall network faster. When the UV-active polymers are cross-linked this solvent effect should rapidly be removed and making a significantly stiffer material.

In this Chapter the work dealing with IPN-materials based on PEG will be presented. The preparation procedures will be reviewed and the results from a study of the UV-spectra of IPN-films containing UV-active polymers will be presented. Finally the material properties of the IPN-materials where both the permanent matrix and the switching segment consist of PEG-polymers will discussed.

5.1 Introduction to inter-penetrating networks

Inter-penetrating polymer networks (IPNs) are a group of materials where two or more polymer networks coexist. The polymer networks are interlaced on the molecular level but there are no covalent linkage between them. In Figure 5.1 a drawing of an IPN of two networks is shown.

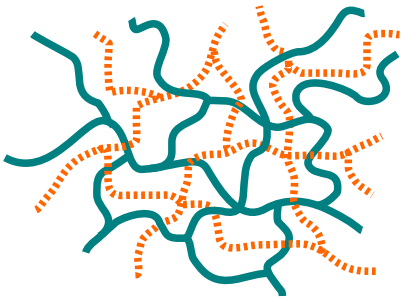

FIGURE 5.1: *An IPN made up of two polymer networks. The networks are interlaced and cannot be separated but no covalent links are formed between the two networks.*

There are several types of IPNs; sequential IPNs, latex IPNs, simultaneous IPNs, gradient IPNs, thermoplastic IPNs and semi-IPNs. Each type is defined by the preparation method and/or the resulting material. Sequential IPNs are made by cross-linking the first network and then immersing this in the liquid monomer of the second network. The liquid monomer diffuses into the cross-linked network and is afterward cross-linked *in situ*. In latex-IPNs the polymers are made as latexes, i.e. suspensions of polymers in water [80]. Each latex-particle contributes with a micro-IPN and by fusing and cross-linking the particles simultaneously the IPN develops. Simultaneous IPNs are produced by mixing the monomers and/or prepolymers with cross-linking agents followed by simultaneous polymerisation and cross-linking via independent reactions. In gradient IPNs the cross-link density varies across the material. Gradient IPNs can be prepared similarly to sequential IPNs but the second monomer is not allowed to fully dissociate into the first cross-linked network. This way materials with e.g. one polymer predominantly on the surface and another in the bulk can be made. Thermoplastic IPNs contains physical cross-links rather than chemical in both polymers and behave like a thermoplastic by flowing at elevated temperatures. Semi-IPNs are systems where a linear or branched polymer is mixed into a cross-linked network [81, 82, 83]. The linear or branched polymers need to form a physical network for the system to be a true semi-IPN but is nevertheless often referred to as semi-IPNs without the physical interactions.

In the work presented here we will prepare permanent cross-linked network into which a secondary (branched) photo-active polymer is mixed and cross-link them with UV-light to form IPNs. The photo-active polymers will be referred to as the switching segment. Upon irradiation with UV-light the switching segment will cross-link and change the material significantly. In Figure 5.2 the transition from network mixed with the switching segment to IPN is shown schematically.

Most often IPNs consist of two different polymers, but in this thesis the term IPN will be used interchangeably for both IPNs consisting of a system with different

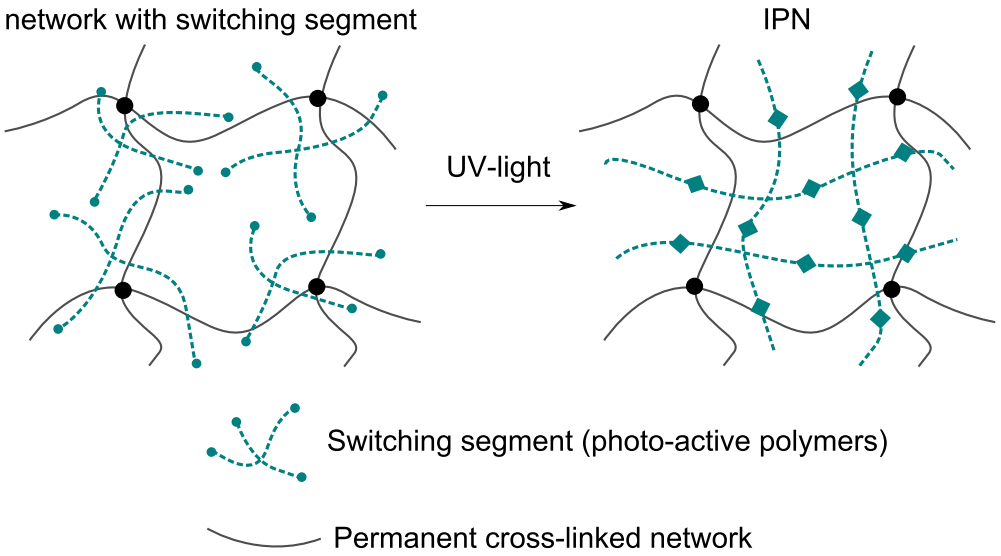

FIGURE 5.2: *A material where the permanent network (—) is mixed with a photo-active switching segment of branched polymers (- - -) is prepared. The switching segment cross-links upon irradiation with UV-light and forms an IPN.*

polymers in the permanent network and the switching segment as well as for systems where both permanent network and switching segment consist of the same polymer.

In this project rheology has been used as a characterisation method to evaluate the networks and to determine whether or not a change in network properties was observed when the IPN was formed.

In Figure 5.3 a schematic representation of the expected development of the rheological properties for the different types of materials is shown. First the permanent network is shown where it is expected that G' governs the material properties since an elastic network is present. When the switching segment of the photo-active polymer is introduced to the network a solvent effect is expected to occur. The switching segment will act as a lubricant for the chains in the network and make the overall dynamics of the material faster. This will be observed as a decrease in G' and G''. When the material is irradiated with UV-light an IPN is formed resulting in a change in G' and G''. A network is formed so again it is expected that $G' > G''$ and that G' dominates the properties.

5.2 Preparation of inter-penetrating network materials

Two different types of IPN-materials where the permanent network was made up by a PEG-polymer were prepared; PEG/HDI/PEGCA-S2 where the PEG-network

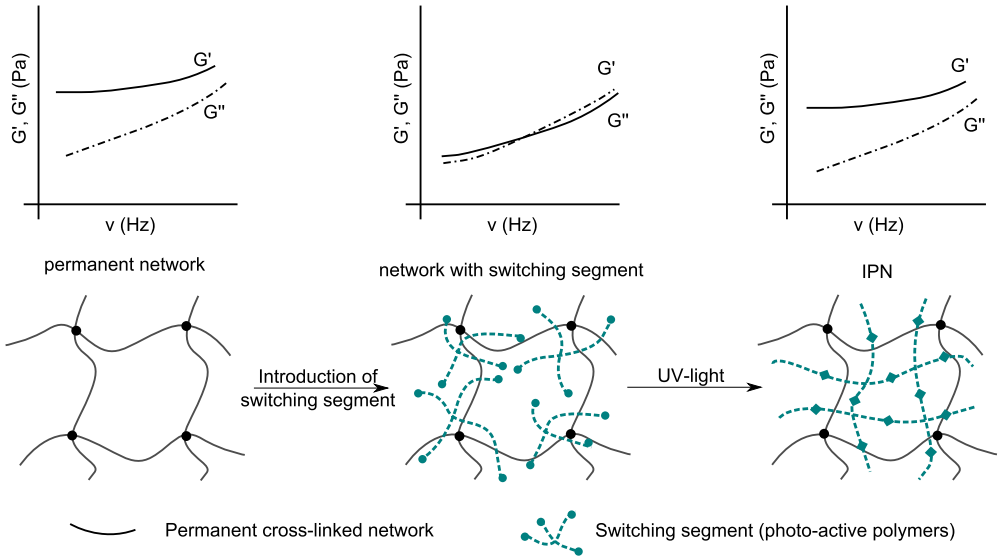

FIGURE 5.3: *The expected change in G' and G'' as a response to changes in the network.*

was cross-linked with hexamethylene diisocyanate and PEG/Desmodur/PEGCA-S2 where the PEG-network was cross-linked with Desmodur.

5.2.1 *Preparation of poly(ethylene glycol) network cross-linked with hexamethylene diisocyanate and with a switching segment consisting of cinnamic acid derivatised 4-armed star poly(ethylene glycol)*

A cross-linker was needed for the OH-functional PEG-polymers. It was decided to focus on the reaction between isocyanates and alcohols, as outlined in Scheme 5.1, for this purpose. This reaction has several advantages but first and foremost it should not be obstructed by the presence of CA-derivatised polymers. Hexamethylene diisocyanate (HDI) was used in the preparations of the PEG-networks.

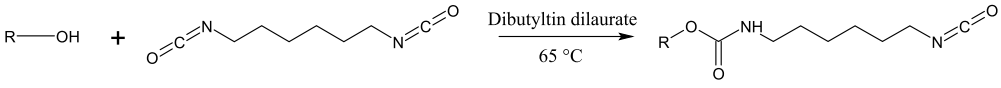

SCHEME 5.1: *Reaction of an isocyanate with an alcohol.*

Two approaches to making IPN-materials based on PEG-polymers cross-linked with HDI in the presence of the UV-active PEGCA-S2 were tested: 1) A one-pot approach where all constituents were mixed, outlined in Scheme 5.2. 2) A two-

step procedure involving firstly the preparation of a four-functional cross-linker and secondly the network formation, outlined in Scheme 5.3.

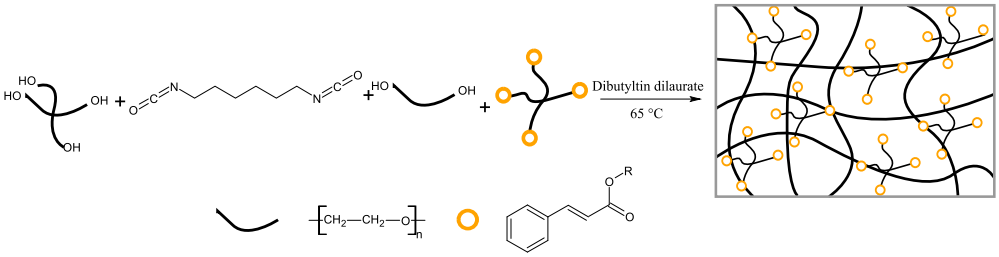

SCHEME 5.2: *One-pot procedure.*

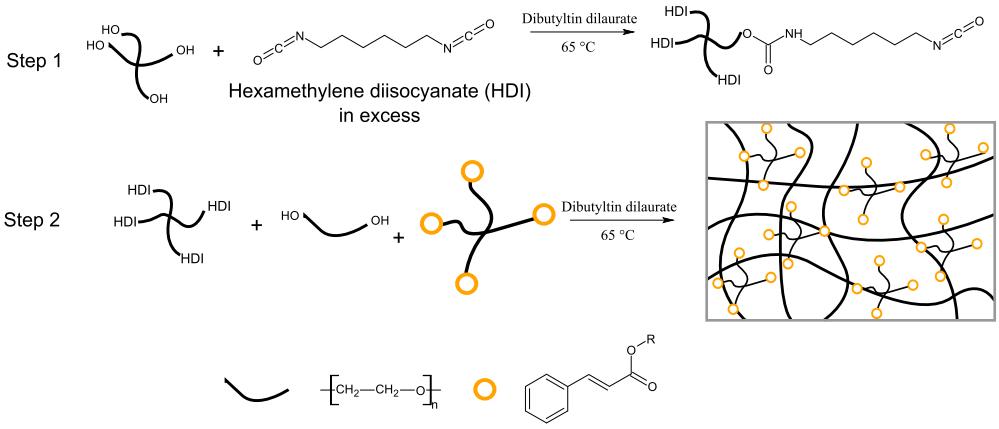

SCHEME 5.3: *Two-step procedure.*

A number of polymers with different molecular weights were used but the applied 4-armed star had M_n=2000 g/mol and typically the linear PEG had M_n=4-10000 g/mol. Details can be found in Appendices A.5 and A.6.

The development of the network was followed with FTIR-spectroscopy, see Figure 5.4. As the Figure shows the modification of PEG-S2 with HDI gives rise to two new stretches in the FTIR-spectrum; at 1720 cm^{-1} as a result of the urethane linkage formed between the polymer and HDI (Scheme 5.1) and at 2245 cm^{-1} as a result of the isocyanate group still present at the end of the arms of the star polymer. Formation of the network occurs after addition of a linear PEG which reacts with the isocyanate on the star polymer. And as Figure 5.4 shows only the urethane linkage is observed in the final network.

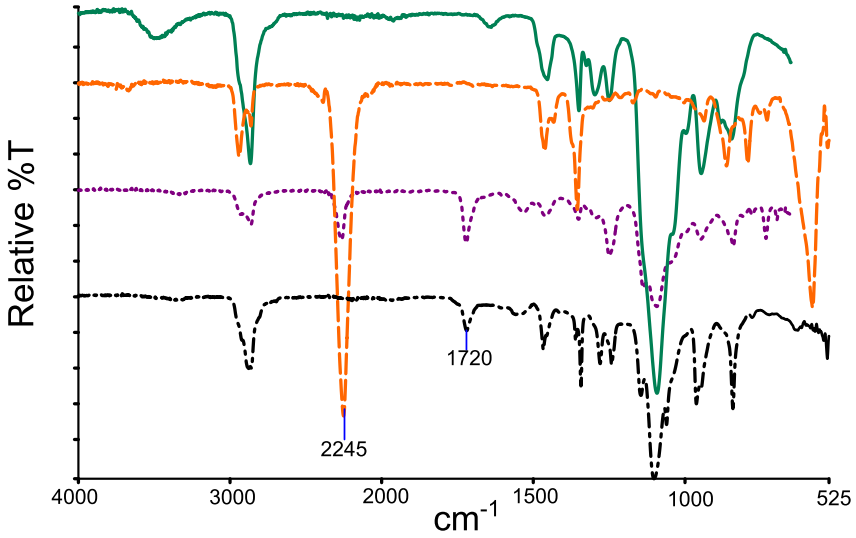

FIGURE 5.4: *The formation of the PEG/isocyanate network. (—) PEG-S2. (- - -) HDI. (· · ·) PEG-S2 reacted with HDI. · – · – ·) The final network. The isocyanate band (2245 cm^{-1}) is present in PEG-S2 modified with HDI but disappears in the final network. The urethane band (1720 cm^{-1}) appears in the modified PEG-S2 and is still present in the final network.*

5.2.2 Preparation of poly(ethylene glycol) network cross-linked with Desmodur and with a switching segment consisting of cinnamic acid derivatised 4-armed star poly(ethylene glycol)

An IPN-system where the permanent network consisted of PEG-chains cross-linked with the 3.4-functional Desmodur N3300 (Desmodur) and the switching segment was PEGCA-S2 was made. Desmodur, which was provided by Bayer, is a isocyanate-functional cross-linker so the advantages of isocyanate as highlighted in the previous section are still valid. The commercially available cross-linker makes the route to the IPN-samples easier since only one step in needed, see Figure 5.5. Desmodur is a 3.4-functional cross-linker meaning that each cross-linking point is in average connected to 3.4 polymer chains. In practice this means that the compound contains a mixture of 3, 4 and possibly higher functional cross-linkers. Polymers of several different molecular weights were tested but mainly linear PEG with M_n=1000 g/mol was used. Further details can be found in Appendices A.8 and A.9.

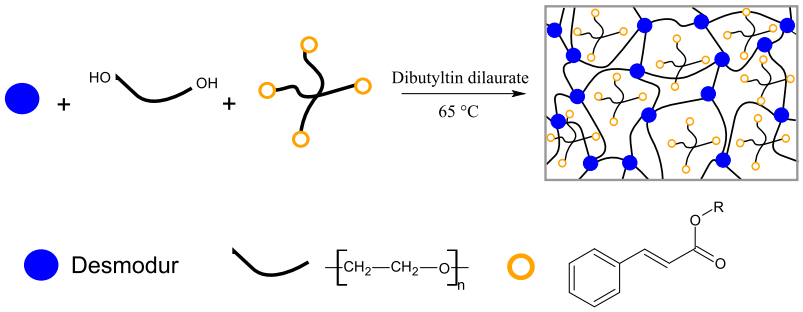

FIGURE 5.5: *Procedure for cross-linking with Desmodur.*

5.3 *UV-study of cinnamic acid derivatised poly(ethylene glycol) in a poly(ethylene glycol) network*

After preparation of the IPN-materials it was needed to determine if the dimerisation of the CA-group attached to the polymers would also take place in the IPN-materials. The mobility of the polymer chains is very different in an IPN-network compared to a sample consisting solely of the UV-active polymer. To understand this issue better a study of thin films of the IPN-material was made. The films were made by cross-linking linear PEG (M_n = 4000 g/mol) with Desmodur in the presence of PEGCA-S2. The mixture of the polymers was made in acetone and thin films (approx 20 µm) were made. Several concentrations of PEGCA-S2 were tested; 0 w%, 1.09 w%, 4.84 w%, 9.59 w%, 13.2 w%, 16.5 w% and 19.4 w%. In Figure 5.6 the UV-spectra of the films can be seen. The data show that the absorption around $\lambda = 274$ nm increased when the concentration was increased. This absorption shows the presence of PEGCA and the increase in concentration can be monitored, as expected.

It would be very useful to be able to link the absorption to the concentration of PEGCA-S2. And the data presented in Figure 5.6 show that the concentration of PEGCA-S2 has an influence on the recorded UV-spectrum. It was tested if the data follow the Beer-Lambert law (Equation 5.1).

$$A = \varepsilon l c \tag{5.1}$$

Equation 5.1 depicts a linear relationship between the absorbance, A, and the concentration, c. ε is the extinction coefficient and l is the thickness of the film. A plot of A as a function of c can verify if the data follow Equation 5.1. This plot can be found in Figure 5.7 for a number of selected wavelengths (λ=265 nm, 270 nm, 280 nm, 285 nm and 290 nm). The plot shows the same trend at all investigated wavelengths and the increase in A as a function of c is also evident. However, the relationship is not linear and the data therefore do not follow the Beer-Lambert law. It is expected that this is due to the high concentrations of the absorbing species. The first three data points are on a straight line indicating the data follow Equation

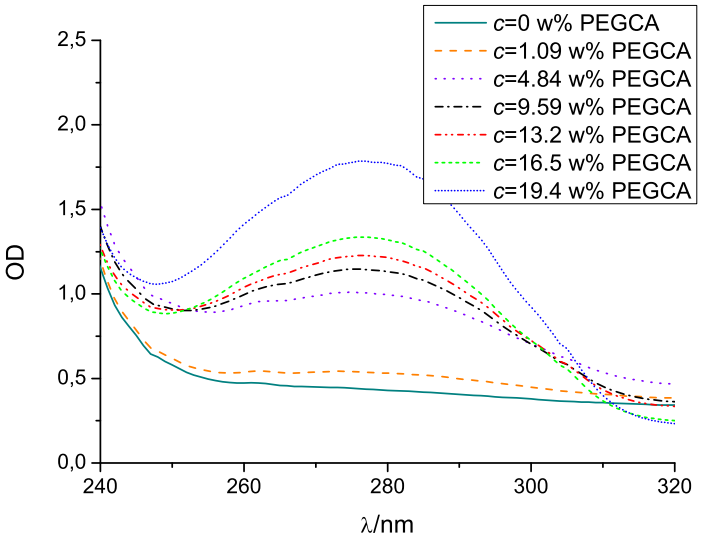

FIGURE 5.6: *UV-absorbance spectra of PEGCA-S2 in PEG/Desmodur (IPN-material). The absorption around λ =274 nm is due to the presence of CA and thus increases with increasing concentration.*

5.1 at lower concentrations. Furthermore, the data show that the concentration of PEGCA-S2 greatly influences A in a non-linear way.

It was also investigated if the exposure to UV-light induced changes in the UV-spectrum of the PEG/Desmodur-network itself. In Figure 5.8 three UV-spectra are shown. The UV-spectra display the changes induced in the PEG/Desmodur-network after 1, 10 and 30 minutes of UV-irradiation. The spectra show no distinct changes and it is therefore concluded that the UV-irradiation does not change the PEG/Desmodur network after up to 30 minutes of irradiation with UV-light.

The data presented in Figure 5.8 were obtained to ensure that the PEG/Desmodur network was not greatly influenced by the incoming UV-radiation. The discussion of the relationship between the concentration and the absorbance along with the discussion of absorbance in the PEG/Desmodur network leads to the conclusion that in case a decrease in A is observed experimentally this is due to a reduction of the concentration of PEGCA-S2 and not due to a changes in the PEG/Desmodur-network.

Figure 5.9 shows UV-spectra of PEG/Desmodur with 19.4 w%, 13.2w% and 4.84 w% PEGCA-S2 before and after UV-irradiation (λ=302 nm) for 30 minutes. For all concentrations a change occurs after irradiation with UV-light as expected. The data also show that the cange occurs even when the photo-active polymer is mixed with another polymer. It is also observed that the concentration of PEGCA-S2 does not

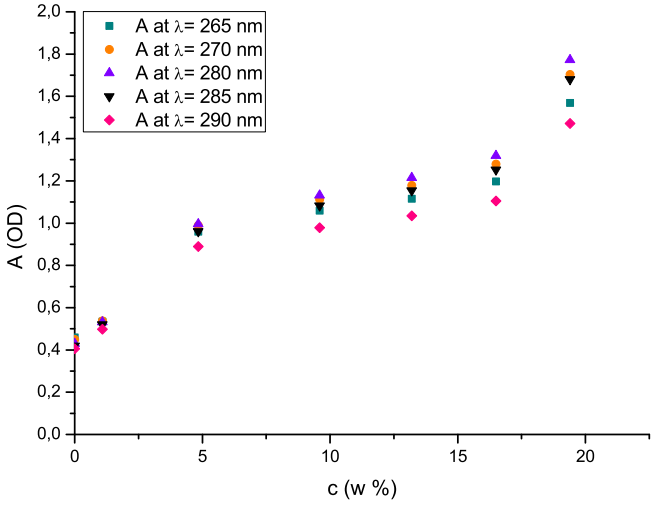

FIGURE 5.7: *Absorbance A as a function of concentration, c, of the photo-active PEGCA-S2 in a PEG/Desmodur-network. A is found at λ = 265 nm (■), 270 nm (●), 280 nm (▲), 285 nm (▼) and 290 nm (♦). It is observed that A increases with c at all the investigated wavelengths. But the relationship is not linear and the data therefore do not follow the Beer-Lambert law.*

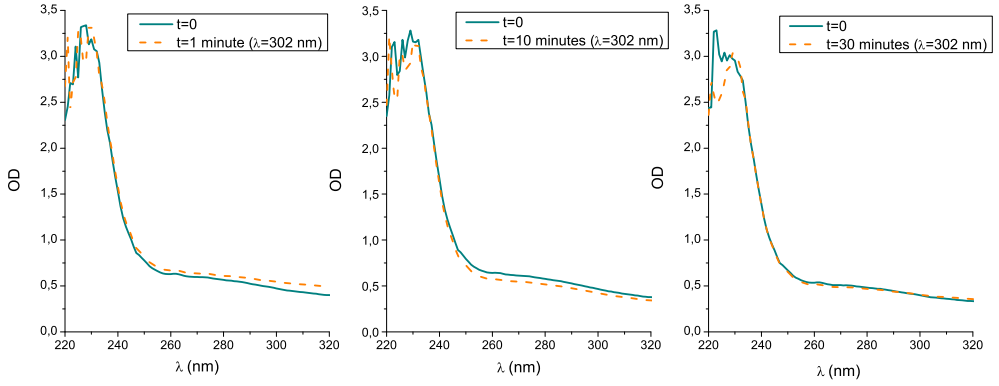

FIGURE 5.8: *Investigation of the PEG/Desmodur network after irradiation with UV. Left: UV-spectrum before (—) and after (- - -) 1 minute of UV-irradiation (λ = 302 nm). Center: UV-spectrum before (—) and after (- - -) 10 minutes of UV-irradiation (λ = 302 nm). Right: UV-spectrum before (—) and after (- - -) 30 minutes of UV-irradiation (λ = 302 nm). No profound changes are observed as a consequence of irradiation with UV.*

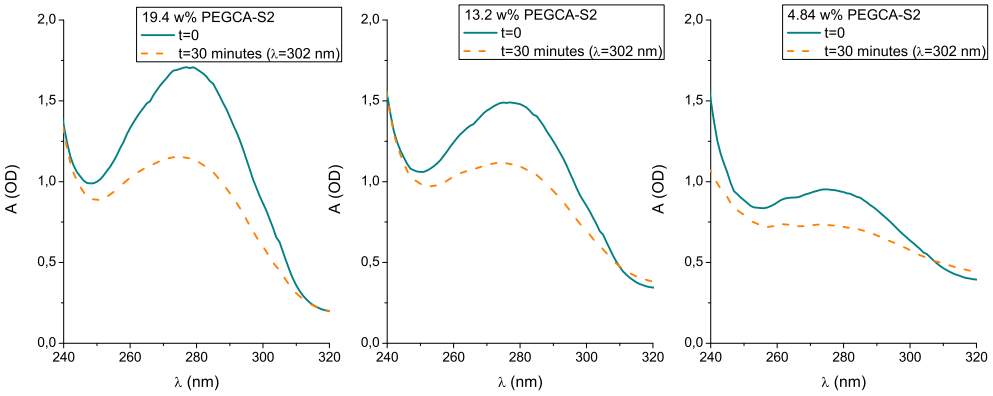

FIGURE 5.9: *Left: The UV-spectrum of PEG/Desmodur-network with a concentration of PEGCA of 19.4 w% before (—) and after (- - -) irradiation with UV-light ($\lambda = 302$ nm) for 30 minutes. Center: The UV-spectrum of PEG/Desmodur-network with a concentration of PEGCA of 13.2 w% before (—) and after (- - -) irradiation with UV-light ($\lambda = 302$ nm) for 30 minutes. Right: The UV-spectrum of PEG/Desmodur-network with a concentration of PEGCA of 4.84 w% before (—) and after (- - -) irradiation with UV-light ($\lambda = 302$ nm) for 30 minutes.*

influence the change in the UV-spectra.

To understand better the influence of the concentration of the UV-active polymer a plot showing the decrease in A, ΔA, at λ =276 nm as a function of the irradiation time was made. ΔA is found by using Equation 5.2.

$$\Delta A = \frac{A(276\text{ nm}) - A(276\text{ nm}_{\text{after irradiation}})}{A(276\text{ nm})} \tag{5.2}$$

The plot is shown in Figure 5.10. Figure 5.10 shows that ΔA increases with increasing irradiation time verifying that the extent of reaction is dependent on the irradiation time, just as expected. Especially for the sample with 19.4 w% PEGCA-S2 it is observed that ΔA increases steeply in the first 1-2 minutes of irradiation and hereafter ΔA increases more slowly. A similar tendency is observed for the samples with 4.48 w% and 13.2 w% PEGCA-S2 but for these samples it is not as pronounced. It can also be observed that the data for the sample with 4.48 w% PEGCA-S2 show large scattering; some of the values for ΔA are even determined to be below 0, indicating an increase in the concentration of PEGCA-S2. This cannot take place and it is suspected that the problem arises due to e.g. unevenness in the surface of the films as a result of the experimental procedure.

The experiment determines that the most pronounced and stable development is observed for the samples with a concentrations of PEGCA-S2 of 19.4 w%.

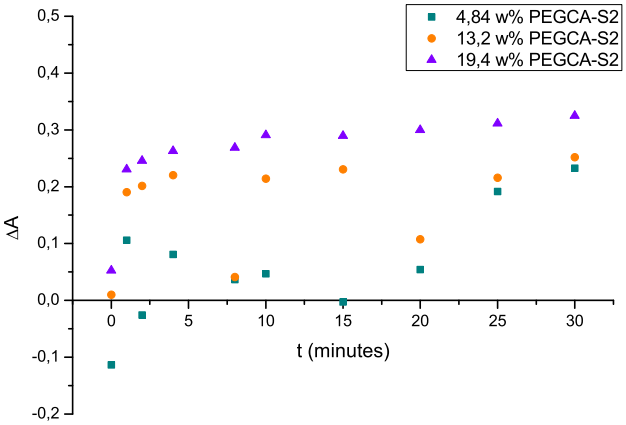

FIGURE 5.10: *The decrease in A, ΔA, at λ =276 nm. The plot shows that ΔA increases with increasing irradiation time (λ = 302 nm). This shows that the concentration of the absorbing species is decreased as a function of irradiation time. A large scattering of the data for the film with the low concentration (4.84 w%) is observed, maybe due to the applied experimental procedure.*

5.4 *Material properties of inter-penetrating network materials with cinnamic acid or cinnamylidene acetic acid derivatised poly(ethylene glycol) as switching segments*

In this section the material properties of the IPN-materials described in Section 5.2 will be presented. Firstly the results from samples where the permanent network consists of PEG-polymers cross-linked with HDI and secondly the samples where the permanent network consists of PEG-polymers cross-linked with Desmodur will be presented.

5.4.1 *Material properties of inter-penetrating network materials with PEG-polymers and a cinnamylidene acetic acid derivatised poly(ethylene glycol) switching segment*

An IPN-material was prepared according to the two step procedure discussed in Section 5.2. In Scheme 5.4 the procedure for this specific IPN-material is outlined: The applied polymers were a linear PEG (M_n=10000 g/mol, PEG-L10), a diisocyanate-modified PEG (4-armed star, M_n=2000 g/mol) (PEGHDI-S2) and the UV-active polymer was a linear CAA-modified PEG (M_n=15000 g/mol) (PEGCAA-L15). The

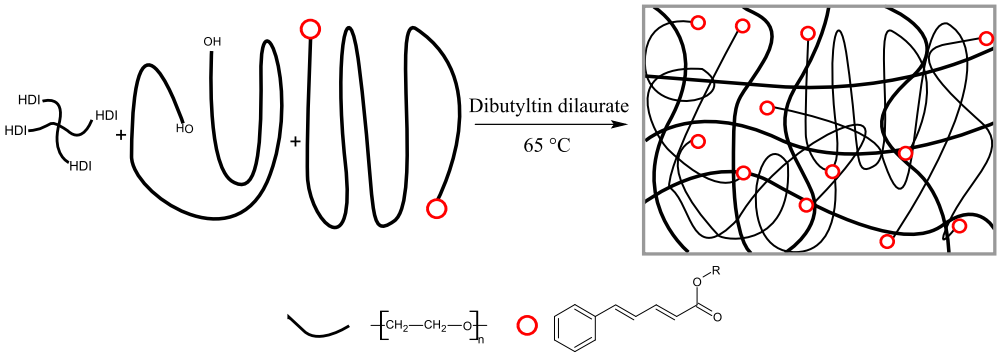

SCHEME 5.4: *Procedure for preparation of the PEG-L10/PEGHDI-S2/PEGCAA-L15 (0.45, 36 w% PEGCAA-L15) material. A linear PEG (M_n=10000 g/mol) was cross-linked with a diisocyanate-modified PEG (4-armed star, M_n=2000 g/mol) in the presence of a linear CAA-modified PEG (M_n=15000 g/mol) (PEGCAA-L15). The concentration of PEGCAA-L15 was 36 w%.*

concentration of PEGCAA-L15 was 36 w% and the r-value of the permanent network was 0.45. The rheological properties of the PEG-L10/PEGHDI-S2/PEGCAA-L15 (0.45, 36 w% PEGCAA-L15) material were determined before and after irradiation with UV-light ($\lambda = 315 - 400$ nm, 30 minutes). The data are shown in Figure 5.11.

Both before and after irradiation the data are dominated by the response from G'' related to the viscous dissipation in the sample. At high frequencies the elasticity is manifested by the cross-over of the data for G' and G''. The data show no significant change in rheological properties after exposure to UV-light. When using a linear polymer as a switching system no secondary network should be formed since the linear photo-active polymers will only form even longer chains, see Figure 5.12. However, the formation of the longer chains should result in a difference in rheological properties due to the molecular weight sensitivity.

It is expected that the primary reason for the lack of detectable change is the entanglement of the polymer chains. This phenomenon results in physical interlocking of chains providing elasticity to the polymer. This behaviour is observed for melts of polymers with molecular weight larger than the so-called molecular entanglement weight, M_e. M_e depends on the specific polymer and for PEG M_e is 1624 g/mol [84]. In general the value for G' increases with increasing molecular weight, and at M_e the polymer chains start to entangle. For molecular weights around 2-3 M_e and above the value for G' is practically constant. Both PEGs used to make the presented IPN have M_n-values far above M_e. Since M_n for both the chains in the switching segment as well as for the permanent network were above M_e the chains are already very entangled. This results in a system where the network properties of the material should not change significantly when M_n for the switching segment is increased.

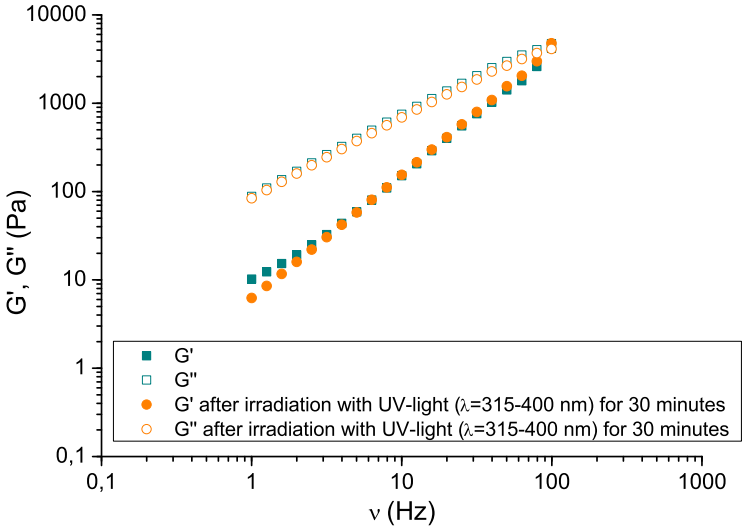

FIGURE 5.11: *Rheological properties of the PEG-L10/PEGHDI-S2/PEGCAA-L15 (0.45, 36 w% PEGCAA-L15) IPN-material before (green) and after (orange) exposure to UV-light. The measurement was carried out at 75 °C with a strain value of 2%. The data before and after exposure to UV-light show no significant changes indicating that no traceable network changes have taken place during the irradiation.*

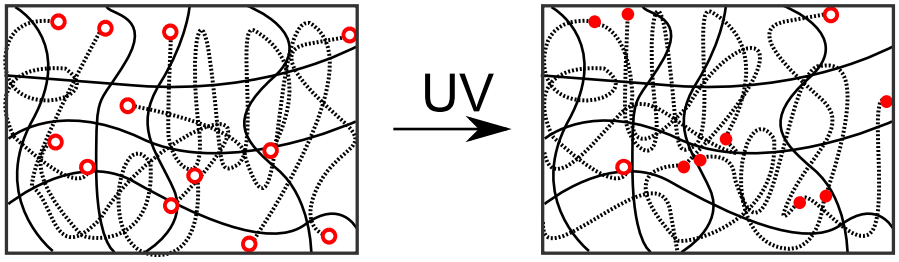

FIGURE 5.12: *This drawing shows the network consisting of PEG-L10 cross-linked with PEGHDI-S2 (—) and the PEGCAA-L15 (···/red open circles). After irradiation with UV-light some of the CAA-groups cross-link (full red circles). The polymer chains are highly entangled both before and after irradiation with UV-light due to the high molecular weights of the chains.*

5.4.2 Initial investigations of the material properties of inter-penetrating network materials with PEG-polymers and a cinnamic acid derivatised poly(ethylene glycol) switching segment

Another IPN-material was prepared according to the two step procedure discussed in Section 5.2. The procedure for preparation and structure of the IPN-material are outlined in Scheme 5.5. The applied polymers were a linear PEG (M_n=4000 g/mol) (PEG-L4), a diisocyanate-modified PEG (4-armed star, M_n=2000 g/mol) (PEGHDI-S2) and the UV-active polymer was a linear CA-modified PEG (M_n=1000 g/mol) (PEGCA-L1). The permanent network had a r-value of 1.05 and the concentration of PEGCA-L1 was approx. 20 w%. This concentration was used based on the study presented in Section 5.3. A film was made by dissolving the components in CH_2Cl_2, placing the mixture in a teflon mold and allowing the solvent to evaporate at atmospheric conditions. A stable, cross-linked film was formed. The rheological properties of the film were determined before and after irradiation with UV-light ($\lambda = 315 - 400$ nm) for 60 minutes. The obtained data are shown in Figure 5.13. The data show that a difference in material properties is induced by the irradiation with UV-light.

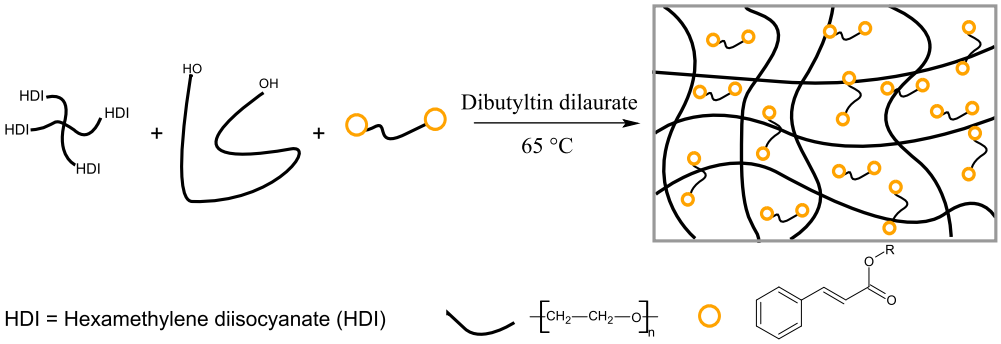

SCHEME 5.5: *Procedure for preparation of the PEG-L4/PEGHDI-S2/PEGCA-L1 (1.05, 20 w% PEGCA-S2) material. A linear PEG (M_n=4000 g/mol) was cross-linked with a diisocyanate-modified PEG (4-armed star, M_n=2000 g/mol) in the presence of a linear CA-modified PEG (M_n=1000 g/mol) (PEGCA-L1). The concentration of PEGCA-L1 was approx. 20 w%.*

It was expected that the short PEGCA-L1 would act as a solvent in the PEG-L4/PEGHDI-S2 network. When a solvent is trapped in a polymer network it acts as a lubricant making the chains move more easily and thus making the entire material less rigid and lowering the values for G' and G''. It was expected that upon exposure to UV-light some of the PEGCA-L1 chains would couple with each other forming longer polymer chains, as shown in Figure 5.14. The longer polymer chains formed by PEGCA-L1 after exposure to UV-light act very differently inside the network compared to single PEGCA-L1 molecules. The longer polymers would have molecular

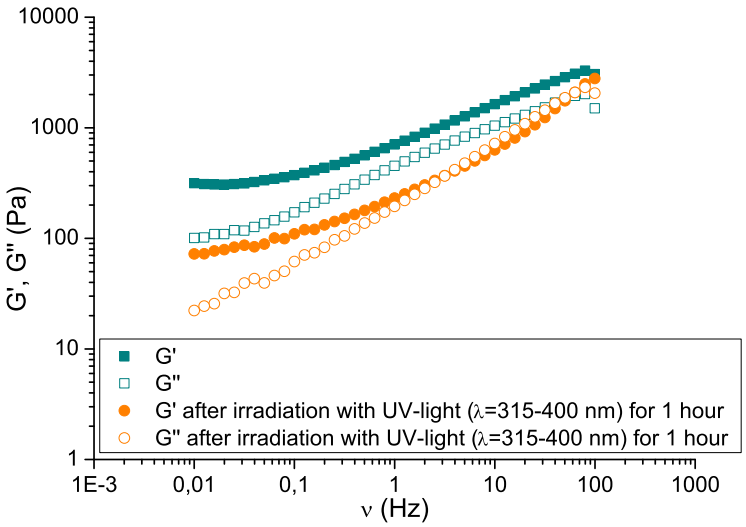

FIGURE 5.13: *Rheological properties of the PEG-L4/PEGHDI-S2/PEGCA-L1 (1.05, 20 w% PEGCA-S2) material before (green) and after (orange) irradiation with UV-light ($\lambda = 315 - 400$ nm) for 1 hour. The measurements were carried out at 50°C with a strain value of 0.4 %.*

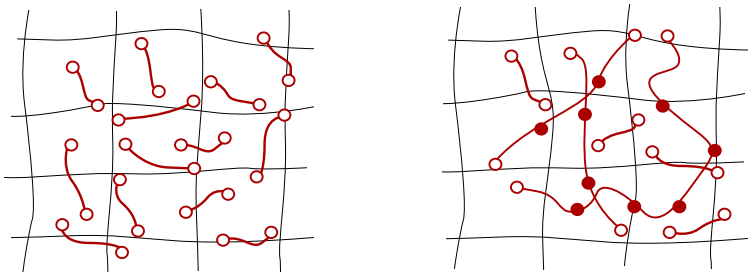

FIGURE 5.14: *This drawing shows the PEG-L4/PEGHDI-S2/PEGCA-L1 (1.05, 20 w% PEGCA-S2) material consisting of PEG-L4 cross-linked with PEGHDI-S2 (black) and the PEGCA-L1 (red/red open circles). After irradiation with UV-light some of the CA-groups cross-link (full red circles) leading to increased entanglement of the chains.*

weight above M_e and therefore the degree of entanglement of the longer polymers both in between themselves as well as with the polymers in the network would increase dramatically. This should result in an increase of the values for G' and G'' as a result of a less dynamic network with more constraints and give a profound change in the rheological properties of the material. This effect is not displayed by the data in Figure 5.13, since a decrease in G' and G'' is observed after irradiation with UV-light. It is uncertain why the results contradict the expectations. It is possible that the observed decrease in G' and G'' is a result of a change in dynamics arising from a change in the glass transition temperature, T_g. But no further investigations were made to confirm this.

Nevertheless, it was decided that the observed change was reason enough to look more thoroughly into what could be achieved with this type of materials.

5.4.3 Inter-penetrating network with hexa-methylene diisocyanate cross-linked PEG-chains and cinnamic acid derivatised poly(ethylene glycol)

In Chapter 4 it was shown how larger irradiation times gave very pronounced changes in the material properties of PEGCA-S2. It was tested if this was the case for IPN-networks too. Two IPN-samples were prepared according to the two step procedure discussed in Section 5.2 and outlined in Scheme 5.3. The applied polymers were a linear PEG (M_n=4000 g/mol) (PEG-L4), a diisocyanate-modified PEG (4-armed star, M_n=2000 g/mol) (PEGHDI-S2) and the UV-active polymer was a CA-modified 4-armed star PEG (M_n=2000 g/mol) (PEGCA-S2). The two samples were prepared in a way where the r-value for the networks was 0.5 and 0.75, respectively. The concentration of PEGCA-S2 was 24 w% for the network with $r = 0.5$ and 28 w% for the network with $r = 0.75$. Two PEG-networks with r-values of 0.5 and 0.75, respectively, without photo-active polymers were also prepared for comparison.

First the results for the PEG-L4/PEGHDI-S2/PEGCA-S2 (0.75, 28 w% PEGCA-S2) material will be presented. In Figure 5.15 the data obtained on the PEG-network and the PEG-L4/PEGHDI-S2/PEGCA-S2 (0.75, 28 w% PEGCA-S2) material are shown. Figure 5.15 shows the differences arising as a consequence of adding the photo-active polymer. The samples with $r = 0.75$ the data show exactly what was expected; the PEG-network has $G' > G''$ indicating an elastic network. Addition of PEGCA-S2 significantly decreases the values for G' and G''. The shape of the data curves are changed too and it is observed that the value of G' and G'' are much closer in the entire frequency range after addition of PEGCA-S2. Furthermore, it is observed that at low frequencies $G'' > G'$ after addition of PEGCA-S2. The data show that the dynamics of the sample after addition of PEGCA-S2 are much faster verifying that PEGCA-S2 acts as a lubricant in the network.

The PEG-L4/PEGHDI-S2/PEGCA-S2 ($r = 0.75$, 28 w% PEGCA-S2) material was irradiated with UV-light for 72 hours and the rheological properties were determined, see Figure 5.16. It was again observed that the sample with $r = 0.75$ behaved exactly as predicted. The irradiation of this sample causes the material properties of

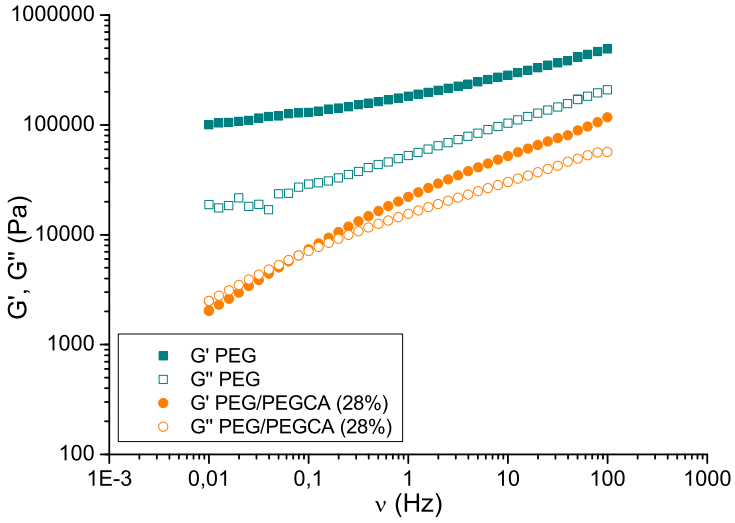

FIGURE 5.15: *Rheological properties of the PEG-network ($r = 0.75$) (green). Rheological properties of PEG-L4/PEGHDI-S2/PEGCA-S2 ($r = 0.75$, 28 w% PEGCA-S2) material (orange). The measurements were carried out at 50 °C with a strain value of 0.08 % for the PEG-network and 1.5 % for the IPN-sample.*

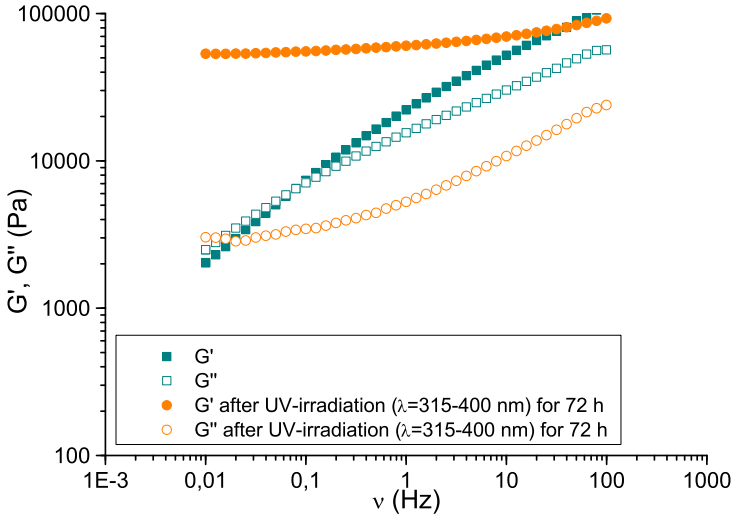

FIGURE 5.16: *Rheological properties of PEG-L4/PEGHDI-S2/PEGCA-S2 ($r = 0.75$, 28 w% PEGCA-S2) material before (green) and after (orange) irradiation with UV-light ($\lambda = 315 - 400$ nm) for 72 h. The measurements were carried out at 50 °C with a strain value of 1.5 % before irradiation and a strain value of 0.2 % after irradiation.*

the sample to change significantly. After irradiation it is observed that $G' > G''$ in the entire frequency range proving the sample to be more elastic than before irradiation. Thus the solvent effect observed prior to irradiation have been removed. This indicates the formation of a secondary network resulting in the pronounced change of rheological properties.

The data obtained on the PEG-network ($r = 0.75$) and the PEG-L4/PEGHDI-S2/PEGCA-S2 ($r = 0.75$, 28 w% PEGCA-S2) material show that the expected solvent effect arising from the addition of PEGCA-S2 is present and furthermore that a development of the rheological properties towards a more elastic material have been verified. The presented data verify our expectations to a material of this type and the work with this type of material was continued.

Now the results for the sample with $r = 0.5$ will be presented. These data show very different tendencies. It is expected that the primary reason for this is that addition of PEGCA-S2 resulted in no network formation. It was observed that after curing the sample was a powder rather than a film. The measurements were carried out at 50 °C where the powder is melted. It was decided to present the data in order to discuss the development of the material and the problems with the film formation. It is noteworthy that a film was formed of the PEG-network with $r = 0.5$. In other words addition of PEGCA-S2 to the sample obstructs the formation of the network. Since this was not observed for the network with $r = 0.75$ it is probably connected

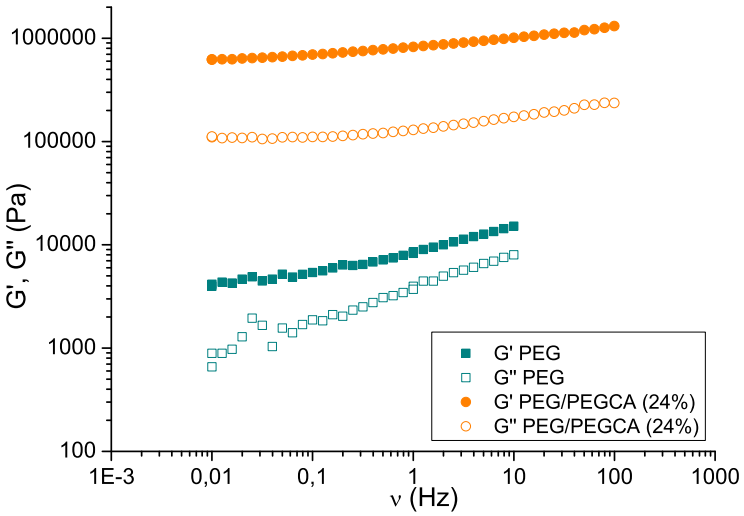

FIGURE 5.17: *Rheological properties of the PEG-network ($r = 0.5$) (green). Rheological properties of the PEG-L4/PEGHDI-S2/PEGCA-S2 ($r = 0.5$, 24 w% PEGCA-S2) material (orange). The measurements were carried out at 60 °C with a strain value of 0.08 % for the PEG-network and at 50 °C with a strain value of 0.5 % for the IPN-sample.*

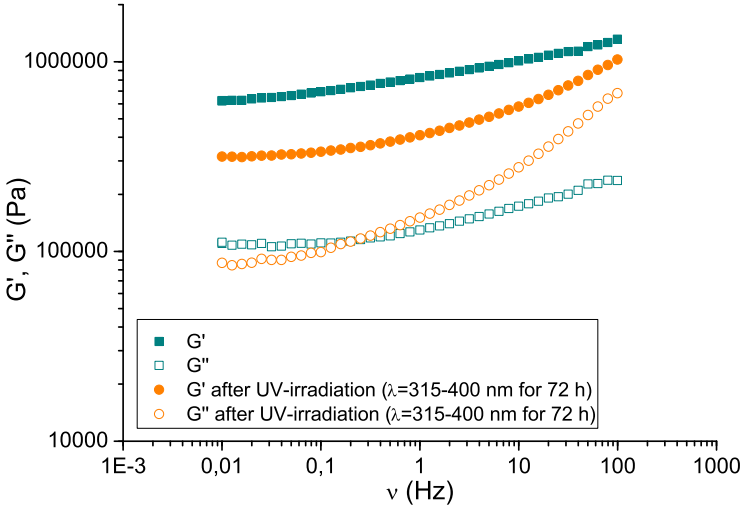

FIGURE 5.18: *Rheological data from PEG-L4/PEGHDI-S2/PEGCA-S2 ($r = 0.5$, 24 w% PEGCA-S2) material before (green) and after (orange) irradiation with UV-light ($\lambda = 315 - 400$ nm) for 72 h. The measurements were carried out at 50 °C with a strain value of 0.5 % before irradiation and a strain value of 0.3 % after irradiation.*

to the r-value of the permanent network.

In Figure 5.17 the data obtained on PEG ($r = 0.5$) and PEG-L4/PEGHDI-S2/PEGCA-S2 ($r = 0.5$, 24 w% PEGCA-S2) are shown. As described above some problems were encountered with the IPN-material and as expected the rheological data on this sample do not correlate with the expected tendency. The presented data actually show a significant increase in both G' and G'' after addition of PEGCA-S2. This contradicts the expectations. Upon irradiation of the sample, Figure 5.18, only a small change in the data is observed. Indicating that the material does not change significantly. It was observed that the irradiated material formed a film indicating that a reaction had taken place. It is difficult to explain exactly what happens with this material expecially since the other IPN ($r = 0.75$) showed precisely what was expected. The difference between the two IPN-materials is the r-value of the permanent PEG-network and these data strongly indicate that this value has a great effect on the material. This is well-known since networks with low r-values have more dangling structures and unreacted chains which influence the properties.

Furthermore, the critical stoichiometric value, r_c, for this material is 0.33. Below r_c no network is formed. The material with $r = 0.5$ is closer to r_c which can also give rise to problems. The problem most probably arises due to the fact that it can be difficult to control the permanent network when working with r-value close to r_c. This is underlined by the order of magnitude of G' and G'' for the materials. For

the material with $r = 0.75$ G' for the PEG-network is in the order of 10^5 Pa while for the irradiated PEG-L4/PEGHDI-S2/PEGCA-S2 ($r = 0.75$, 28 w% PEGCA-S2) IPN-material it is in the order of 10^4 Pa. These values are relatively close showing that the properties of the IPN-material are similar to the initial network. But for the material with $r = 0.5$ G' for the PEG-network is in the order of 10^3 Pa while for the irradiated PEG-L4/PEGHDI-S2/PEGCA-S2 ($r = 0.5$, 24 w% PEGCA-S2) IPN-material it is in the order of 10^5 Pa. This indicates large changes in the material that the secondary network formed after irradiation dominates the properties to a large extent.

This study showed that a high irradiation time of IPN-samples could give a change in material properties and that the r-value for the permanent network was very important. A significant development of the rheological properties of the material with $r = 0.75$ was observed. It was decided to continue the work with this type of material.

5.4.4 Inter-penetrating network with Desmodur cross-linked poly(ethylene glycol)-chains and cinnamic acid derivatised poly(ethylene glycol)

As the data presented in the former sections show it was possible to prepare an IPN-material by cross-linking a PEG-polymer with an isocyanate-functional cross-linker in the presence of photo-active CA- or CAA-derivatised PEG-polymers. It was also possible to observe changes in the material properties of the materials as a result of exposure to UV-light. The irradiation time was large (72 h) but the data from UV-spectroscopy showed that the dimerisation of CA occurs on much shorter timescales. This gave reason to believe that changes in the rheological properties of the IPN could be achieved on much shorter timescales.

In the following section the material properties of IPN-samples cross-linked with Desmodur N3300 (Desmodur) will be presented. The commercially available Desmodur cross-linker made it possible to skip the preparation of the HDI-functional cross-linker and thus save time. This was highly appreciated since the focus of this work has been a possible commercialisation of the final product wherefore a short and simple route to the product was desired. The irradiation times used in this work are much shorter (15 minutes) since this was the timescale UV-spectroscopy predicted.

It was found that the PEG-L1/Desmodur/PEGCA-S2 ($r = 0.84$, 19.2 w% PEGCA-S2) material resulted in the most stable films, see Figure 5.19. Two samples were made and irradiated with UV-light for 15 minutes at RT and 60 °C, respectively. First the influence of PEGCA-S2 in the matrix was investigated, see Figure 5.20. It can be observed that the original network is quite stiff since G' is constant in the entire frequency range. Addition of PEGCA-S2 only influence G'' which is slightly decreased. The r-value of the PEG/Desmodur-network is smaller than for the PEG-L1/Desmodur/PEGCA-S2 material so it is expected that the PEG-L1/Desmodur/PEGCA-S2 ($r = 0.84$, 19.2 w% PEGCA-S2) material is stiffer. The data show that the material is not significantly altered by addition of PEGCA-S2.

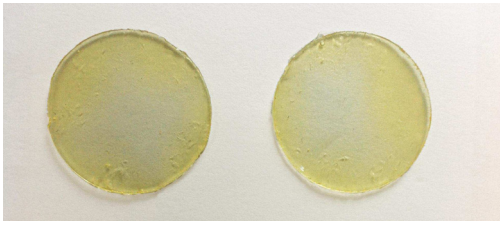

FIGURE 5.19: *Films of the PEG-L1/Desmodur/PEGCA-S2 ($r = 0.84$, 19.2 w% PEGCA-S2) material.*

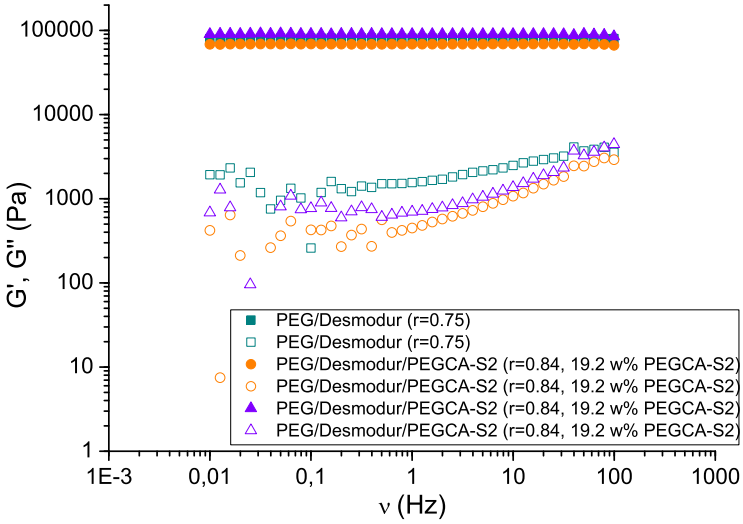

FIGURE 5.20: *Rheological properties of the PEG/Desmodur ($r = 0.75$) network and two PEG-L1/Desmodur/PEGCA-S2 ($r = 0.84$, 19.2 w% PEGCA-S2) samples. The measurements were carried out at 60 °C with a strain value of 1.0 %.*

In Figure 5.21 the rheologcial data obtained before and after irradiation with UV-light are shown. The two data sets presented in Figure 5.21 show the data obtained on the film irradiated at RT and at 60 °C, respectively. It is seen that no profound change occurs upon irradiation.

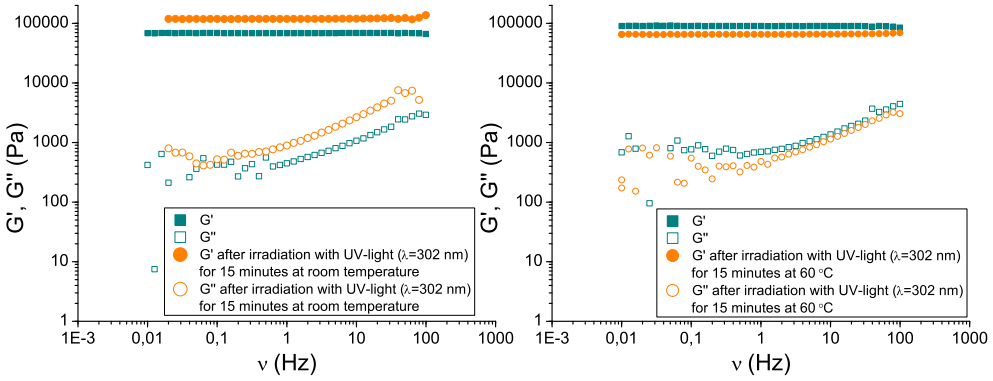

FIGURE 5.21: *Rheological properties of two PEG-L1/Desmodur/PEGCA-S2 (r = 0.84, 19.2 w% PEGCA-S2) samples before (green) and after (orange) irradiation with UV-light (λ = 302 nm). Left: Irradiated for 15 minutes at RT. Right: Irradiated for 15 minutes at at 60 °C. The measurements were carried out at 60 °C with a strain value of 1.0 %.*

Two important factors have been altered from Section 5.4.3 to this Section: 1) M_n of the PEG-chains in the permanent network which was 4000 g/mol in Section 5.4.3 and 1000 g/mol in this Section). 2) The irradiation time which was 72 hours in Section 5.4.3 and 15 minutes in this Section. Using significantly shorter chains in the permanent network will make the overall material harder and reduce flexibility. This will make it more difficult for the PEGCA-S2 chains to diffuse and react. There are no reason to believe that the shorter irradiation time would cause problems. As mentioned before the data from UV-spectroscopy show that the timescale of the reaction in minutes rather than hours.

The data shown in this Section show no indications on changes in the IPN material after 15 minutes irradiation with UV-light. It is expected that this problem arise due to limitations of the mobility of the chains.

5.5 Conclusion

Four different types of PEG/cross-linker/photo-active PEG materials were successfully prepared; namely PEG-L10/PEGHDI-S2/PEGCAA-L15, PEG-L4/PEGHDI-S2/PEGCA-L1, PEG-L4/PEGHDI-S2/PEGCA-S2 and PEG-L1/Desmodur/PEGCA-

S2. All materials have been thoroughly presented and their rheological properties have been discussed.

PEG-L10/PEGHDI-S2/PEGCAA-L15 (0.45, 36 w% PEGCAA-L15) showed no change in rheological properties upon irradiation with UV-light. This is ascribed to the entanglement of the polymer chains which will not increase due to the large value for M_n in this system. The large value for M_n results in a system that is already highly entangled before irradiation with UV-light.

The material consisting of PEG-L4/PEGHDI-S2/PEGCA-L1 (1.05, 20 w% PEGCA-S2) responded to the UV-light by changing its rheological properties. But the values for G' and G'' decreased, even though an increase was expected. It is uncertain why this effect is observed. It was concluded that the fact that a change was observed was reason enough to carry on the work with this type of system.

Two systems consisting of PEG-L4/PEGHDI-S2/PEGCA-S2 were made with $r = 0.75$ and $r = 0.5$. The material PEG-L4/PEGHDI-S2/PEGCA-S2 ($r = 0.75$, 28 w% PEGCA-S2) confirmed the expectations to the fullest: Incorporation of PEGCA-S2 in the PEG-network showed a solvent effect and upon irradiation with UV-light for 72 hours an elastic network was formed. This results proves that the type of material this thesis strive to find can indeed be achieved. The material PEG-L4/PEGHDI-S2/PEGCA-S2 ($r = 0.5$, 24 w% PEGCA-S2) behaved differently most probably due to the significantly lower value for r which gave rise to problems with the film formation.

PEG-L1/Desmodur/PEGCA-S2 ($r = 0.84$, 19.2 w% PEGCA-S2) was tested with short irradiation times and no change was observed.

Chapter 6

Inter-penetrating network materials

So far IPNs which were made up by the same polymer in both the permanent network as well as the switching segment have been considered. It is also possible to prepare IPNs which have different polymers for the permanent network and the switching segment. This way unique materials exploiting the properties of different polymers can be prepared.

In this Chapter the work done on IPNs with different polymers will be outlined. A PPO/PEGCA-S2 material where the permanent network consists of a cross-linked poly(propylene oxide) network as well as PDMS/PEGCAA-S2 where the permanent network consists of a cross-linked poly(dimethyl siloxane) network will be presented.

6.1 Preparation of inter-penetrating network materials

Here the preparation for the PPO/PTM/PEGCA-S2 network as well as the PDMS-/PEGCAA-S2 network will be presented.

6.1.1 Preparation of poly(propylene oxide) network with a switching segment consisting of cinnamic acid derivatised 4-armed star poly(ethylene glycol)

An IPN with a permanent poly(propylene oxide) (PPO) network and a PEGCA-S2 switching segment was prepared. The PPO-network was prepared by a thiolene reaction, see Scheme 6.1, where a vinyl double bond and a thiol-group react to form a thioether. In the conducted experiments vinyl-terminated PPO-chains ($M_n = 13500$ g/mol) and a four-functional thiol-cross-linker (PTM) were used. The films were cured under UV-light (λ =315-400 nm), see Appendices A.10 and A.11 for details.

PEGCA-S2 was introduced to the network by swelling the PPO-network in a solution of PEGCA-S2 in $CHCl_3$ (10 w%). It was expected that the UV-absorbance

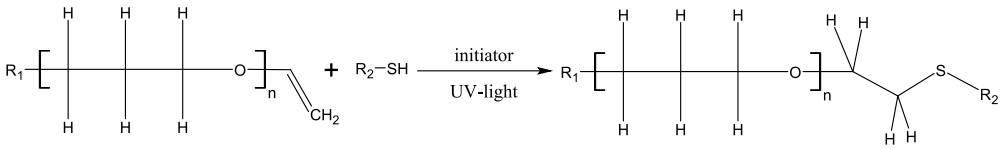

Scheme 6.1: *Thiolene reaction between a vinyl functional polymer and a thiol.*

of the CA-groups would influence the efficiency of the thiolene reaction and therefore the photo-active polymers were added after curing of the PPO.

6.1.2 Preparation of poly(dimethyl siloxane) network with a switching segment consisting of cinnamylidene acetic acid derivatised 4-armed star poly(ethylene glycol)

It was attempted to simply mix PEGCAA-S2 into a PDMS-network. The PDMS-network is made by mixing the two premixes S1 and S2 in a given ratio to control the r-value of the resulting PDMS-network. S1 contains the vinyl-functional PDMS and the four-functional hydride cross-linker, while S2 contains vinyl-functional PDMS and the Pt-catalyst. In Scheme 6.2 the general reaction for the cross-linking of vinyl functional PDMS with the active hydride groups on the four functional cross-linker is shown.

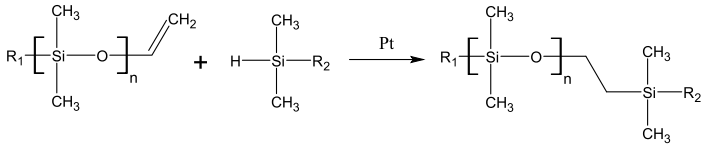

SCHEME 6.2: *Cross-linking of vinyl-terminated PDMS with a hydride-functional cross-linker.*

When producing PDMS-networks the mentioned premixes, S1 and S2, are simply weighed out, mixed thoroughly and left to cure at RT.

It was attempted to simply add PEGCAA-S2 to the mixture by adding a little solvent to ensure proper mixing, see Appendix A.7 for details. Two important observations were made. First of all it was observed that it was difficult to fully mix the two polymers. This was expected since PEG and PDMS are very different; PEG being a hydrophilic polymer, while PDMS is highly hydrophobic. It was observed that $CHCl_3$ dissolved both polymers but this proved not to solve the issues with mixing the polymers. Secondly it was observed that the PDMS did not cross-link when PEGCAA-S2 was present. Cross-linking was only observed for one of the investigated samples in which an obvious phase separation was present since the PEGCAA-S2 was agglomerated inside the cross-linked PDMS-film. For the other samples no cross-linking was observed. It was attempted to add extra catalyst to see if this would accelerate the cross-linking reaction but the reaction did not occur.

It is unclear why the cross-linking reaction was obstructed in the presented experiments. A reason could be that the Pt in the catalyst coordinates to the conjugated double bonds in PEGCAA rather than on the vinyl groups in the PDMS. Molberg *et al.* [85] report problems with Pt-catalysed cross-linking with systems with compounds containing nitrogen and argue that this problem occurs because Pt coordinates to

N. This shows that the cross-linking reaction can be disturbed by the presence of other compounds but it does not verify that coordination of Pt is the problem in the presented work.

Since the cross-linking of the PDMS proved to be unsuccessful no further work was conducted with this type of IPN-material.

6.2 Inter-penetrating network materials with a poly(propylene oxide) network and a cinnamic acid derivatised poly(ethylene glycol) switching segment

PEGCA-S2 was introduced to the PPO network by swelling. Swelling is a procedure that involves immersing the sample fully in a solvent and allowing it to absorb the solvent. The absorption of the solvent in the network results in a large increase in the volume of the sample and in the swelled state it is possible for compounds and larger molecular structures to diffuse in and out of the network. A swelling experiment can therefore be used to remove compounds from a network but also to introduce new compounds.

The swelling experiment is governed by thermodynamics and thus it is not possible to remove all the compounds in the network since equilibrium concentration of the compound inside and outside the network will be established. This concentration can be lowered by repeating the experiment a number of times.

From general network theory it is well-known that an ideal network where all polymer chains are a part of an infinite network is not equal to the experimental outcome. Prepared networks, regardless of the polymer type, are more accurately described as a system made up of an elastic infinite network fraction and a so-called sol fraction that consists primarily of unreacted chains and larger branched structures, see Figure 6.1. Alongside the work presented in this thesis a study of the rheological properties of PDMS-networks and their extracted network fraction was also made and published, see Appendix D.3 [86]. This study showed that removing the sol fraction from a PDMS-network by conducting a swelling experiment made a very large difference in the rheological properties of the material.

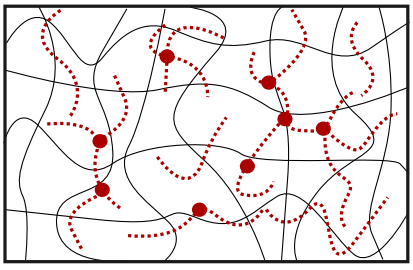

FIGURE 6.1: *A network consists of cross-linked network chains (—) and a sol fraction (- - -) made up of larger branched structures and unreacted chains.*

To ensure similar properties of all the PPO-samples they were swelled in CH_2Cl_2 to remove unreacted chains and larger branched structures before introducing PEGCA-S2 in the network. The swelling experiments were carried out in two steps:

- Step 1: Swelling of the cured PPO network in CH_2Cl_2 to remove unreacted chains and small structures from the network. After the swelling the sample was left at atmospheric conditions to allow the solvent to evaporate.
- Step 2: Swelling of PPO network in a solution of PEGCA-S2 in CH_2Cl_2 ($c = 53$ mmol/L) to introduce PEGCA-S2 in the network. After the swelling the sample was left at atmospheric conditions to allow the solvent to evaporate.

The prepared PPO-networks were clear and sticky. The swelling procedure (Step 1) made the networks less sticky while the introduction of PEGCA-S2 (Step 2) changed the colour of the samples from clear to opaque yellow, see Figure 6.2. The opacity of the sample is a result of mixing two polymers with different refractive indices. During the evaporation of the solvent after Step 2 it was observed that excess PEGCA-S2 was squeezed out of the sample and occurred on the surface. The reason for this is simply that the volume to accommodate PEGCA-S2 molecules in the PPO-network is larger in the swelled sample than in the dry sample. The excess of the non-volatile PEGCA-S2 diffuses out of the network and occurs on the surface of the films.

FIGURE 6.2: *Photograph of the PPO network (right) and the PPO/PTM/PEGCA-S2 (1.2, 40.5 w% PEGCA-S2) material (left). The PPO/PEGCA-S2 has an opaque yellow colour.*

The rheological properties of the washed PPO-network and the PPO/PTM/-PEGCA-S2 (1.2, 40.5 w% PEGCA-S2) material were determined and the obtained data are shown in Figure 6.3. The result shows that the rheological properties of the PPO/PEGCA-S2 material are very similar to those for the washed PPO-network. The introduction of PEGCA-S2 polymers in the network only influence the dynamics of the PPO-network to a very small degree.

After determining the rheological properties of the PPO/PTM/PEGCA-S2 (1.2, 40.5 w% PEGCA-S2) material the sample was exposed to UV-light. Two types irradiation experiments were performed: 1) Irradiation with UV light (λ =302 nm) for

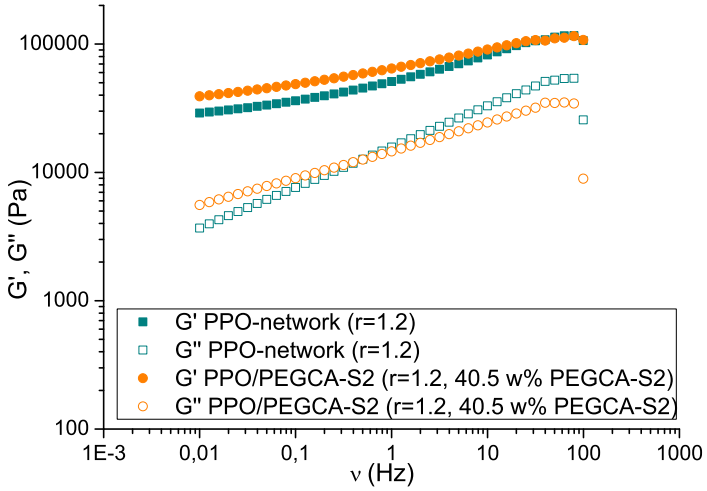

FIGURE 6.3: *Rheological properties of the PPO-network and the PPO/PTM/PEGCA-S2 (1.2, 40.5 w% PEGCA-S2) material. The measurements were carried out at 23 °C with a strain value of 2.0 %.*

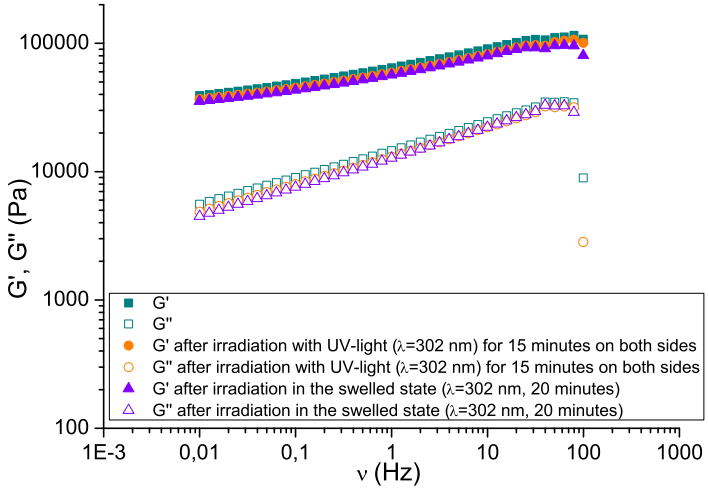

FIGURE 6.4: *Rheological properties of PPO/PTM/PEGCA-S2 (1.2, 40.5 w% PEGCA-S2) material(green), after irradiation with UV-light ($\lambda = 302$ nm) for 15 minutes at RT on both sides (orange) and after irradiation in the swelled state ($\lambda = 302$ nm) for 20 minutes (purple). The measurements were carried out at 23 °C with a strain value of 2.0 %.*

15 minutes at RT. Both sides of the film were irradiated. 2) Irradiation in the swelled state with UV light (λ =302 nm) for 20 minutes at RT. The sample was swelled in a solution PEGCA-S2 in CH_2Cl_2 ($c = 53$ mmol/L). By irradiating the sample in its swelled state the mobility of the chains in the switching segment is ensured.

Figure 6.4 show the rheological data obtained on the samples before and after irradiation and it is observed that the irradiation induces no changes in rheological properties of the samples. It is unclear why no change is observed but it could be due to the opacity of the sample. The opacity will most likely influence the way the sample interacts with the UV-light and cause the penetration depth of the light to diminish. This was the reason for irradiating the samples on both sides.

6.3 Conclusion

Two IPNs were prepared; one based on PDMS and one based on PPO. The system based on PDMS failed to cross-link after addition of PEGCAA-S2 and no further work was done with this type of IPN. The IPN based on PPO was successfully prepared and yielded opaque yellow films which were tested with rheology before and after irradiation with UV-light. The addition of PEGCA-S2 to the PPO-matrix did not change the properties significantly. Nor did irradiation of the samples induce any traceable change in rheologial properties.

Chapter 7

Mobility and reactivity

As has been discussed in the previous Chapters the conducted work showed that the timescale determined by the models and data presented in Chapter 3 proved to be too short to obtain traceable changes in the material properties of the photo-active materials. In other words a disagreement between the data obtained by UV-spectroscopy and rheology was observed. In the following Chapter this issue will be discussed and supporting results from NMR and SEC will be presented.

In this Chapter a discussion of mobility in crystals versus polymer materials will be made, followed by a discussion of the results obtained from NMR and SEC on irradiated samples. Initially NMR and SEC were discarded for use on irradiated systems due to insolubility of the samples. However, this issue was overcome partially by irradiating the photo-active polymer in solution and partially by producing a number of mono-functional photo-active polymers.

7.1 Crystals and mobility

The photo-activated dimerisation of CA in crystals have been extensively studied since the reaction is a good example of solid state [2π+2π] photo-dimerisation [87, 88]. In a crystal the CA-molecules will be placed in a lattice and depending on the experimental procedure for obtaining the crystals the molecules can be positioned either head-to-head (α-CA), head-to-tail (β-CA) or in a vaguely defined unfavorable pattern (γ-CA) [89, 90]. In 7.1 drawings of α-CA and β-CA can be seen. Both α-CA and β-CA readily undergo dimerisation, while no photo-activity is observed for γ-CA.

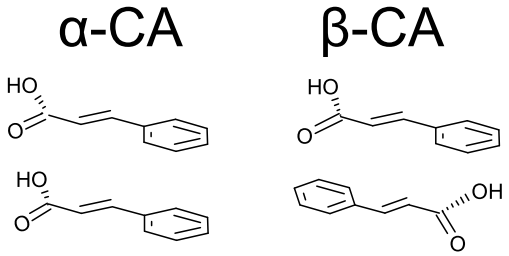

FIGURE 7.1: *In α-CA two CA molecules are positioned head-to-head and in β-CA they are head-to-tail.*

In CA-crystals the crystal lattice ensures to keep the CA-molecules in favorable position for photo-dimerisation. In polymers this is far more difficult to obtain. The motion of the polymer chain is governed by Brownian motions and can thus not be controlled to a larger extent. Some research groups have overcome this by fixing the CA-groups at specific positions in the network and thereby increasing the possibility for positive cross-linking [15, 78].

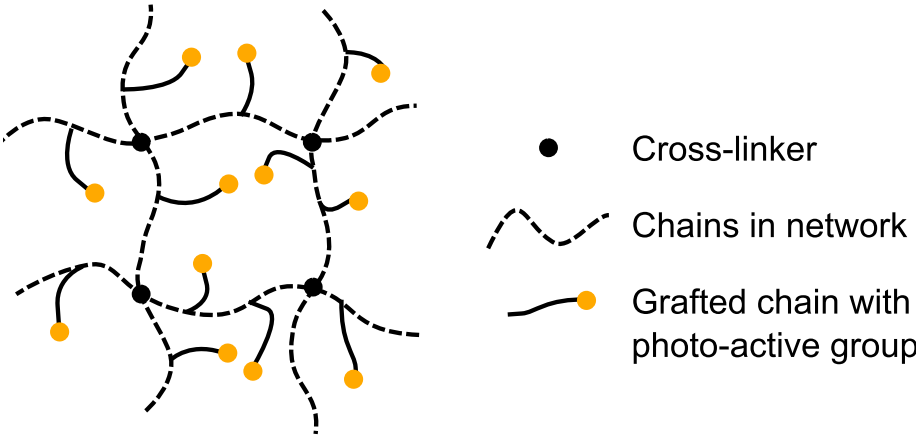

FIGURE 7.2: *A way of controlling the position of the photo-active groups is to graft them onto the network chains. This ensures that the photo-active groups are in close proximity.*

7.2 NMR-study of cinnamic acid derivatised poly(ethylene glycol

As mentioned earlier it was initially decided not to use NMR-spectroscopy on the irradiated systems since the samples were insoluble. The reason behind this was primarily that the irradiated samples formed networks. NMR was therefore discarded as a method to follow the cross-linking reaction of CA and CAA. The technique came back into focus after a number of CA-derivatised linear mono-functional PEGs were made. Two linear mono-functional PEGs (m-PEG) were derivatised with CA, namely m-PEG (M_n = 750 g/mol) (m-PEGCA-L0.75) and m-PEG (M_n = 2000 g/mol) (m-PEGCA-L2), see Figure 7.3. m-PEGCA-L0.75, m-PEGCA-L2 as well as PEGCA-S2 were dissolved and irradiated with UV-light (λ = 302 nm) for 60 minutes. NMR-spectra of the compounds were obtained before and after irradiation with UV-light.

In Figure 7.5 a section of the NMR-spectrum for PEGCA-S2 is displayed. The NMR-data obtained for PEGCA-S2 are described in details earlier (Chapter 4.3.1), but briefly the protons in the benzene ring occur as two multiplets at 7.46 ppm and 7.33 ppm. The protons on the double bond occur as two distinct doublets; at 7.65

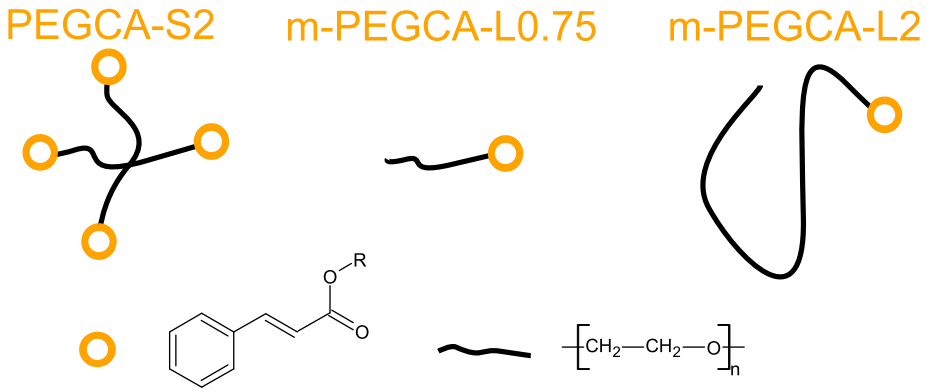

FIGURE 7.3: *Structures of PEGCA-S2, m-PEGCA-L0.75 and m-PEGCA-S2.*

ppm (H_{1A}) and 6.44 ppm (H_{1B}), respectively. The coupling constant, J, for H_{1A} and H_{1B} is 16.0 Hz which confirms that the protons in question are in *trans*-position.

After irradiation the spectrum also shows the pattern described above, but two new doublets have occurred at 6.89 ppm (H_{2A}) and 5.90 (H_{2B}). For these doublets J is 12.1 Hz. The chemical shifts of H_{2A} and H_{2B} indicate that they, just like H_{1A} and H_{1B}, are connected to a double bond. But the coupling constants show that the protons are in *cis*-configuration.

In other words the NMR-data suggest that PEGCA-S2 isomerises to its *cis*-isomer when irradiated in DMF-solution. The molecular structures of *trans*-CA and *cis*-CA are shown in Figure 7.4. The NMR-data for m-PEGCA-L2 and m-PEGCA-L0.75 show the same tendency and can be found in Appendix C.2.

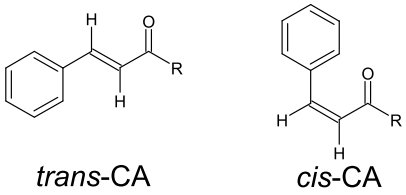

FIGURE 7.4: *The molecular structure of trans-CA (left) and cis-CA (right).*

It must be noted that the irradiation of the samples was carried out in solution which makes the environment of the polymers very different from a polymer network. However, it is expected that the photo-induced isomerisation of *trans*-CA to *cis*-CA is occurring alongside the dimerisation. In practise meaning that in case a CA-molecule is irradiated with UV-light and has no possibility of dimersation, which is the preferred reaction, it will isomerise instead [73, 91].

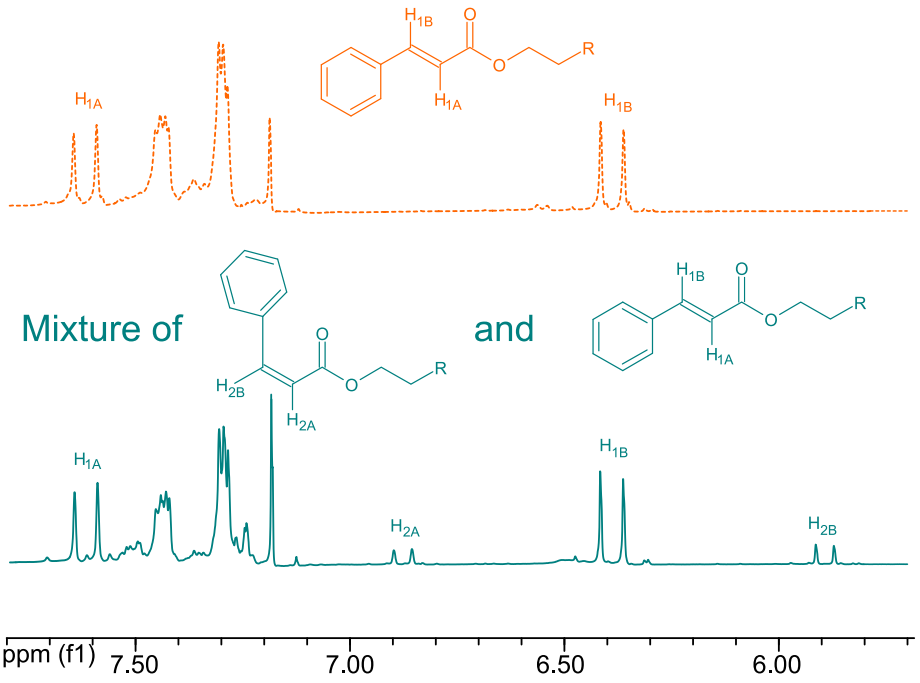

FIGURE 7.5: *The NMR-spectrum of PEGCA-S2 before (- - -) and after (—) irradiation with UV-light (λ = 302 nm) for 60 minutes. Before irradiation (- - -)the characteristic traces for the CA-group is observed with the protons from the benzene ring occurring around 7.46-7.3 ppm 3 and the protons attached to the double bond occurring at 7.65 ppm (H_{1A}) and 6.44 ppm (H_{1B}), respectively. The coupling constant J is 16 Hz confirming the trans-conformation of H_{1A} and H_{1B}. After irradiation (—) a similar pattern is observed. But two new protons occur at 6.89 ppm (H_{2A}) and 5.90 (H_{2B}). J is 12.1 Hz indicating that H_{2A} and H_{2B} are in cis-conformation. The data confirm the possibility of forming the cis-isomer of CA upon irradiation with UV-light.*

The isomerisation of the double bond in CA is documented in literature. Isomerisation is in general inhibited in solid polymer matrices but several authors argue that photo-isomerisation of polymer-bound photo-active molecules does proceed [73, 91]. The dimerisation is reported to be the dominant reaction.

The NMR-study suggests that the isomerisation occurs in solution. This is thought to be linked to the concentration of active groups and in fact the concentration of PEGCA-S2 in the solution used for the NMR-experiment was 0.079 mol/L which is similar to the concentration of PEGCA-S2 in the PEG/Desmodur/PEGCA-S2 material described in Section 5.4.4 which was 0.076 mol/L. So the isomerisation could possibly be taking place in the material too.

This and the previous section highlight two important things: Firstly the alignment of the CA-groups has an influence on the reactivity. Secondly the concentration of the photo-active polymer seems to allow for isomerisation. These two things combined reduce the possibility of positive cross-linking and may very well be part of the solution to some of the issues reported.

7.3 Size exclusion chromatography study of cinnamic acid derivatised poly(ethylene glycol

Size exclusion chromatography (SEC) cannot be applied to networks since it is essential the molecules in the sample can be dissolved and elute through the SEC-column. SEC was therefore not used to characterise PEGCA-S2 after irradiation. However, the linear mono-functional PEGs (m-PEG) could be examined both before and after UV-irradiation. It was expected that derivatised m-PEGs would dimerise upon irradiation giving rise to samples with unchanged polymers with a general M_n of M g/mol as well as the formed dimers with an M_n of $2M$ g/mol, see Figure 7.6.

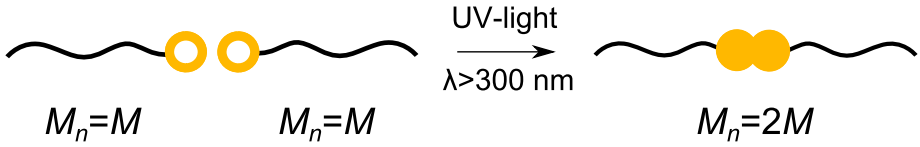

FIGURE 7.6: *Schematic drawing of the dimerisation of two mono-functional PEGCA-chains (m-PEGCA). The m-PEGCA-chains dimerise upon irradiation with UV-light. The molecular weight of the dimers is twice that on the m-PEGCA, which should make it possible to clearly distinguish the two molecules using SEC.*

Three mono-functional PEGs were derivatised with CA, namely m-PEGCA-L0.75, m-PEGCA-L2 and m-PEG-L5 (m-PEGCA-L5). The compounds were irradiated with UV-irradiation for up to 60 minutes. The irradiation was carried out both on the solid polymers as well as on solutions of the polymers. In Figure 7.7 the data obtained for m-PEGCA-L2 irradiated in solid phase can be seen.

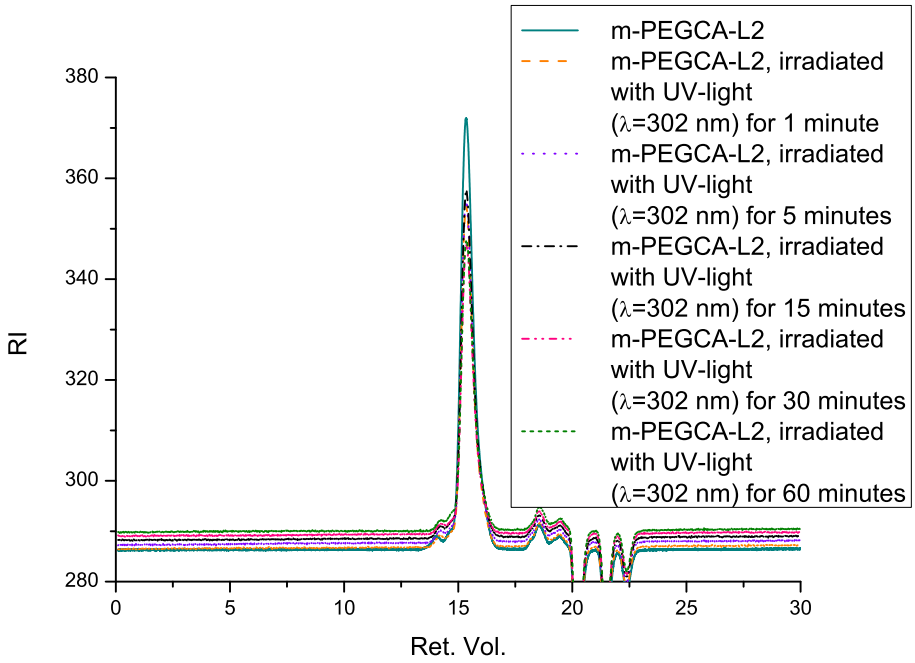

FIGURE 7.7: *SEC-traces of m-PEGCA-L2 after irradiation with UV-light ($\lambda = 302$ nm) for 0, 1, 5, 15, 30 and 60 minutes. The SEC-traces does not change after irradiation indicating no formation of dimers.*

As described earlier it was expected that the irradiation with UV-light would give rise to samples containing compounds of two different molecular weights. If this would be the case it would be displayed as two distinct peaks in the SEC-trace of the sample. But as Figure 7.7 shows only one peak occurs both before and after irradiation with UV. This indicates that the dimerisation has not taken place in the samples.

The data for m-PEG-L0.75 and m-PEG-L5 as well as the data for the irradiation in solution show the same results. The SEC-traces can be found in Appendix C.1.

7.4 Conclusion

This Chapter highlights some issues regarding the used photo-active reaction. First of all the literature suggests that the spatial orientation of the CA-group is important to achieve positive cross-linking. CA can take three possible crystal forms; α, β and γ of which only the first two can dimerise. This can be difficult to achieve with polymers since they diffuse. The possibility of the end groups to be in positive pairing position might thus be low.

Results from an NMR-study of irradiated photo-active polymers were presented.

This study showed that in solution *trans*-CA isomerises to *cis*-CA. It is argued that the isomerisation primarily occurs in cases where dimerisation is not possible due to e.g. concentration.

Finally a SEC-study of mono-functional photo-active polymers showed no trace of dimerisation.

Chapter 8

Summary and concluding remarks

The aim of this project was to develop stimuli-adaptable materials to be used in skin adhesives. The first steps into a realisation of this were taken.

A literature study was carried out and based on this it was decided to focus on UV-activated chemistry, namely the dimerisation of cinnamic acid and its derivatives. This reaction has been applied in several different polymer materials and for many different purposes. Furthermore, the reversibility of the reaction was very appealing for the suggested application. Lendlein *et al.*[15] published an increase in Young's modulus of 26 % in a system based on CA-derivatised polymers which was found to be very promising.

The first steps into the project were to determine the timescale of the reaction. Two simple models were presented and evaluated. The first was the Beer-Lambert law which proved that a large amount of UV-radiation would be absorbed in the photo-active compounds. To evaluate the timescale a simple kinetic model was developed based on the results presented by Tanaka *et al.*[33] This simple kinetic model proved that the dimerisation reaction should run to completion within approximately 1 hour. This confirmed that the timescale of the dimerisation was in the right order of magnitude, namely minutes.

It was highly desirable to be able to follow the dimerisation reaction closely by spectroscopy and the readily available FTIR- and UV-absorption spectroscopy methods were used for this. FTIR-spectroscopy proved to be very useful in determining the presence of the photo-active groups. Furthermore, FTIR-spectra of cinnamylidene acetic acid derivatised PEG showed distinct changes after irradiation with UV-light, while FTIR-spectra of CA-derivatised PEG also showed changes though not as pronounced. It was evident that changes which could be identified by FTIR-spectroscopy occurred in the compounds but it was concluded that FTIR was not the right tool to follow the reaction and other possibilities were explored.

A thorough study of the UV-absorption spectra of CA and CA-derivatised PEG were made and showed that UV was a powerful tool in the study of the dimerisation reaction. It was observed that both the UV-induced dimerisation (irradiation with $\lambda > 300$ nm) as well as the dissociation of the dimers (irradiation with $\lambda < 300$ nm) gave rise to changes in the UV-absorption spectra of the compound. It was found that for the CA-derivatised PEG after 60 minutes of irradiation with UV-light no

further changes were observed for the dimerisation reaction.

The outcome of the study of the models and the FTIR- and UV-spectroscopy was that a timescale of minutes for the dimerisation reaction could be expected. This was sufficient and the work was continued with cinnamic acid based photo-active polymers.

A study of the photo-active polymers and their material properties was carried out. PEG-polymers derivatised with cinnamylidene acetic acid groups showed macroscopic changes after irradiation with UV-light. However, some issues with using cinnamylidene acetic acid were identified. A large excess of the compound was needed in the derivatisation reaction wherefore it was synthesised in-house via the Knoevenagel reaction. The yields were low and after it other possibilities were discussed. Several published studies used cinnamic acid with promising results and it was therefore decided to use this photo-active compound instead of cinnamylidene acetic acid.

A number of cinnamic acid derivatised PEG-polymers were produced and their properties were studied thoroughly. Two linear and one 4-armed star shaped cinnamic acid derivatised PEGs were prepared and the rheological properties of mixtures of the polymers were determined before and after irradiation with UV-light for one hour. It was found that the most profound development of material properties occurred for the sample consisting solely of the star shaped cinnamic acid derivatised PEG. A time-dependence study was carried out to determine the development of the rheological properties as a function of irradiation time. It was observed that after approx. 24 hours of irradiation a film was formed and after approx. 70 hours of irradiation the properties were stable.

The irradiation time needed was significantly larger than expected and it was observed that the reversibility of the reaction was obstructed. It also proved difficult to fully reproduce all the data.

It was expected that some of the issues regarding the systems consisting solely of the photo-active polymers would be resolved when the photo-active polymers were incoporated into a permanent network. Several different inter-penetrating networks of this type were prepared. Firstly systems where both the permanent and the switchable network consisted of PEG-polymers were investigated.

An UV-study proved that a reaction was occurring in the IPN-materials and that the observed differences were not due to break-down of the permanent network. Furthermore, the study proved that the most pronounced and stable development were obtained with networks with approx. 20 w% photo-active polymer.

Irradiation of PEG-L10/PEGHDI-S2/PEGCAA-L15 (0.45, 36 w% PEGCAA-L15) gave no changes in rheological properties. This is expected to be because M_n of the applied polymers is above the molecular entanglement weight.

A material consisting of PEG-L4/PEGHDI-S2/PEGCA-L1 (1.06, 20 w% PEGCA-L1) showed a decrease of G' and G'' after irradiation for 30 minutes. The reason for the decrease in the rheology parameters is unclear but the change encouraged further work with this type of systems.

The PEG-L4/PEGHDI-S2/PEGCA-S2 (0.75, 28 w% PEGCA-S2) material proved the expectations by clearly showing a solvent effect when the photo-active polymer was introduced into the permanent network. Furthermore, a significant increase of G' and G'' was observed after 72 h of irradaition with UV-light proving the formation of a second network consisting of the photo-active polymers.

A similar sample, namely PEG-L4/PEGHDI-S2/PEGCA-S2 (0.5, 24 w% PEGCA-S2), was also investigated but gave very different results due to the lower r-value. The applied r-value is significantly closer to r_c and thus resulted in problems with the film formation. Nevertheless, a film was formed after irradiation for 72 h and the data showed that the secondary network dominates the rheological properties of this network.

A material with shorter chains in the permanent network (PEG-L1/Desmodur/-PEGCA-S2 (0.84, 19.2 w% PEGCA-S2)) was also investigated but showed no change after irradiation with UV-light for 15 minutes. This is related to the stiffness of permanent matrix.

The first steps into preparing IPN-materials with different polymers in the permanent network and the switching segment were also taken. Incorporating cinnamylidene acetic acid derivatised PEG in a PDMS-network resulted in no cross-linking of the PDMS. This could be due to deactivation of the catalyst.

Cinnamic acid derivatised PEG was swelled into PPO-networks forming PPO/-PTM/PEGCA-S2 materials. It was observed that introducing the photo-active PEG into the PPO-network changed the appearance of the material from a clear sample to an opaque yellow sample. Two UV-irradiation procedures were tested but none of the samples displayed a change in rheological properties after irradiation with UV-light.

To address some of the questions that occurred during the project a discussion of the mobility and the reactivity of the polymers was made. The mobility and structure of the polymers give a system where it can be difficult for two end groups to meet and dimerise. This statement is underlined by data from NMR and SEC. The NMR-data proved the formation of the *cis*-isomer of cinnamic acid and SEC showed no trace of dimerisation of mono-functional photo-active polymers. The formation of the *cis*-isomer should only occur in case dimerisation is somehow hindered. We expect that this is closely related to the concentration of the photo-active polymers.

All things considered this thesis shows that:

- It is possible to create a UV-controllable material and determine the rheological properties of this. In fact the PEG-L4/PEGHDI-S2/PEGCA-S2 (0.75, 28 w% PEGCA-S2) material fully meet the expected development of properties.

- There is an issue regarding the irradiation times. Our preliminary studies, namely the simple models and the UV-studies, show that the dimerisation re-

action occurs within minutes. The obtained results suggest that several hours are needed for significant changes in the properties. This is not fully explained but it is expected that a key to this question is related to the concentration of the photo-active group. NMR-data confirm the formation of the *cis*-isomer of the photo-active group which should only occur in case the dimerisation is not favoured. This is expected to be related to the concentration and design of the photo-active polymer.

Chapter 9

Future work and outlook

This thesis presents a number of interesting results which form the first steps towards the realisation of a switchable adhesive based on CA-derivatised polymers. In this section the next steps are outlined.

9.1 Final work with cinnamic acid derivatised poly(ethylene glycol)

First of all the possibility of determining the extent of reaction in detail would be very much appreciated. It is expected that carrying out Raman-spectroscopy on the CA-derivatised polymers could give important information on this. Raman spectroscopy gives a quite unique possibility to focus on carbon-carbon double bonds which would be very useful. Knowledge of the extent of reaction would give the final answer to whether the dimerisation of CA is in fact applicable for the proposed adhesive as our findings suggest.

It was observed that the concentration of the photo-active group is of high importance and it could therefore be interesting to examine if a higher concentration of photo-active polymers would improve the materials. Another way to achieve this could be to test a different design of the switching segment. As presented in Chapter 7 this could be polymers with grafted photo-active groups instead of active end groups.

If the results from these investigations are good the system should be ready to proceed to the next phase by further development of IPN-materials.

9.2 Further work with photo-active inter-penetrating network materials

The experiments conducted suggest that the mobility of the components in the IPN-materials are too low. This is due to the length of the chains between the cross-linking points and permanent networks with longer chains in the switching segment could be interesting to investigate. First steps into this were taken with longer PEG-chains, some of the results have been shown earlier. The mobility is increased but the preparation of the samples is more difficult since the PEG crystallises. This can probably be overcome by curing at elevated temperatures.

At this stage using polymers better applicable in adhesives could also be used. First steps were made to derivatised OH-functional PDMS with CA but a number of obstacles were met and the focus was put elsewhere. It is expected that these

obstacles can be overcome with a focused study. Another possibilty could be to use PPO.

9.3 Alternative photo-activated chemistry

It could also be interesting to screen alternative types of photo-activated reactions and primarily we find the dimerisation of coumarine interesting. This reaction offers many of the same appealing features of the dimerisation of CA.

Bibliography

[1] A. Solga, Z. Cerman, B.F. Striffler, M. Spaeth, and W. Barthlott. The dream of staying clean: Lotus and biomimetic surfaces. *Bioinspir. Biomim.*, 2(4):S126, 2007.

[2] H. Lee, B.P. Lee, and P.B. Messersmith. A reversible wet/dry adhesive inspired by mussels and geckos. *Nature*, 448(7151):338–341, 2007.

[3] A. Mahdavi, L. Ferreira, C. Sundback, J.W. Nichol, E.P. Chan, D.J.D. Carter, C.J. Bettinger, S. Patanavanich, L. Chignozha, E. Ben-Joseph, et al. A biodegradable and biocompatible gecko-inspired tissue adhesive. *Proc. Natl. Acad. Sci. USA*, 105(7):2307–2312, 2008.

[4] E. Mattsson. *Basic corrosion technology for scientists and engineers*. Ellis Horwood, second edition edition, 1996.

[5] J.R. Capadona, K. Shanmuganathan, D.J. Tyler, S.J. Rowan, and C. Weder. Stimuli-responsive polymer nanocomposites inspired by the sea cucumber dermis. *Science*, 319(5868):1370, 2008.

[6] M. Kamperman and A. Synytska. Switchable adhesion by chemical functionality and topography. *J. Mater. Chem.*, 22:19390–19401, 2012.

[7] J.F. Kenney, T.H. Haddock, R.L. Sun, and H.C. Parreira. Medical-Grade Acrylic Adhesives for Skin Contact. *J. Appl. Polym. Sci.*, 45:355–361, 1992.

[8] M.K. Jensen. *Rheology of Cross-linked Polymer Networks*. PhD thesis, Technical University of Denmark DTU, 2010.

[9] J. Comyn. *Adhesion science*. Royal Society of Chemistry, Cambridge, UK, 1997.

[10] S. Venkatraman and R. Gale. Skin Adhesives and Skin Adhesion 1. Transdermal Drug Delivery Systems. *Biomaterials*, 19:1119–1136, 1998.

[11] S. Reddy, E. Arzt, and A. del Campo. Bioinspired surfaces with switchable adhesion. *Adv. Mater.*, 19(22):3833–3837, 2007.

[12] M.W. Urban. *Handbook of stimuli-responsive materials*. Wiley Online Library, 2011.

[13] X. Yan, F. Wang, B. Zheng, and F. Huang. Stimuli-responsive supramolecular polymeric materials. *Chem. Soc. Rev.*, 41:2985–2689, 2012.

[14] R.J. Wojtecki, M.A. Meador, and S.J. Rowan. Using the dynamic bond to access macroscopically responsive structurally dynamic polymers. *Nature mater.*, 10(1):14–27, 2010.

[15] A. Lendlein, H. Jiang, O. Jünger, and R. Langer. Light-induced shape-memory polymers. *Nature*, 434(7035):879–882, 2005.

[16] Z. Ge, J. Hu, F. Huang, and S. Liu. Responsive supramolecular gels constructed by crown ether based molecular recognition. *Angew. Chem. Int. Ed.*, 48(10):1798–1802, 2009.

[17] D. Ratna and J. Karger-Kocsis. Recent advances in shape memory polymers and composites: a review. *J. Mater. Sci.*, 43(1):254–269, 2008.

[18] F. Liu and M. W. Urban. Recent advances and challenges in designing stimuli-responsive systems. *Prog. Polym. Sci.*, 35:3–23, 2010.

[19] T. Baltes, F. Garret-Flaudy, and R. Freitag. Investigation of the LCST of polyacrylamides as a function of molecular parameters and the solvent composition. *J. Polym. Sci. A. Polym. Chem.*, 37(15):2977–2989, 1999.

[20] A.C.W. Lau and C. Wu. Thermally sensitive and biocompatible poly(N-vinylcaprolactam): Synthesis and characterization of high molar mass linear chains. *Macromolecules*, 32(3):581–584, 1999.

[21] F. Liu and M.W. Urban. 3D directional temperature responsive (N-(DL)-(1-Hydroxymethyl) propylmethacrylamide-co-n-butyl acrylate) colloids and their coalescence. *Macromolecules*, 41(2):352–360, 2008.

[22] I. Idziak, D. Avoce, D. Lessard, D. Gravel, and X.X. Zhu. Thermosensitivity of aqueous solutions of poly(N,N-diethylacrylamide). *Macromolecules*, 32(4):1260–1263, 1999.

[23] Y.G. Takei, T. Aoki, K. Sanui, N. Ogata, Y. Sakurai, and T. Okano. Dynamic contact angle measurement of temperature-responsive surface properties for poly(N-isopropylacrylamide) grafted surfaces. *Macromolecules*, 27(21):6163–6166, 1994.

[24] Y. Osada and A. Matsuda. Shape memory in hydrogels. *Nature*, 376(6537):219, 1995.

[25] F. Liu and M.W. Urban. Dual Temperature and pH Responsiveness of Poly(2-(N,N-dimethylamino) ethyl methacrylate-co-n-butyl acrylate) Colloidal Dispersions and Their Films. *Macromolecules*, 41(17):6531–6539, 2008.

[26] I. Bellin, S. Kelch, R. Langer, and A. Lendlein. Polymeric triple-shape materials. *Proc. Natl. Acad. Sci. USA*, 103(48):18043–18047, 2006.

[27] M. Behl and A. Lendlein. Triple-shape polymers. *J. Mater. Chem.*, 20(17):3335–3345, 2010.

[28] H. Koerner, G. Price, N.A. Pearce, M. Alexander, and R.A. Vaia. Remotely actuated polymer nanocomposites - stress-recovery of carbon-nanotube-filled thermoplastic elastomers. *Nature Mater.*, 3(2):115–120, 2004.

[29] S. Tamesue, Y. Takashima, H. Yamaguchi, S. Shinkai, and A. Harada. Photoswitchable supramolecular hydrogels formed by cyclodextrins and azobenzene polymers. *Angew. Chem.*, 122(41):7623–7626, 2010.

[30] R. Rojanathanes, B. Pipoosananakaton, T. Tuntulani, W. Bhanthumnavin, J.B. Orton, S.J. Cole, M.B. Hursthouse, M.C. Grossel, and M. Sukwattanasinitt. Comparative study of azobenzene and stilbene bridged crown ether *p-tert*-butylcalix[4]arene. *Tetrahedron*, 61(5):1317–1324, 2005.

[31] S.L. Gilat, S.H. Kawai, and J.M. Lehn. Light-triggered molecular devices: photochemical switching of optical and electrochemical properties in molecular wire type diarylethene species. *Chemistry*, 1(5):275–284, 1995.

[32] H. Y. Jiang, S. Kelch, and A. Lendlein. Polymers Move in Response to Light. *Adv. Mater.*, 18:1471–1475, 2006.

[33] H. Tanaka and K. Honda. Photoreversible Reactions of Polymers Containing Cinnamylideneacetate Derivatives and the Model Compounds. *J. Polym. Sci., Polym. Chem. Ed.*, 15:2985–2689, 1977.

[34] T. Yamaoka, K. Ueno, and T. Tsunoda. A study on phenoxy-resin esters of cinnamylideneacetic acid and its derivatives. *Polymer*, 18:81–86, 1977.

[35] F. M. Andreopoulos, C. R. Deible, M. T. Stauffer, S. G. Weber, W. R. Wagner, E. J. Beckman, and A. J. Russell. Photoscissable Hydrogel Synthesis via Rapid Photopolymerization of Novel PEG-Based Polymers in the Absence of Photoinitiators. *J. Am. Chem. Soc.*, 118:6235–6240, 1996.

[36] F. M. Andreopoulos, E. J. Beckman, and A. J. Russell. Light-induced tailoring of PEG-hydrogel properties. *Biomaterials*, 19:1343–1352, 1998.

[37] X. Coqueret. Photoreactivity of polymers with dimerizable side-groups: Kinetic analysis for probing morphology and molecular organization. *Macromol. Chem. Phys.*, 200:1567–1579, 1999.

[38] K.M. Gattás-Asfura, Weisman; E., F. M. Andreopoulos, M. Micic, B. Muller, S. Sirpal, S. M. Pham, and R. M. Leblanc. Nitrocinnamate-Functionalized Gelatin: Synthesis and "smart" hydrogel formation via photo-cross-linking. *Biomacromolecules*, 6:1503–1509, 2005.

[39] J. Lanzo, FP Nicoletta, G. De Filpo, and G. Chidichimo. From nematic emulsions to polymer dispersed liquid crystals. *J. Appl. Phy.*, 92:4271, 2002.

[40] G. Liu and X. Zhao. Electroresponsive behavior of gelatin/alginate semi-interpenetrating polymer network membranes under direct-current electric field. *J. Macromol. Sci. A*, 43(2):345–354, 2006.

[41] A.G. Bejenariu, L. Yu, and A.L. Skov. Low moduli elastomers with low viscous dissipation. *Soft Matter*, 8(14):3917–3923, 2012.

[42] P. Brochu and Q. Pei. Advances in dielectric elastomers for actuators and artificial muscles. *Macromol. Rapid Commun.*, 31(1):10–36, 2009.

[43] A.M. Kushner, J.D. Vossler, G.A. Williams, and Z. Guan. A biomimetic modular polymer with tough and adaptive properties. *J. Am. Chem. Soc.*, 131(25):8766–8768, 2009.

[44] L. Tskhovrebova, J. Trinick, et al. Titin: properties and family relationships. *Nat. Rev. Mol. Cell Bio.*, 4(9):679–689, 2003.

[45] K.E. Feldman, M.J. Kade, E.W. Meijer, C.J. Hawker, and E.J. Kramer. Phase behavior of complementary multiply hydrogen bonded end-functional polymer blends. *Macromolecules*, 43(11):5121–5127, 2010.

[46] J. Li, C.L. Lewis, D.L. Chen, and M. Anthamatten. Dynamic Mechanical Behavior of Photo-Cross-linked Shape-Memory Elastomers. *Macromolecules*, 44(13):5336–5343, 2011.

[47] G. Ligthart, H. Ohkawa, R.P. Sijbesma, and E.W. Meijer. Complementary quadruple hydrogen bonding in supramolecular copolymers. *J. Am. Chem. Soc*, 127(3):810–811, 2005.

[48] J.M.J. Paulusse and R.P. Sijbesma. Reversible mechanochemistry of a Pd^{II} coordination polymer. *Angew. Chem.*, 116(34):4560–4562, 2004.

[49] D. Roy, J.N. Cambre, and B.S. Sumerlin. Future perspectives and recent advances in stimuli-responsive materials. *Prog. Polym. Sci.*, 35(1):278–301, 2010.

[50] D. Szabo, G. Szeghy, and M. Zrinyi. Shape transition of magnetic field sensitive polymer gels. *Macromolecules*, 31(19):6541–6548, 1998.

[51] P.M. Xulu, G. Filipcsei, and M. Zrínyi. Preparation and responsive properties of magnetically soft poly(N-isopropylacrylamide) gels. *Macromolecules*, 33(5):1716–1719, 2000.

[52] Z. Zhi and D.T. Haynie. Direct evidence of controlled structure reorganization in a nanoorganized polypeptide multilayer thin film. *Macromolecules*, 37(23):8668–8675, 2004.

[53] M. Orlov, I. Tokarev, A. Scholl, A. Doran, and S. Minko. pH-Responsive Thin Film Membranes from Poly (2-vinylpyridine): Water Vapor-Induced Formation of a Microporous Structure. *Macromolecules*, 40(6):2086–2091, 2007.

[54] A. Gasnier, G. Royal, and P. Terech. Metallo-Supramolecular Gels Based on a Multitopic Cyclam Bis-Terpyridine Platform . *Langmuir*, 25(15):8751–8762, 2009.

[55] J.M. Lehn. Supramolecular chemistry - Scope and perspectives: Molecules - Supermolecules - Molecular devices. *J. Incl. Phenom. Macro.*, 6(4):351–396, 1988.

[56] D. Montarnal, F. Tournilhac, M. Hidalgo, J.L. Couturier, and L. Leibler. Versatile One-Pot Synthesis of Supramolecular Plastics and Self-Healing Rubbers. *J. Am. Chem. Soc*, 131(23):7966–7967, 2009.

[57] Y. Ito, M. Casolaro, K. Kono, and Y. Imanishi. An insulin-releasing system that is responsive to glucose. *J. Control. Release*, 10(2):195–203, 1989.

[58] F. Liu, S.C. Song, D. Mix, M. Baudyš, and S.W. Kim. Glucose-induced release of glycosylpoly(ethylene glycol) insulin bound to a soluble conjugate of concanavalin A. *Bioconjugate Chem.*, 8(5):664–672, 1997.

[59] I. Hisamitsu, K. Kataoka, T. Okano, and Y. Sakurai. Glucose-responsive gel from phenylborate polymer and poly(vinyl alcohol): prompt response at physiological pH through the interaction of borate with amino group in the gel. *Pharmaceut. Res.*, 14(3):289–293, 1997.

[60] R.V. Ulijn. Enzyme-responsive materials: a new class of smart biomaterials. *J. Mater. Chem.*, 16(23):2217–2225, 2006.

[61] Z.R. Lu, P. Kopečková, and J. Kopeček. Antigen responsive hydrogels based on polymerizable antibody Fab' fragment. *Macromol. Biosci.*, 3(6):296–300, 2003.

[62] F. Meng, W.E. Hennink, and Z. Zhong. Reduction-sensitive polymers and bioconjugates for biomedical applications. *Biomaterials*, 30(12):2180–2198, 2009.

[63] K. Sumaru, M. Kameda, T. Kanamori, and T. Shinbo. Characteristic phase transition of aqueous solution of poly(N-isopropylacrylamide) functionalized with spirobenzopyran. *Macromolecules*, 37(13):4949–4955, 2004.

[64] R. Bogue. Recent developments in adhesive technology: a review. *Assembly Automation*, 31(3):207–211, 2011.

[65] S.L.R. Barker, D. Ross, M.J. Tarlov, M. Gaitan, and L.E. Locascio. Control of flow direction in microfluidic devices with polyelectrolyte multilayers. *Anal. Chem.*, 72(24):5925–5929, 2000.

[66] A. Kikuchi and T. Okano. Pulsatile drug release control using hydrogels. *Adv. Drug Deliv. Rev.*, 54(1):53–77, 2002.

[67] L.K. Ista, V.H. Pérez-Luna, and G.P. López. Surface-grafted, environmentally sensitive polymers for biofilm release. *Appl. Environ. Microb.*, 65(4):1603–1609, 1999.

[68] C. de las Heras Alarcón, S. Pennadam, and C. Alexander. Stimuli responsive polymers for biomedical applications. *Chem. Soc. Rev.*, 34(3):276–285, 2005.

[69] H.C. Kim, S. Kreiling, A. Greiner, and N. Hampp. Two-photon-induced cycloreversion reaction of coumarin photodimers. *Chem. Phys. Lett.*, 372(5):899–903, 2003.

[70] F. Chambon and H.H. Winter. Linear viscoelasticity at the gel point of a crosslinking PDMS with imbalanced stoichiometry. *J. Rheol.*, 31(8):683–697, 1987.

[71] J. Clayden, N. Greeves, S. Warren, and P Wothers. *Organic Chemistry*. Oxford University Press, 2001.

[72] R. Venkatasamy, L. Faas, A. R. Young, A. Raman, and R. C. Hider. Effects of piperidine analogues on stimulation of melanocyte proliferation and melanocyte differentiation. *Bioorgan. Med. Chem.*, 12:1905–1920, 2004.

[73] P. Gupta, S.R. Trenor, E. Timothy, and G.L. Wilkes. In situ photo-cross-linking of cinnamate functionalized poly (methyl methacrylate-co-2-hydroxyethyl acrylate) fibers during electrospinning. *Macromolecules*, 37(24):9211–9218, 2004.

[74] T. Fujiwara, Y. Kimura, and I. Teraoka. Tailoring of block copolymers based on the stoichiometric control of the end-functionality of telechelic oligomers and the utilization of large-scale fractionation by phase fluctuation chromatography: A synthetic strategy for the preparation of end-functionalized poly(L-lactide)-block-poly(oxyethylene). *J. Polym. Sci. A. Polym. Chem.*, 38(13):2405–2414, 2000.

[75] M. Sandholzer, S. Bichler, F. Stelzer, and C. Slugovc. UV-induced crosslinking of ring opening metathesis block copolymer micelles. *J. Polym. Sci. A. Polym. Chem.*, 46(7):2402–2413, 2008.

[76] Y. Nakayama and T. Matsuda. Preparation and Characteristics of Photocrosslinkable Hydrophilic Polymer Having Cinnamate Moiety. *J. Polym. Sci. A. Polym. Chem.*, 30:2451–2457, 1992.

[77] E. Lemaitre, X. Coqueret, R. Mercier, A. Lablache-Combier, and C. Loucheux. Photochemistry of polymeric systems VII. Photo-cross-linking of liquid polysiloxanes including cinnamic groups. *J. Appl. Polym. Sci.*, 33(6):2189–2201, 1987.

[78] L. Wu, C. Jin, and X. Sun. Synthesis, Properties, and Light-Induced Shape Memory Effect of Multiblock Polyesterurethanes Containing Biodegradable Segments and Pendant Cinnamamide Groups. *Biomacromolecules*, 12(1):235–241, 2010.

[79] Y. Jiao, J. Guo, X. Dong, R. Li, and J. Wei. Kinetic analysis of solid-state photodimerization reaction of photosensitive monomers and a polymer with cinnamoyl moieties. *J. Appl. Polym. Sci.*, 116(6):3569–3580, 2010.

[80] J.R. Fried. *Polymer science and technology*. Prentice Hall PTR, 2nd edition, 2003.

[81] S.C. Kim, D. Klempner, K.C. Frisch, HL Frisch, and H. Ghiradella. Polyurethane - polystyrene interpenetrating polymer networks. *Polym. Eng. Sci.*, 15(5):339–342, 1975.

[82] H.L. Frisch. Interpenetrating polymer networks. *Brit. Polym. J.*, 17(2):149–153, 1985.

[83] L.H. Sperling and V. Mishra. The current status of interpenetrating polymer networks. *Polymer. Adv. Tech.*, 7(4):197–208, 1996.

[84] L.J. Fetters, D.J. Lohse, D. Richter, T.A. Witten, and A. Zirkel. Connection between polymer molecular weight, density, chain dimensions, and melt viscoelastic properties. *Macromolecules*, 27(17):4639–4647, 1994.

[85] M. Molberg, D. Crespy, P. Rupper, F. Nüesch, J.A.E. Månson, C. Löwe, and D.M. Opris. High breakdown field dielectric elastomer actuators using encapsulated polyaniline as high dielectric constant filler. *Adv. Funct. Mater.*, 20(19):3280–3291, 2010.

[86] S.M.G. Frankær, M.K. Jensen, A.G. Bejenariu, and A.L. Skov. Investigation of the properties of fully reacted unstoichiometric polydimethylsiloxane networks and their extracted network fractions. *Rheol. Acta*, 51:559–567, 2012.

[87] K. Tanaka and F. Toda. Solvent-Free Organic Reactions. *Chem. Rev*, 100:1025–1074, 2000.

[88] I. Abdelmoty, V. Buchholz, L. Di, C. Guo, K. Kowitz, V. Enkelmann, G. Wegner, and B.M. Foxman. Polymorphism of cinnamic and α-truxillic acids: New additions to an old story. *Cryst. Growth Des.*, 5(6):2210–2217, 2005.

[89] G. Kaupp. Photodimerization of cinnamic acid in the solid state: new insights on application of atomic force microscopy. *Angew. Chem. Int. Ed.*, 31(5):592–595, 2003.

[90] S.D.M. Allen, M.J. Almond, J.L. Bruneel, A. Gilbert, P. Hollins, and J. Mascetti. The photodimerisation of *trans*-cinnamic acid and its derivatives: a study by vibrational microspectroscopy. *Spectrochim. Acta A Mol. Biomol. Spectrosc.*, 56(12):2423–2430, 2000.

[91] P.L. Egerton, E. Pitts, and A. Reiser. Photocycloaddition in solid poly(vinyl cinnamate). The photoreactive polymer matrix as an ensemble of chromophore sites. *Macromolecules*, 14(1):95–100, 1981.

Appendix A

Synthesis

A.1 Chemicals

Poly(ethylene glycol) (PEG) (4-armed star, M_n=2000 g/mol) was acquired from Creative PEGWorks. Linear PEG (M_n=1000, 4000 and 15000 g/mol) was acquired from MERCK-Schuchardt. Mono-functional PEG (M_n=750 g/mol) was acquired from Acros Chemicals. Desmodur N3300 was kindly provided by Bayer. Vinyl functional poly(dimethyl siloxane) (PDMS) (M_n=28000 g/mol), the 3-functional cross-linker phenyltris(dimethylsilyloxy) silane (HMS) and the catalyst (SIP6828, a platinum-cyclovinylmethylsiloxane complex) was acquired from Gelest Inc. Cinnamylidene acetic acid (5-phenylpenta-2,4-dienoic acid) (CAA) was acquired from Apollo Scientific. All other chemicals were acquired from Sigma-Aldrich.

A.2 $SOCl_2$-mediated derivatisation of poly(ethylene glycol) with cinnamylidene acetic acid and cinnamic acid

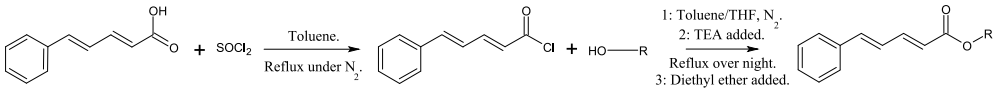

Cinnamylidene acetic acid (CAA) (7.89 g, 0.045 mol, app. 100 equiv) was dissolved by stirring in dry toluene under N_2-atmosphere. $SOCl_2$ (16.5 mL, 0.2272 mol, app. 500 eq) was added dropwise and the mixture was refluxed at 75 °C for 3.5 hours. Dry PEG (4-armed star, M_n = 2000 g/mol, 0.952 g, $0.476 \cdot 10^{-3}$ mol, 1 eq) was dissolved in dry toluene/tetrahydrofurane and stirred for 20 minutes. The solution of CAA/$SOCl_2$ was added dropwise to the solution of PEG and 1 mL triethyl amine (TEA) was added slowly. The mixture refluxed under N_2 overnight at 80 °C. The solution was concentrated and 80 mL diethyl ether was added. The product was recovered by filtration as a white solid (47% yield).

TABLE A.1: *Details from the preparation of PEGCAA.*

m(PEG) g	m(CAA) g	V($SOCl_2$) mL	V(TEA) mL	Yield
0.952[1]	7.89	16.5	1.00	47 %
0.6[1]	5.27	11.0	0.80	6 %
7.22[2]	4.12	8.60	0.80	101 %[3]
0.634[1]	4.48[4]	11.0	1.00	59 %
1.02[5]	7.44[4]	21.0	1.00	40 %
1.05[1]	7.53[4]	19.0	1.00	-

[1] 4-armed star, M_n=2000 g/mol.
[2] Linear, M_n=15000 g/mol.
[3] Probably due to residual solvent trapped in the product.
[4] Cinnamic acid used instead of cinnamyldiene acetic acid. Used for preparation of PEGCA.
[5] Linear, M_n=1000 g/mol.

A.3 Synthesis of cinnamylidene acetic acid

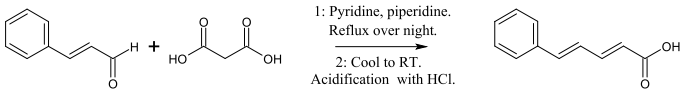

Cinnamaldehyde (12.1 mL, 0.102 mol, 1 equiv) and malonic acid (10.0 g, 0.096 mol, 0.94 eq) was stirred in pyridine (9 mL) for 10 min. Piperidine (0.05 mL, 0.0005 mol, 0.005 eq) was added and the mixture refluxed overnight at 115 °C. The mixture was cooled to RT and acidified with 1 M HCl yielding a yellowish precipitate. Recrystallisation from ethanol (two times) yielded a white-yellow solid (9% yield).

TABLE A.2: *Details from synthesis of CAA.*

V(cinnamaldehyde) mL	m(malonic acid) g	V(pyridine) mL	V(piperidine) mL	Yield
12.1	10.00	9, 10	0.05	9 %[1]
1.2	2.002	20	-	-[2]
1.2	2.007	20	0.01	-[2]
1.2	2.007	20	0.05	-[2]
1.2	2.000	1	0.05	-[3]

[1] 9 mL pyridine added initially. 10 mL added after reflux over night.
[2] 1 eq CA to 2 eq malonic acid. No product could be isolated.
[3] 1 eq CA to 2 eq malonic acid. Additional 6 mL of pyridine was added after reflux over night. No product could be isolated.

A.4 General procedure for preparation of cinnamic acid derivatised poly(ethylene glycol) via N,N'-dicyclohexylcarbodiimide/4-dimethylamidopyridine mediated esterification

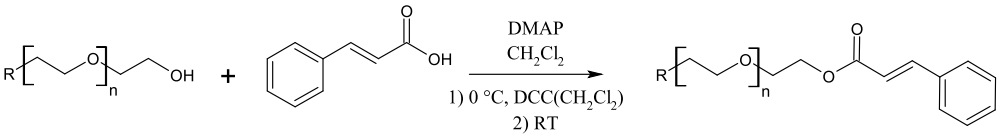

PEG (4-armed star, 6.07 g, 3.03 mmol, 12.1 mmol OH-groups, M_n=2000 g/mol) was dried by dissolution in CH_2Cl_2 and toluene followed by evaporation *in vacuo*. A solution of cinnamic acid (CA) (2.36 g, 15.9 mmol) and 4-dimethylamidopyridine (DMAP) (0.454 g, 3.64 mmol) in CH_2Cl_2 (3 mL) was added and the mixture was stirred at 0 °C under N_2. To the mixture a solution of *N,N'*-dicyclohexylcarbodiimide (DCC) (3.26 g, 15.8 mmol) in CH_2Cl_2 (2 mL) was added dropwise. The mixture was

stirred at RT for 15 hours. The product was recovered by precipitation in cold dry ether as a yellow oil (5.50 g, 72% yield, $T_g = -52.4$°C, $T_m = 0.11$°C, $M_n \approx= 3500$ g/mol, PDI=1.06). IR(cm^{-1}): 3061 (=C-H stretch), 2869 (C-H stretch), 1710 (C=O stretch), 1636 (C=C stretch), 1093 (C-O stretch). ^{1}H-NMR ($CDCl_3$, 300 MHz)(ppm): 7.69 (d, 4H, J=16.0 Hz, (C_6H_5)-CH=CH), 7.51 (m, 8H, (C_6H_5)-CH=CH), 7.37 (m, 12H, (C_6H_5)-CH=CH), 6.46 (d, 4H, J=16.0 Hz, (C_6H_5)-CH=CH), 4.35 (m, 8H, CH=CH-C(O)OCH_2CH_2), 3.76 (m, 8H, CH=CH-C(O)OCH_2CH_2), 3.61 (m, 208H, C(O)$OCH_2CH_2(OCH_2CH_2)_n$).

TABLE A.3: *Details from the preparation of PEGCA.*

m(CA) g	m(PEG-S2) g	m(DCC) g	m(DMAP) g	Yield
0.750	1.95[1]	1.20	0.145	-
0.730	1.98[1]	1.02	0.145	71%
0.301	3.28[2]	0.433	0.061	114%[3]
1.32	3.57	1.84	0.260	35%
13.2	3.57	1.84	0.261	42%
0.708	1.90[1]	0.995	0.139	45%
1.89	5.01	2.66	0.366	52%
0.468[4]	1.02	1.11	0.075	26%
3.71	10.1	5.17	0.736	57%
1.86	5.01[1]	2.57	0.368	-
0.465	5.01[2]	0.688	0.093	-
5.55	15.0	7.77	1.10	97%
1.93	5.00[1]	2.72	0.372	66%
0.483	5.00	0.689	0.094	69%
2.36	6.07	3.26	0.454	72%
3.73	1.00	5.28	0.755	83%
3.71	1.00	5.18	0.739	80%
0.037	1.01[5]	0.057	0.010	-
0.998	2.09[6]	1.43	0.197	63%
0.379	2.01[7]	0.638	0.079	72%

[1] PEG-L1 used instead of PEG-S2.
[2] PEG-L4 used instead of PEG-S2.
[3] Residual solvent in the product.
[4] CAA used instead of CA.
[5] m-PEG-L5 used instead of PEG-S2.
[6] m-PEG-L0.75 used instead of PEG-S2.
[7] m-PEG-L2 used instead of PEG-S2.

A.5 One-pot procedure for preparation of samples with a permanent poly(ethylene glycol) network cross-linked with hexamethylene diisocyanate and with a switching segment of cinnamylidene acetic acid or cinnamic acid derivatised poly(ethylene glycol)

PEG (4-armed star, 0.113 g, M_n=2000 g/mol) and PEG (linear, 1.83 g, M_n=20000 g/mol) were dried and dissolved in toluene. 0.069 mL hexamethylene diisocyanate and dibutyltin dilaurate (DBTDL) was added and the mixture was transferred to a mold and left to cure at 65°C over night.

TABLE A.4: *Details from the one-pot preparation procedure.*

m(PEG-L) g	m(PEG-S2) g	HDI mL	m(PEGCAA-L15) g	DBTDL
1.88[1]	0.113	0.069[2]		0.004[2]
	2.01	0.081[2]		0.010[2]
0.552[1]	0.400	0.133[2]		0.007[2]
	2.01	0.400		
	0.531	0.170	0.104	1 dr
	0.545	0.170		2 dr
	0.241	0.070	0.208	2 dr

[1] M_n=20000 g/mol
[2] Amount of HDI given g.

A.6 Two-step procedure for preparation of samples with a permanent poly(ethylene glycol) network cross-linked with hexamethylene diisocyanate and with a switching segment of cinnamylidene acetic acid or cinnamic acid derivatised poly(ethylene glycol)

Step 1: PEG (4-armed star, 0.405 g, M_n=2000 g/mol) was dried and dissolved in toluene. HDI (1.00 mL) and DBTDL (2 dr) was added and the mixture was stirred at 65 °C for 2 hours. Concentrated *in vacuo* and dissolved in toluene.
Step 2: The product from step 1 (1.03 g) was mixed with PEG (linear, 0.8002 g, M_n=1000 g/mol) in toluene. DBTDL and PEGCAA/PEGCA was added and the mixture was left to cure in a mold at 65 °C over night.

TABLE A.5: *Details from the two-step preparation procedure.*

m(PEG-L) g	*m*(PEG-S2) g	HDI mL	*m*(PEGHDI-S2) g	*m*(PEGCAA-L15) g	DBTDL
	2.00	3.70			1 dr
0.800[1]			1.03		2 dr
	0.405	1.00			2 dr
0.895[2]			0.120		2 dr
0.564[2]			0.034	0.337	2 dr
0.973[2]	0.200				2 dr
0.761 [3]	0.213	0.450			2 dr, 2 dr
	0.198	0.450		0.200[4]	2 dr, 2 dr
	2.04	3.8			2 dr
0.640[3]	0.169	0.40		0.208[5]	2 dr, 3 dr
2.00[3]			0.333	0.751[6]	yes[7]
2.00[3]			0.500	0.970[6]	yes[7]

[1] M_n=1000 g/mol.
[2] M_n=10000 g/mol.
[3] M_n=4000 g/mol.
[4] PEGCAA-S2 added instead of PEGCAA-L15.
[5] PEGCA-L1 added instead of PEGCAA-L15.
[6] PEGCA-S2 added instead of PEGCAA-L15.
[7] The reagents were dissolved in warm anisol. The films were cures at 75 °C for 1 hour.

A.7 Preparation of PDMS-networks containing PEGCAA

Two premixes, S1 and S2, were made from PDMS (vinyl end groups, M_n=28000 g/mol), a 3-functional hydride cross-linker phenyltris(dimethylsilyloxy) silane (HMS) and the catalyst (SIP6828, a *platinumcyclovinylmethylsiloxane complex*) , see Table A.6 for details.

TABLE A.6: *Components in premix S1 and S2.*

	PDMS g	Cross-linker g	Catalyst g
S1	98	2.0	-
S2	96.99	-	3.01

For the formation of PDMS-networks S1 and S2 were mixed thoroughly in a small plastic cup and left to cure at room temperature.
For the formation of PDMS-networks containing PEGCAA-S2, additional PDMS-V31 and PEGCAA was mixed with a little solvent to dissolution. S2 added and the mixture was left to cure at room temperature.

TABLE A.7: *Details from the preparation of PDMS-films containing PEGCAA.*

m(PEGCAA-L15) g	m(PEGCAA-S2) g	m(S1) g	m(S2) g	m(PDMS-V31) g	Cross-linking observed
0.701	0.069	1.24	2.79		no[1]
0.003		1.01	0.535	1.01	yes[2]
0.014		0.996	0.506	1.01	no[3]

[1] PEGCAA-L15 and PEGCA-S2 was dissolved in toluene and S1 was added. S2 added. Additional Pt-catalyst added.
[2] PEGCAA-L15/S1/PDMS-V31 dissolved in CH_3Cl3. S2 added. PEGCAA and PDMS were not fully mixed. PEGCAA were agglomerated inside the cross-linked PDMS-film.
[3] S1 and PDMS-V31 mixed. PEGCAA-L15 dissolved in CH_3Cl_3 was added dropwise. S2 added.

A.8 Procedure for preparation of samples with a permanent poly(ethylene glycol) network cross-linked with Desmodur and with a switching segment of cinnamic acid derivatised poly(ethylene glycol)

PEG (linear, 0.040 g, $M_n = 4000$ g/mol), PEGCA-S2 (0.010 g) and Desmodur (0.004 g) were dissolved in solvent and transferred to mold. Left to cure at RT.

TABLE A.8: *Details from the preparation of PEG/Desmodur/PEGCA-networks.*

m(PEG-L4) g	m(Desmodur) g	r	m(PEGCA-S2) g	Solvent
3.06	0.302	0.986		$CHCl_3$
1.10	0.100	0.916		acetone
1.01	0.104	1.02		acetone
1.01	0.094	0.930		acetone
0.040	0.004	1.01	0.010	acetone
0.021	0.002	0.962		acetone
0.512	0.050	0.968		acetone
0.501	0.049	0.983	0.031	acetone
0.499	0.047	0.942		acetone
0.509	0.044	0.865	0.028	acetone

[1] Curing at 60°C for 60 min.
[2] Curing at 70°C for 30 min.

A.9 Procedure for preparation of samples with a permanent poly(ethylene glycol) network cross-linked with Desmodur and dibutyltin dilaurate-catalyst and with a switching segment of cinnamic acid derivatised poly(ethylene glycol)

PEG (linear, 2.01 g, M_n = 4000 g/mol) and Desmodur (0.858 g) were dissolved in solvent. DBTDL was added and the mixture was vigorously stirred. The mixture was cured at 120 °C for 1 h.

TABLE A.9: *Details from the preparation of PEG/Desmodur/PEGCA materials.*

m(PEG-L4) g	m(Desmodur) g	r	Solvent	Catalyst[1]
2.01	0.858	1.07	$CHCl_3$	+[2]
0.513	0.228	1.11	DCM	+[2]
2.01	0.835	1.04	DCM	+[2]
2.50	1.01	1.01	DCM	+[3]
1.50	0.652	1.08	DCM	+[3]
1.51	0.482	0.797	DCM	+[3]
1.00	0.300	0.750	DCM	+[3]
0.639	0.215	0.842	DCM	+[4]
1.00	0.143	0.356	DCM	-[3]
2.00	0.511	0.639	DCM	-[3]
2.00	0.592	0.740	DCM	-[2]
1.99	0.509	0.638	DCM	-[2]
0.989	0.293	0.741	-	-[2]
1.05	0.240	0.569	H_2O	-[2]
2.02	0.558	0.691	-	+[5]
2.02	1.01	1.25		+[5]
0.506	0.254	1.26	10 dr DCM	+[2]
2.02	0.427	0.530	0.4 mL DCM	7.1 mg[6]
0.199	0.417	5.22	0.2 mL DCM	1.3 mg[7]
2.01	0.438	0.545	0.2 mL DCM	-[7]
2.01	0.441	0.549	0.3 mL $CHCl_3$	5 mg[8]
1.01	0.230	0.572	0.1 mL $CHCl_3$	18 mg[8]
0.860	0.218	0.633	-	15.1 mg[8]
0.202	0.444	5.49	0.3 mL $CHCl_3$	16.4 mg[9]

[1] + = catalyst added.
[2] Curing over night at RT.
[3] Solvent removed with vacuum. Cured at RT.
[4] 0.2030 g PEGCA-S2 added (19.2 w%). Solvent removed with vacuum. Cured at RT.
[5] Cured at 60°C.
[6] Cured at 135°C.
[7] Cured at 100°C.
[8] Cured at 120°C.
[9] Cured at 80°C.

A.10 Preparation of PPO-networks

The initiator (2,2-Dimethoxy-2-phenylacetophenone, 0.026 g) (DMPA) and the four-functional cross-linker (Pentaerythritol tetra(3-mercaptopropionate) , 1.20 g) (PTM) were dissolved in toluene. Di-vinyl terminated PPO (2.08 g, M_n=13500 g/mol) was added and the compounds were thoroughly mixed. The mixture was transferred to a mold and cured under UV ($315 - 400$ nm) for 45 minutes at RT.

TABLE A.10: *Details from the preparation of PPO-networks.*

m(PPO) g	m(initiator) mg	m(PTM) mg	r
2.08	25.7	30.6	1.2
2.00	25.0	1.75	0.7
2.00	77.9	25.7	1.1
1.02	13.0	13.7	1.1
1.02	13.4	15.5	1.2
2.05	26.0	29.2	1.2

A.11 Procedure for preparation of samples with a permanent poly(propylene oxide) network cross-linked with pentaerythritol tetra(3-mercaptopropionate) and with a switching segment of cinnamic acid derivatised poly(ethylene glycol)

PEGCA-S2 was introduced into PPO networks by swelling. A solution of 6.68 g PEGCA-S2 in 50 mL CH_2Cl_2 was made. The cross-linked PPO networks were washed with CH_2Cl_2 (app. 6-20 % weight-loss). The washed networks were covered with the PEGCA-S2-solution and left for seven hours. Afterwards the residual solvent were allowed to evaporate at atmospheric conditions. networks were dried. The resulting films were opaque yellow and contained between 40 and 65 w% PEGCA-S2.

TABLE A.11: *Details from the preparation of PPO/PTM/-PEGCA materials.*

m(PPO) g	m(PPO/PEGCA) g	w% PEGCA
0.287	0.815	65%
0.067	0.112	40%
0.070	0.117	40%

Appendix B

Methods

B.1 UV-irradiation methods

Irradiation was carried out with on of the lamps specified below. The sample was placed in a distance d from the lamp and irradiated for the time specified for each experiment. If the experimental data mention that the temperature was raised this was done by placing the samples on an electrical heating plate set to the specified temperature.
UV-lamp: UV-irradiation in the $\lambda = 315 - 400$ nm range was carried out with a SolData Ultra Violet Lamp UVA 315-400 nm (mercury vapour lamp) and the intensity of the UV-light was measured with a Sentry® UV-detector (detection range: from 280-400 nm). The main peak of the emitted light is at 365 nm.
3UV-lamp: A UV-lamp with three available wavelengths ($\lambda = 254, 302$ and 365 nm) from UVP (3UVLamp, mercury lamp, 8 W) was used for irradiation of samples. Primarily it was used to irradiate with $\lambda = 254$ nm, but $\lambda = 302$ nm was also used.
UV-apparatus: An Atlas UVTest^{TM}apparatus was used for irradiation of samples. The light has $\lambda = 300 - 400$ (main peak at 340 nm) and an intensity of 0.55 W/m^2.

B.2 Spectroscopy, chromatography and rheology

NMR-spectroscopy was conducted on a Bruker 300 MHz spectrometer using CDCl3 or deuterated DMSO as solvent. Fourier-transformed infrared spectroscopy (FT-IR) was conducted on a Perkin-Elmer Spectrum One model 2000 Fourier transform infrared system with a universal attenuated total reflection sampling accessory on a ZnSe/diamond composite. The spectra were recorded in the range of 4000-525 cm^{-1} with 4 cm^{-1} resolution and 16 scans. UV-absorbance spectra were recorded with a BMG Labtech POLARstar Omega micro plate reader in the range from 220 nm to 400 nm. Molecular weights were estimated by size exclusion chromatography (SEC) carried out on a Viskotek GPCmax VE-2001 equipped with Viscotek TriSEC Model 302 triple detector array (refractive index detector, viscometer detector, and laser light scattering detector) and a Knauer K-2501 UV-detector using two PLgel mixed-D columns (from PL). The samples were run in THF at 30°C (1 mL/min). Molecular weights were estimated using polystyrene (PS) standards from PL. Differential Scanning Calorimetry (DSC) measurements were performed with a TA Instruments DSC Q1000 with a heating rate of 10 °C/min. The samples were heated to 100 °C, cooled

to -90 °C and consecutively heated to 100 °C. T_g was measured upon the second heating cycle and T_m was determined by the peak maximum of the melting peak. Small amplitude oscillatory shear (SAOS) measurements were made with a TA 2000 Rheometer from TA Instruments set to a controlled strain mode, where the chosen strain value was ensured to be within the linear regime of the materials by means of strain-sweeps. The measurements were done with parallel plate geometry of 10 or 20 mm in the frequency range from 100 Hz to 0.01 Hz and at 50°C.

B.3 Film formation

B.3.1 General film formation

In general the components were dissolved in solvent and the mixture was transferred to a mold. The mixture was cured at RT or elevated temperatures.

B.3.2 Thin film of PEGCAA-mixture on PE-backing

Thin film of a PEGCAA-mixture was prepared using an in-house designed coating device consisting of a stainless steel plate and a knife with a nominal coating height of 100 μm. The mixture of the polymers in solution were poured onto a sheet of PE-film and the knife is moved smoothly over the foil to form the film. The solvent was evaporated at atmospheric conditions overnight.

B.4 UV-absorbance of CA and PEGCA-S2 in aqueous solution.

Solutions of CA and PEGCA-S2 were made in H_2O, a few drops of aqueos NaOH (1 M) was added to ensure dissolution. The solutions of CA and PEGCA were irradiated with UV-light with $\lambda = 254$ nm and $\lambda = 302$ nm for different amounts of time, see Table B.1. After irradiation 60 μL of the solution was placed in a well on a microplate which was shielded from light until the UV-spectra could be recorded.

B.5 UV-absorbance of solid films of cinnamic acid derivatised 4-arm star poly/ethyelen glycol and inter-penetrating networks comprising this photo-active polymer

Thin films of PEGCA-S2 and PEGCA-S2/PEG/Desmodur-mixtures were made by dissolving the compounds in acetone. 60 μL of the solution was transferred to a well on the microplate and the solvent was removed by evaporation at atmospheric conditions over night.

Details from the UV-irradiation of PEGCA-S2/PEG/Desmodur-films can be found in Table B.2

TABLE B.1: *Solutions*

Photoactive compound	Solvent	c mM	UV-irradiation time minutes ($\lambda = 254$ nm)	UV-irradiation time minutes ($\lambda = 302$ nm)	UV-irradiation time minutes ($\lambda = 254$ nm)
CA	H_2O	0.344	0, 1, 2, 5, 10, 15	0, 1, 2, 3, 4, 5, 7.5, 10, 15, 30	1, 2, 5, 15
PEGCA	H_2O	0.199	-	0, 1, 2, 3, 4, 5, 7, 10, 15, 20, 25, 30, 30+30[1]	20, 30
PEGCA	H_2O	0.199	-	0, 60	60

[1] Irradiation for 30 minutes, 10 minutes break under aluminum foil, irradiation for 30 minutes.

TABLE B.2: *Networks*

w% PEGCA	r[1]	UV-irradiation time minutes ($\lambda = 302$ nm)
0	1.20	1, 2, 4, 8, 10, 15, 20, 25, 30
1.09	1.22	1, 2, 4, 8, 10, 15, 20, 25, 30
4.84	1.40	1, 2, 4, 8, 10, 15, 20, 25, 30
9.59	1.33	1, 2, 4, 8, 10, 15, 20, 25, 30
13.2	1.21	1, 2, 4, 8, 10, 15, 20, 25, 30
16.5	1.29	1, 2, 4, 8, 10, 15, 20, 25, 30
19.4	1.04	1, 2, 4, 8, 10, 15, 20, 25, 30

[1] r-value for PEG/Desmodur-matrix.

Appendix C

Supporting data

In this Appendix supporting data can be found.

C.1 SEC data from mono-functional cinnamic acid derivatised poly(ethylene glycol)

C.1.1 m-PEGCA-L0.75 irradiated in solid state

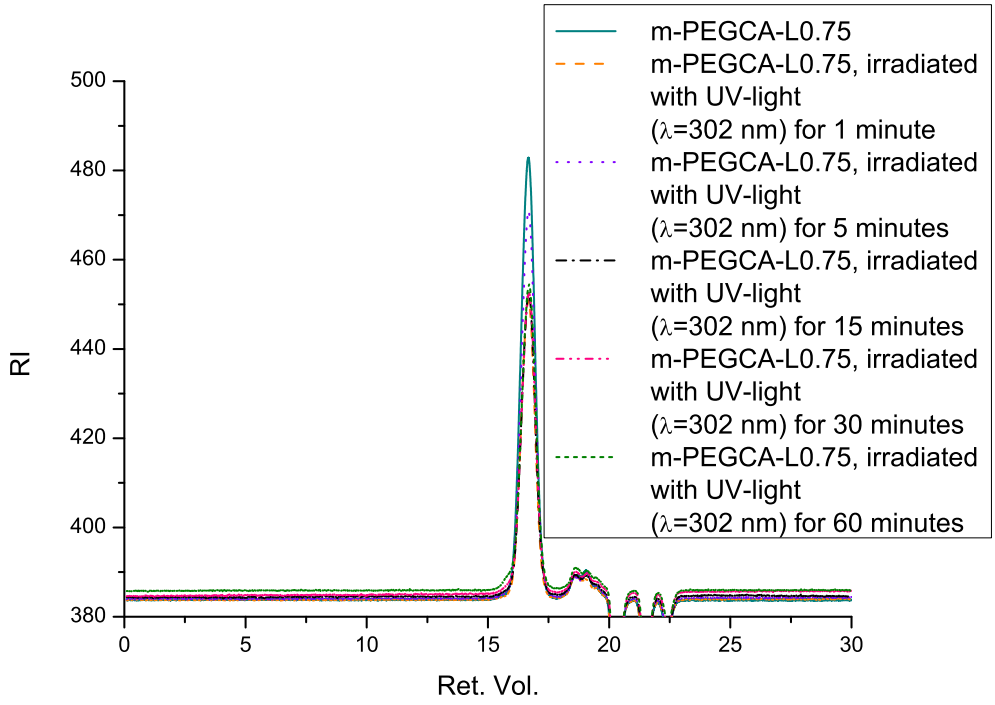

C.1.2 m-PEGCA-L5 irradiated in solid state

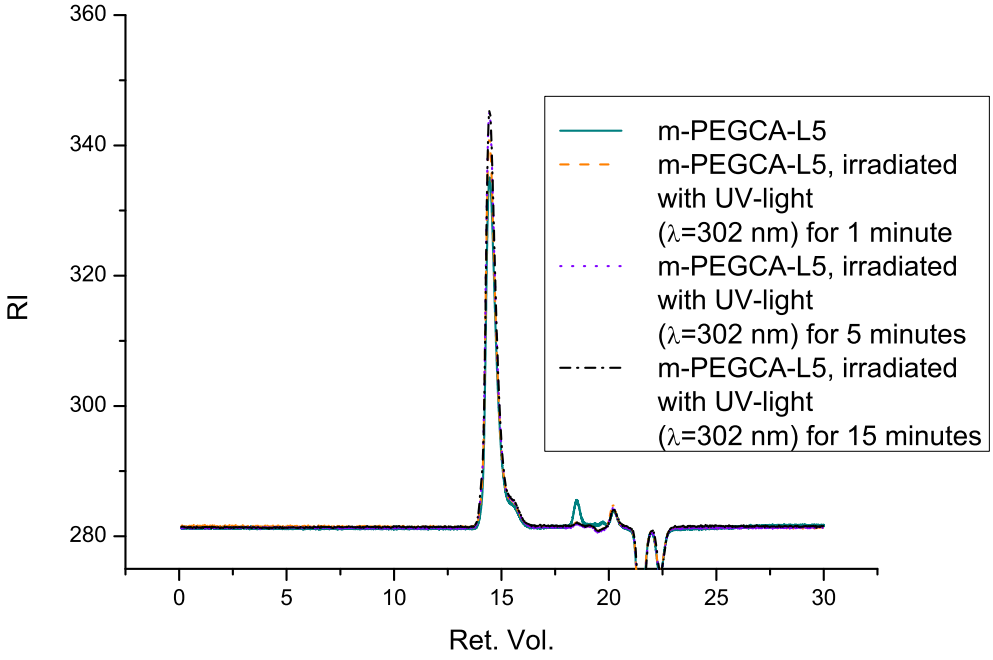

C.1.3 m-PEGCA-L0.75 irradiated in solution

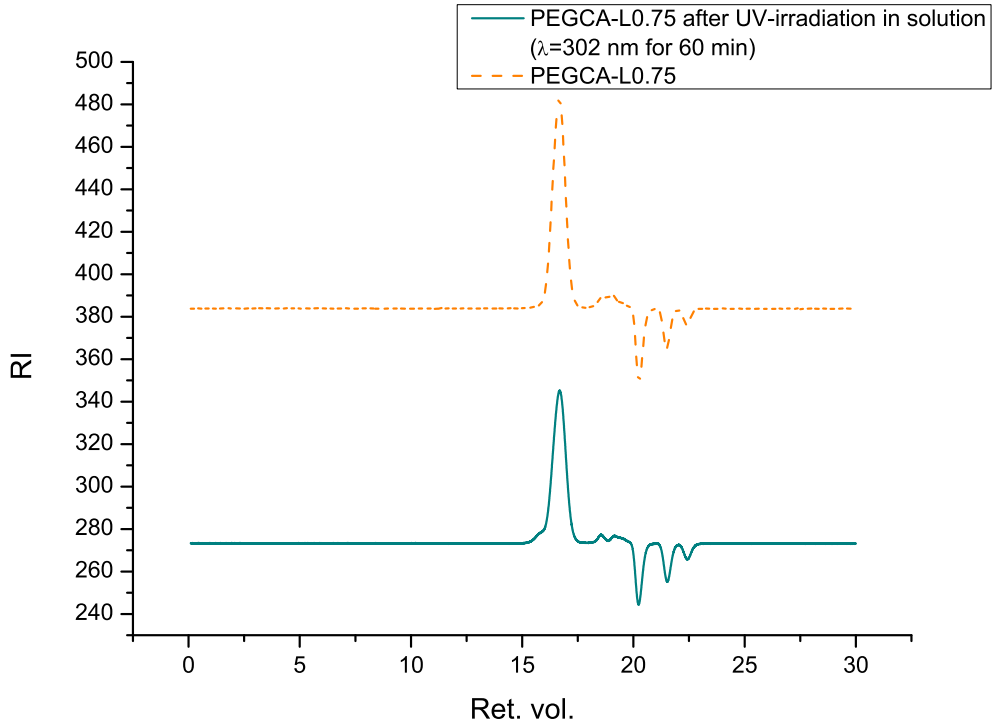

C.1.4 m-PEGCA-L2 irradiated in solution

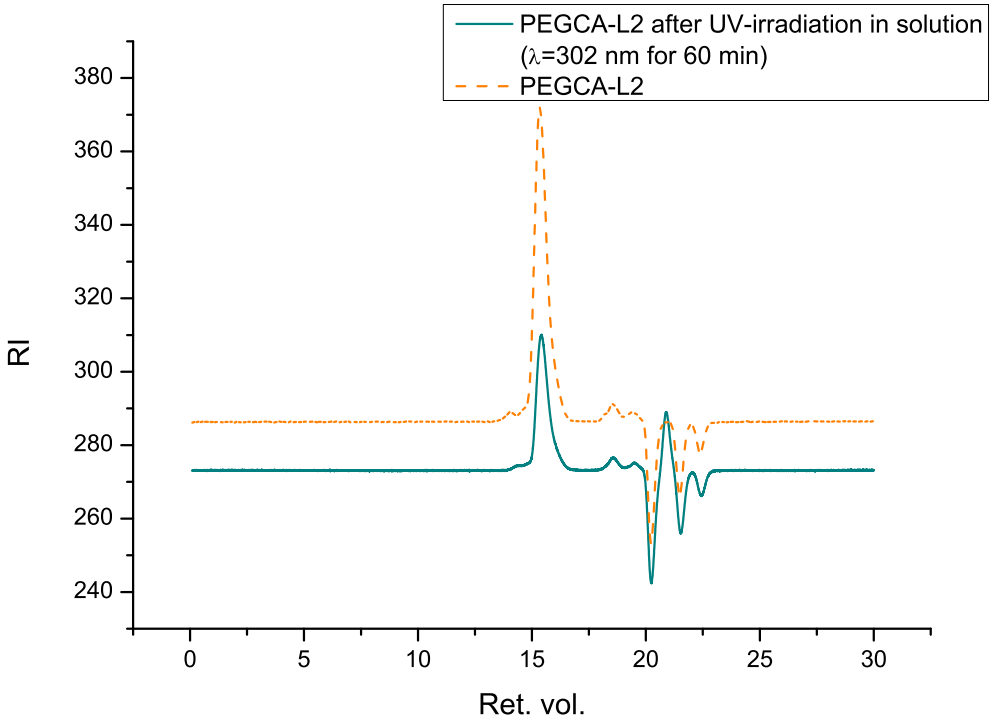

C.2 NMR-data from mono-functional cinnamic acid derivatised poly(ethylene glycol)

C.2.1 m-PEGCA-L0.75

Full spectrum.

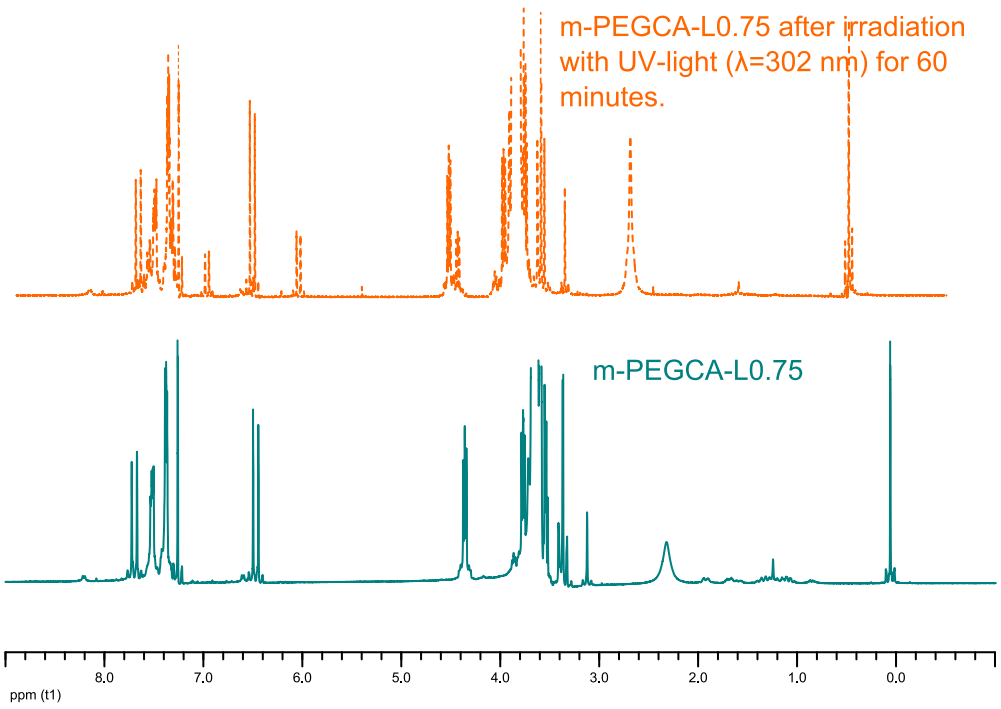

Selection of spectrum

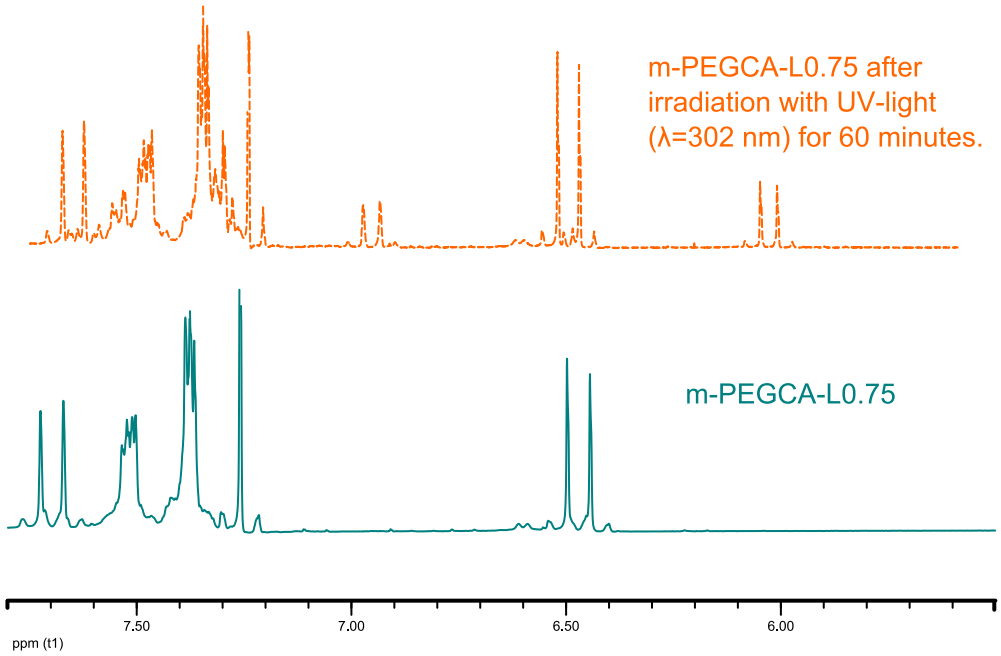

C.2.2 m-PEGCA-L2

Full spectrum.

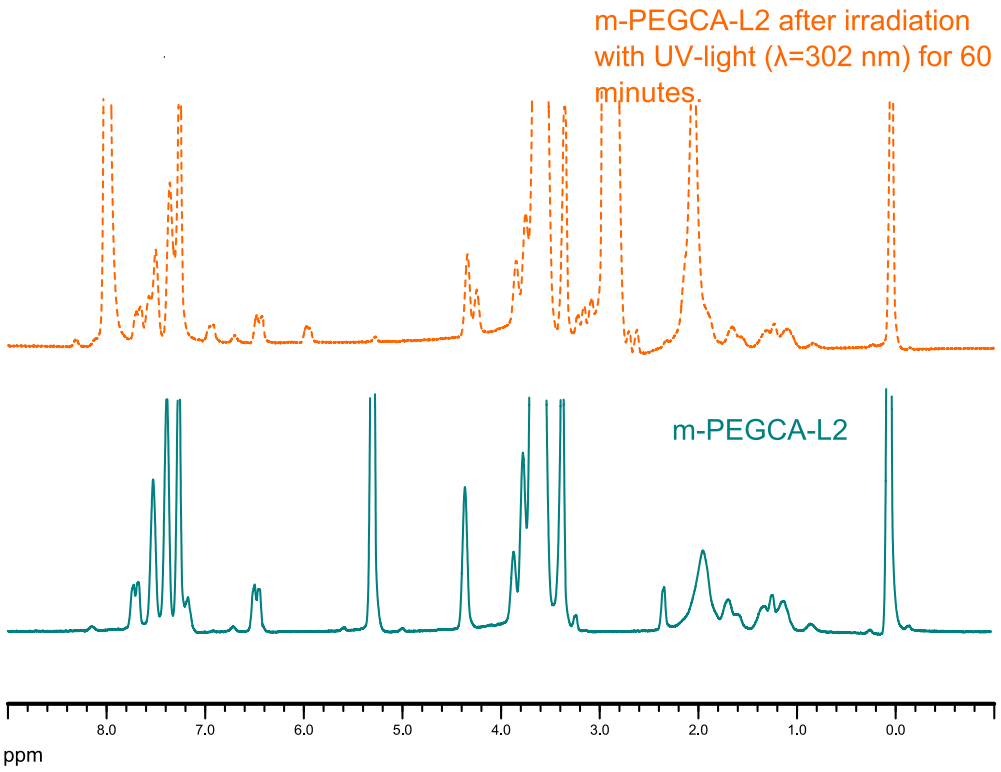

Selection of spectrum

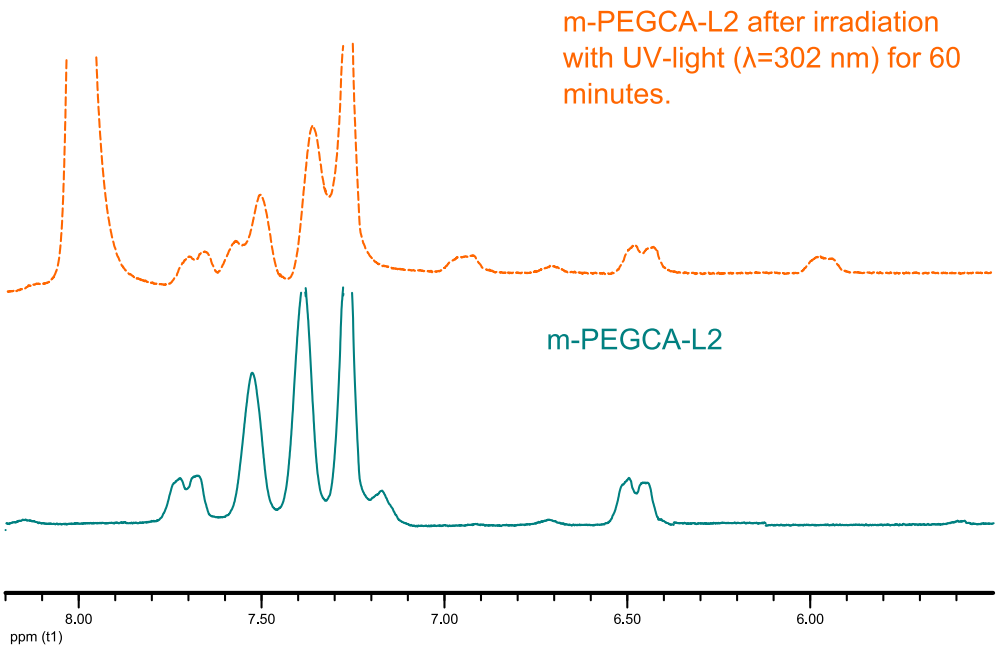

Appendix D

Articles

D.1 Article 1: Fremstilling af UV-aktive polymerer

S.M.G. Frankær, A.L.H. Di Vaia, A.E. Daugaard, S. Kiil & A.L. Skov.
Fremstilling af UV-aktive polymerer.
Dansk Kemi, **2011** (92):24-27

KEMITEKNIK

Fremstilling af UV-aktive polymerer

Naturens mangfoldighed har givet inspiration til nye materialetyper. Det gælder bl.a. søagurken, som har resulteret i materialer baseret på UV-aktive kanelsyrederivatiserede polymerer.

Af Sarah Maria Grundahl Frankær[1], Ayelén Luna Helling Di Vaia[1], Anders Egede Daugaard[1], Søren Kiil[2] og Anne Ladegaard Skov[1]
[1]Dansk Polymer Center. DTU-Kemiteknik.
[2]CHEC Forskningscentret, DTU-Kemiteknik

De seneste år er antallet af videnskabelige artikler omhandlende materialer, som efterligner dyr og planters egenskaber, steget kraftigt. Naturen har igennem lang tids udvikling løst komplicerede problemstillinger og kan derfor ofte give inspiration til fremstilling af morgendagens materialer. Et eksempel er søpølsen, der kan beskytte sig mod fjender ved at ændre sin bløde og fleksible hud til et hårdt og ufleksibelt skjold på få sekunder. Denne proces er reversibel, så når faren er drevet over, kan et stimulus fra søpølsen få den modsatrettede reaktion til at forløbe, hvormed søpølsen er tilbage til sin normale tilstand [1].

I dag kendes et stort antal reaktioner og materialer, der kan udvise sådanne stimuli. Mange af disse reaktioner aktiveres af en bestemt type udefrakommende stimuli [2]. Disse reaktioner kan overføres til polymermaterialer ved organisk syntese. Dvs. man kan fremstille stimuli-responsive polymermaterialer, og med tiden kan det resultere i en række helt nye materialetyper.

Dimerisering af kanelsyre

Et eksempel på en stimuli-responsiv reaktion er dimerisering af kanelsyre (KS), som aktiveres ved bestråling med UV-lys (boks 1). Reaktionen er blevet brugt af mange forskere. Lendlein et al. [5] har brugt den til at fremstille en "shape-memory polymer" – en polymer, som kan huske og genvinde sin oprindelige form efter deformation. KS er velegnet, da det har relativ lav giftighed, og dertil er det let at derivatisere polymerer via estersyntese. Den lave giftighed giver rig mulighed for at anvende stoffet i bioapplikationer.

Ideen bag projektet er at bruge KS-kemien til at fremstille fotoaktive polymerer. De fotoaktive polymerer skal bruges til at fremstille et materiale med et netværk, som kan krydsbindes ("tændes") og dekomponeres ("slukkes") vha. UV-lys med den rette bølgelængde. Dette materiale giver mulighed for at undersøge det "tændte" netværk bestående af fotoaktive polymerer, men også mulighed for at fremstille interpenetrerende netværk (IPN),

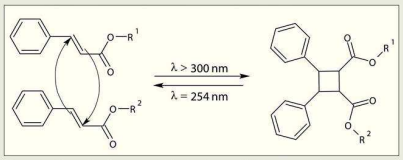

Figur 1. Dimeriseringen af derivater af KS kan opnås ved bestråling med UV-lys med bølgelængder over 300 nm. Reaktionen er reversibel, og dimererne kan dekomponeres ved bestråling med UV-lys med en lavere bølgelængde.

Boks 1. Krydsbinding af kanelsyre

Derivater af kanelsyre (KS) kan krydsbindes ved bestråling med UV-lys. Derved dannes dimerer, som vist på figur 1. Indbygges denne funktionalitet i et polymersystem, kan det bruges til krydsbinding med UV-lys med bølgelængder over 300 nm. Krydsbindingen er reversibel, og ved bestråling med UV-lys med en bølgelængde på 254 nm kan den fjernes, og den oprindelige struktur af molekylet gendannes [3]. Denne reaktion er velkendt, rapporteret i mange artikler og på mange måder attraktiv bl.a. pga. KS-gruppens lave giftighed. Dertil kan kemien anvendes i mange forskellige polymermaterialer [4-7].

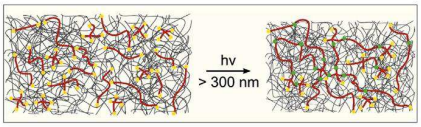

Figur 2. Illustration af "tænd"/"sluk"-netværkets funktion. Før reaktion (venstre side): Her består systemet af et permanent netværk (grå) og de fotoaktive polymerer (røde kæder og krydsbindere, gul markerer den aktive gruppe). Efter bestråling med UV-lys (λ>300 nm) (højre side): De fotoaktive polymerer har reageret, og systemet består nu af to sammenfiltrede netværk (grøn markerer reagerede grupper). Materialets egenskaber vil være ændrede pga. den øgede krydsbindingstæthed. Krydsbindingstætheden er koncentrationen af krydsbindere i netværket. Jo højere denne er, jo mere rigidt bliver materialet.

(boks 2), ved at blande de fotoaktive polymerer i et permanent bundet netværk (figur 2). Herved kan der fremstilles et materiale, der har potentiale til at efterligne f.eks. søpølsens egenskaber. Ved dannelsen af et IPN sker der en forøgelse af krydsbindingstætheden i materialet, hvorved der opnås højere værdier for det elastiske modul, G_0, for materialet samt en formindskelse af det viskøse tab.

Fremstilling af PEG-polymerer

I denne undersøgelse er KS-krydsbindingen og netværksdannelsen analyseret ved anvendelse af et polyethylenglycol-baseret (PEG-baseret) modelsystem. PEG blev valgt, da det er lettilgængeligt, har lav giftighed og er relativt let at derivatisere.

Der blev fremstillet en række forskellige KS-derivatiserede PEG-polymerer; en 4-armet stjerne (Mn=2000 g/mol) (PEGKS(2000)) samt to lineære PEG-kæder med hhv. Mn=1000 g/mol (PEGKS(1000)) og Mn=4000 g/mol (PEGKS(4000)). ▶

Boks 2. Interpenetrerende netværk

Et interpenetrerende netværk, IPN, består af to separate polymernetværk, der sameksisterer i et materiale og er fysisk uadskillelige, men hvor der ikke er nogle kemiske bindinger imellem netværkene. På figur 3 ses en skematisk illustration af et IPN. Materialer bestående af IPN giver mulighed for at kombinere to forskellige polymernetværk og ved den rette kombination opnå optimale mekaniske egenskaber for en given applikation.

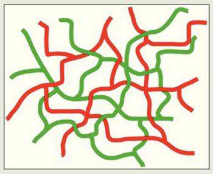

Figur 3. Illustration af et interpenetrerende netværk (IPN). Den grønne og den røde polymer er sammenfiltrede, men der er ingen kemiske bindinger imellem polymererne.

Prøve	PEGKS(2000)	PEGKS(1000)	PEGKS(4000)	Bestrålingstid	ΔG_0
A	100 vægt-%	-	-	1 time	2500 %
B	50 vægt-%	50 vægt-%	-	1 time	700 %
C	30 vægt-%	-	70 vægt-%	1 time	300 %

Tabel 1. Detaljer for de fremstillede prøver. Bestrålingen blev udført med UV-lys med λ=315-400 nm (11W, 1,98 W/cm²). De rheologiske målinger blev udført ved 50°C.

I tabel 1 ses en oversigt over de fremstillede prøver. Den mest udtalte ændring fandtes, når PEGKS(2000) blev brugt alene. I dette tilfælde blev der fundet en stigning i det elastiske modul, G_0, på 2500%. Det var forventet, at den stjerneformede polymer, PEGKS(2000), ville give den største ændring, da polymerens relativt korte arme (Mn=500 g/mol pr. arm) giver et hårdt bundet netværk pga. den høje krydsbindingstæthed.

Der blev også observeret en stærk tidsafhængighed af krydsbindingsreaktionen. I figur 4 ses udviklingen af G_0 som funktion af bestrålingstiden. Udviklingen af G_0 viser, at materialet ændrer sig gradvist fra at være en væske til at være et fast stof efter de første ca. 20 timers bestråling. Ud fra figur 4 ses det, at mindst 70 timers bestråling er nødvendig for at opnå en tilnærmelsesvis konstant værdi for G_0. Dvs. at der går flere timer, inden der kan måles en signifikant ændring i materialeegenskaberne. Det er normalt ønskeligt, at ændringen opstår væsentligt hurtigere. Søpølsen ville f.eks. være dårligt stillet, hvis det tog den et døgn at blive klar til at modstå et angreb fra et rovdyr.

Den udtalte tidsafhængighed hænger sammen med, at dimeriseringen af KS styres af den energi, UV-lyset afsætter i materialet. Derfor er effekten/intensiteten samt spektret af det anvendte UV-lys vigtigt. Som eksempel kan nævnes, at Sandholzer et al. [8], som arbejder med block-copolymerer med KS-grupper, har rapporteret 70% dimerisering efter 10 minutters bestråling med UV-lys (3000 mW/cm²) [8]. Det må derfor antages, at det kan lade sig gøre at få en hurtigere reaktionstid ved f.eks. at anvende UV-lys med en højere intensitet.

Reaktionens hastighed styres af UV-lyset og molekylernes diffusion, så længe de har fuld bevægelighed. Reaktionshastigheden sænkes efterhånden som netværket dannes, da sandsynligheden for at to aktive grupper kommer så tæt på hinanden, at de kan reagere, formindskes.

Dvs. at man ud fra samme startmateriale kan bruge metoden til at fremstille materialer med forskellige specifikke mekaniske egenskaber. Det kan gøres ved udelukkende at anvende eksterne stimuli, hvilket muliggør anvendelser svært tilgængelige steder. Det blev observeret, at UV-bestråling af en KS-derivatiseret PEG-polymer (4-armet stjerne) kunne ændre materialet fra at være en væske til et viskoelastisk materiale med G_0 på op til 1 MPa.

Søpølsen kan beskytte sig mod fjender ved at ændre sin bløde og fleksible hud til et hårdt og ufleksibelt skjold på få sekunder.

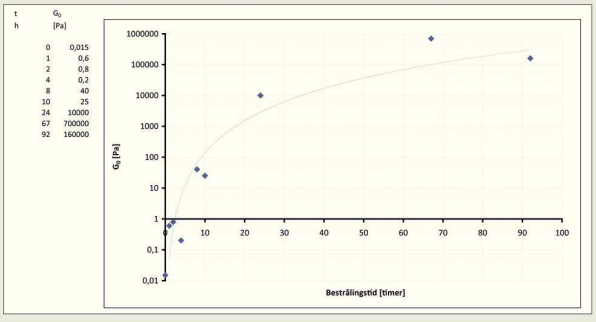

Figur 4. G_0 som funktion af bestrålingstiden (i timer). Det ses, at materialet går fra at være en væske (lave tider) til at være et fast stof (ca. 20 timer og højere). G_0 stabiliseres ved høje tider på en værdi omkring 1 MPa.

Boks 3. Typer af stimuli
En lang række stimuli, der kan aktivere stimuli-responsive polymerer, er identificeret. Hvilken stimulus, som passer til en given applikation afhænger naturligvis af denne, men alsidigheden i typer af stimuli gør, at der i de fleste tilfælde kan identificeres et brugbart system.
Her ses et udsnit af typiske stimuli [2]:

Fysiske
- Temperatur
- Elektromagnetisk stråling
- Spænding
- Magnetisme

Kemiske
- pH
- Ionstyrke
- Elektrokemi

Processen er meget tidskrævende og kræver lange belysningstider, hvilket skal forbedres, før det er praktisk muligt at anvende materialet i et egentligt produkt.

Forbedring af mekaniske egenskaber

Skal man skabe materialer med bedre mekaniske egenskaber end de undersøgte PEG-polymerer, vil det være en stor fordel, hvis KS-kemien kan overføres til andre typer af polymerer, f.eks. silikone. Den beskrevne krydsbinding af KS-gruppen er allerede rapporteret mange steder i litteraturen og i mange materialer [4-7]. På baggrund af den alsidighed, som de mange rapporter i litteraturen vidner om, samt den opnåede baggrundsviden fra arbejdet med PEG-systemet, håber vi at kunne udnytte KS-kemien til at fremstille f.eks. KS-funktionelle silikoner og derpå bruge disse til at fremstille innovative fotoaktive materialer med silikonernes velkendte egenskaber.

E-mail-adresser
Sarah Maria Grundahl Frankær: saf@kt.dtu.dk
Anne Ladegaard Skov: al@kt.dtu.dk

Referencer:
1. J. R. Capadona, K. Shanmuganathan, C. J. Tyler, S. J. Rowan, C. Weder (2008), Stimuli-responsive polymer Nanocomposites Inspired by the Sea Cucumber Dermis, Science 319: 1370-1374
2. F.Liu, M. W. Urban (2010), Recent advances and challenges in designing stimuli-responsive polymers, Progress in Polymer Science 35: 3-23
3. A. Lendlein, V. P. Shastri (2010), Stimuli-Sensitive Polymers, Advanced Materials 22: 3344-3347
4. X. Coqueret (1999), Photoreactivity of polymers with dimerizable side-groups: Kinetic analysis for probing morphology and molecular organization,Macromol. Chem. Phys. 200: 1567-1579
5. A. Lendlein, H. Jiang, O. Jünger, R. Langer (2005), Light-induced shape-memory polymers, Nature 434: 879-882
6. K. M. Gattás-Asfura, E. Weisman, F. M. Andreopoulos, M. Micic, B. Muller, S. Sirpal, S. M. Pham, R. M. Leblanc (2005), Nitrocinnamate-Functionalized Gelatin: Synthesis and "Smart" Hydrogel Formation via Photo-Cross-Linking, Biomacromolecules 6: 1503-1509
7. L. Wu, C. Jin, X. Sun (2011), Synthesis, Properties, and Light-Induced Shape Memory Effect of Multiblock Polyesterurethanes Containing Biodegradeable Segments and Pendant Cinnamamide Groups, Biomacromolecules 12: 235-241
8. M. Sandholzer, S. Bichler, F. Stelzer, C. Slugovc (2008): UV-Induced Cross-slinking of Ring Opening Metathesis Block Copolymer Micelles, Journal of Polymer Science Part A: Polymer Chemistry 46: 2402-2413

D.2 Article 2: Cinnamic Acid Derivatised Poly(Ethylene Glycol) as a UV-Active Bio-Inspired Material

S.M.G. Frankær, A.L.H. Di Vaia, A.E. Daugaard, S. Kiil & A.L. Skov.
Cinnamic Acid Derivatised Poly(Ethylene Glycol) as a UV-Active Bio-Inspired Material.
Macromol. Chem. Phys., submitted.

Table of contents

Photo-active materials are coming into focus for several novel applications. Here photo-active chemistry is used to create a bio-inspired UV-responsive material which can significantly change its properties upon exposure to UV-light. This gives an opportunity to develop polymer materials with light-switchable properties

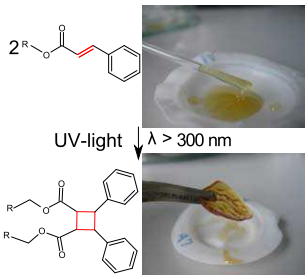

Cinnamic Acid Derivatised Poly(Ethylene Glycol) as a UV-Active Bio-Inspired Material

Sarah Maria Grundahl Frankær[1], Ayelén Luna Helling Di Vaia[1], Anders Egede Daugaard[1], Søren Kiil[2], Anne Ladegaard Skov[1]*

[1]Danish Polymer Center
DTU Chemical Engineering
Technical University of Denmark, DTU
Søltofts Plads, Building 229
2800 Kgs. Lyngby
Denmark

[2]CHEC Research Center
DTU Chemical Engineering
Technical University of Denmark, DTU
Søltofts Plads, Building 229
2800 Kgs. Lyngby
Denmark

*al@kt.dtu.dk

Abstract
Three different polymers were derivatised with cinnamic acid (CA), namely a 4-arm star PEG (M_n=2000 g/mol) (P4), a short linear PEG (M_n=1000 g/mol), and a long linear PEG (M_n=4000 g/mol). The rheological properties of the CA-derivatised polymers changed after irradiation with UV-light (=315-400 nm, main peak 365 nm) for one hour. It was observed that film formation occurred for P4 after approx. 24 hours of irradiation while approx. 70 hours were needed to obtain stable rheological properties. UV-spectroscopy confirmed a change the solid film and reversibility after short irradiation times. The conducted work showed that the reversibility was obstructed after long irradiation times. NMR-spectroscopy confirmed the possibility of isomerisation of CA from *trans* to *cis* which could explain the low efficiency.

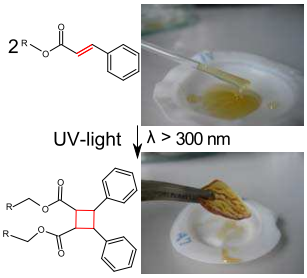

Introduction
Stimuli-responsive polymer materials are a wide-ranging field with many intriguing promises for the future and in recent years many studies in this field have been published. A stimuli-responsive material is a material that has one or more properties that can be significantly changed in a controlled fashion by external stimuli. This stimuli can be changes in the chemical environment (e.g. pH, ionic strength, or redox/electrochemical properties) as well as changes in the physical environment (e.g. temperature, electric field, electromagnetic radiation, magnetic field, or mechanical).[1,2] The chemistry behind the responsiveness is very diverse and can be a consequence of formation or scission of covalent bonds (e.g. photo-activated dimerisation of CA[3]), changes in the non-covalent interactions between the species (e.g. molecular recognition between dibenzo[24]-crown-8 and di-benzylammonium salt moieties[4]) or physical adaptation to the environment (e.g. thermo-responsive shape-memory polymers[5]). The most extensive studies were done on stimuli-responsive polymer materials used as shape-memory polymers[6] but stimuli-responsive polymers have potential for many other applications as well. The greatest difference between physical and chemical stimuli is the rate with which the response happens. In general, physical stimuli will give a quicker response than chemical stimuli, because physical stimuli most often are of a switchable nature (either on or off) e.g. hydrogen bonds or van der Waals interactions.

The research presented here is based on the work presented by Lendlein *et al.*[4] who reported a photo-activated shape-memory polymer which could retain an imposed deformed shape after irradiation with UV-light (>260 nm for 60 minutes) and afterwards regain its original shape by irradiation with shorter wavelength UV-light (<260 nm for 60 minutes). The shape-memory effect

was demonstrated in two types of materials; a network where the light-sensitive group was grafted onto the network and in an inter-penetrating network where photo-active poly(ethylene glycol) (PEG) four-armed stars were distributed in a butyl acrylate network.

The present work was initially inspired by the sea cucumber which is able to quickly transform its soft skin into a hard shield when threatened by enemies.[7] A polymer material mimicking abilities of the sea-cucumber could be a material where it would be possible to quickly increase the plateau modulus (G_0) by a chemical reaction and also quickly reverse the reaction and regain the original G_0. A material of this type could find many different applications such as a part of a switch-able adhesive similar to those made by Lumina Adhesives.[8] The aim of this work is a system that can be controlled by externally applied physical stimuli and therefore photo-activated chemistry was chosen. There are a number of photo-activated reactions available such as isomerisation of azo-benzenes[9], dimerisation of coumarine derivatives[10], and dimerisation of *trans*-cinnamic acid (CA) derivatives.[9] CA type derivatives were selected because of the many published studies with this type of material and the reversible nature of the reaction. The general reaction scheme for the UV-activated dimerisation of CA-groups is shown in Figure 1.

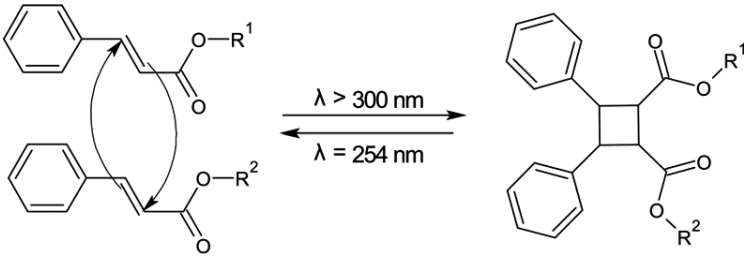

Figure 1: The dimerisation or cross-linking of *trans*-cinnamic acid. R^1 and R^2 indicate where the functional groups are linked to the polymer. In this work, R^1 and R^2 are poly(ethylene glycol)-polymers.

The dimerisation of CA occurs upon irradiation with UV-light with wavelengths above 300 nm and can be reversed by irradiation with UV-light with a shorter wavelength (254 nm). The reaction takes place between trans-isomers only since they allow for both favourable stacking of molecules as well as favourable bonding.[9] Several research groups have worked with this reaction in different types of materials and for many different purposes.[3,10-13] The primary focus of this work is to use networks that are softer than those based on acrylates e.g. poly(dimethyl siloxane) (PDMS). PDMS-networks are often based on a four-functional cross-linker[14], which is used to cross-link di-functional PDMS-chains and it was decided to work with a 4-armed star PEG and di-functional PEG-chains to make a system that had a structure similar to the PDMS-systems.

In this study it is shown that a UV-activated stimuli-responsive polymer material can change from being a liquid to an elastic material upon irradiation with broad spectrum UV-light and the rheological properties of the polymer materials before and after exposure to UV-light are reported. The perspective of the study is to develop stimuli-responsive materials which change reversibly upon external stimuli. The systems presented in this study are different from those presented by

Lendlein *et al.* [3] since they consist solely of photo-active polymers. This gives a unique possibility to understand the reactivity and properties of photo-active polymers without interference from the secondary networks and undesired effects such as micro-phase separation.

Materials and general methods

General methods. NMR spectroscopy was conducted on a Bruker 300 MHz spectrometer using $CDCl_3$ as solvent. Infrared spectroscopy (ATR-FTIR) was conducted on a Perkin-Elmer Spectrum One model 2000 Fourier transform infrared system with a universal attenuated total reflection (ATR) sampling accessory on a ZnSe/diamond composite. The spectra were recorded in the range of 4000-525 cm^{-1} with 4 cm^{-1} resolution and 16 scans. UV-spectra were recorded with a BMG Labtech POLARstar Omega micro plate reader in the range from 220 nm to 400 nm on approx. 20 µm thick films. Molecular weights were estimated by size exclusion chromatography (SEC) carried out on a Viskotek GPCmax VE-2001 equipped with Viscotek TriSEC Model 302 triple detector array (RI detector, viscometer detector and light scattering detector, and a Knauer K-2501 UV-detector) using two PLgel mixed-D columns (from PL). The samples were run in THF at 30°C (1 mL/min). Molecular weights were estimated using polystyrene (PS) standards from PL. Small amplitude oscillatory shear (SAOS) measurements were made with a TA 2000 Rheometer from TA Instruments set to a controlled strain mode, where the chosen strain value was ensured to be within the linear regime of the materials by means of strain-sweeps. The measurements were done with parallel plate geometry of 10 or 20 mm in the frequency range from 100 Hz to 0.01 Hz and 50°C. UV-irradiation (=315-400 nm, main peak 365 nm) was carried out with a SolData Ultra Violet Lamp UVA 315-400 nm (mercury vapour lamp) and the intensity of the UV-light was measured with a Sentry® UV-detector (detection range: from 280-400 nm). UV-irradiation (=254 nm) was carried out with a UVP 3UVLamp (mercury lamp, 8 W) (=254 nm, 302 nm and 365 nm).

Chemicals. 4-armed PEG star (M_n=2000 g/mol) was acquired from Creative PEGWorks and linear PEG (Mn=1000 and 4000 g/mol) was acquired from MERCK-Schuchardt. All other chemicals were acquired from Sigma-Aldrich.

General procedure for CA- derivatisation of PEG, CA-derivatised PEG (4-armed star) (P4). PEG (4-armed star, 6.07 g, 3.03 mmol, 12.1 mmol OH-groups, M_n=2000 g/mol) was dried by dissolution in CH_2Cl_2 and toluene followed by evaporation *in vacuo*. A solution of CA (2.36 g, 15.9 mmol) and 4-dimethylamidopyridine (DMAP) (0.454 g, 3.64 mmol) in CH_2Cl_2 (3 mL) was added and the mixture was stirred at 0 °C under N_2. To the mixture a solution of *N,N'*-dicyclohexylcarbodiimide (DCC) (3.26 g, 15.8 mmol) in CH_2Cl_2 (2 mL) was added dropwise. The mixture was stirred at RT for 15 hours. The product was recovered by precipitation in cold dry ether as a yellow oil (5.50 g, 72% yield, M_n=3482 g/mol, PDI=1.06). IR(cm^{-1}): 3061 (=C-H stretch), 2869 (C-H stretch), 1710 (C=O stretch), 1636 (C=C stretch), 1093 (C-O stretch). ^{1}H NMR ($CDCl_3$, 300 MHz)(ppm): 7.69 (d, 4H, J=16.0 Hz, (C_6H_5)-C*H*=CH), 7.51 (m, 8H, (C_6H_5)-CH=CH), 7.37 (m, 12H, (C_6H_5)-CH=CH), 6.46 (d, 4H, J=16.0 Hz, (C_6H_5)-CH=C*H*), 4.35 (m, 8H, CH=CH-C(O)OCH_2CH_2), 3.76 (m, 8H, CH=CH-C(O)OCH$_2$CH_2), 3.61 (m, 208H, C(O)OCH$_2$CH$_2$(OCH_2CH_2)$_n$).

CA-derivatised PEG (linear, M_n=1000 g/mol) (P2S). Following the general procedure for derivatisation with CA a linear PEG (5.00 g, 5.00 mmol, 10.0 mmol OH-groups, M_n=1000 g/mol) was derivatised. The product was a yellow oil (4.18 g, 66%, M_n=1202 g/mol, PDI=1.10). IR(cm^{-1}):

3061 (=C-H stretch), 2866 (C-H stretch), 1711 (C=O stretch), 1637 (C=C stretch), 1096 (C-O stretch). ^{1}H NMR ($CDCl_3$, 300 MHz)(ppm): 7.70 (d, 2H, J=16.0 Hz, (C_6H_5)-C*H*=CH), 7.52 (m, 4H, (C_6H_5)-CH=CH), 7.38 (m, 6H, (C_6H_5)-CH=CH), 6.47 (d, 2H, J=16.0 Hz, (C_6H_5)-CH=C*H*), 4.35 (m, 4H, CH=CH-C(O)OCH_2CH$_2$), 3.77 (m, 4H, CH=CH-C(O)OCH$_2$CH_2), 3.66 (m, 71H, C(O)OCH$_2$CH$_2$(OCH_2CH_2)$_n$).

CA-derivatised PEG (linear, M_n=4000 g/mol) (P2L). Following the general procedure for derivatisation with CA a linear PEG (5.00 g, 1.25 mmol, 2.50 mmol OH-groups, M_n=4000 g/mol) was derivatised. The product was a light yellow solid (3.69 g, 69%, M_n=7042 g/mol, PDI=1.08). IR(cm^{-1}): 3061 (=C-H stretch), 2868 (C-H stretch), 1714 (C=O stretch), 1637 (C=C stretch), 1097 (C-O stretch). ^{1}H NMR ($CDCl_3$, 300 MHz)(ppm): 7.70 (d, 2H, J=16.0 Hz, (C_6H_5)-C*H*=CH), 7.59 (m, 4H, (C_6H_5)-CH=CH), 7.38 (m, 6H, (C_6H_5)-CH=CH), 6.47 (d, 2H, J=16.0 Hz, (C_6H_5)-CH=C*H*), 4.36 (m, 4H, CH=CH-C(O)OCH_2CH$_2$), 3.77 (m, 4H, CH=CH-C(O)OCH$_2$CH_2), 3.64 (m, 344H, C(O)OCH$_2$CH$_2$(OCH_2CH_2)$_n$).

Preparation of photo-active materials. The photo-active materials **A**, **B** and **C** are made by mixing P4, P2S and P2L in different ratios: **A** is 100 weight-% (w%) P4. **B** is 50 w% P4 and 50 w% P2S. **C** is 23 w% P4 and 77 w% P2L.

*Procedure for irradiation of **A**, **B** and **C** with UV-light.* **A**, **B** and **C** were irradiated with UV-light (=315-400 nm, *I*=1.98 mW/cm^2) in a distance of 2.5 cm for one hour. The temperature was kept at 60°C**.**

Procedure for irradiation of $\mathbf{A_T}$-samples with UV-light. The samples used in the time dependence study ($\mathbf{A_T}$ samples=100 w% P4) were irradiated with UV-light (=315-400 nm, *I*=2.36-4.70 mW/cm^2) in a distance of 2 cm from the light source. The irradiation times were 0, 1, 2, 4, 8, 10, 15, 24, 31, 50, 65, 80, 95 and 120 h. The temperature was kept at 60°C.

Procedure for irradiation of solution of P4. 0.2003 g P4 was dissolved in 1 mL DMF and placed under a UV lamp (=302 nm) in a distance of 1.5 cm from the light source. The solution was irradiated for 1 h at room temperature.

Results and Discussion

Three different CA-derivatised PEG-polymers were prepared by esterification of commercially available PEG-polymers, namely a 4-armed star polymer (P4, Mn=2000 g/mol) and two linear polymers (P2S and P2L, Mn=1000 g/mol and 4000 g/mol, respectively), as shown in Figure 2 and 3.

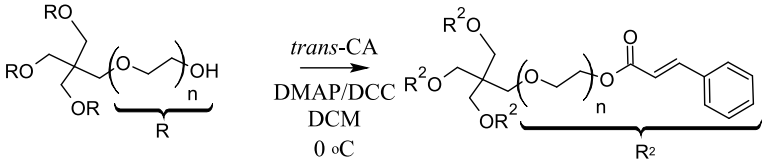

Figure 2: General reaction scheme for the preparation of trans-CA derivatised PEG. Four-armed star PEG is reacted with *trans*-CA in the presence of DCC and DMAP. The alcohol groups are esterified and the photo-active CA-derivatised PEG is formed.

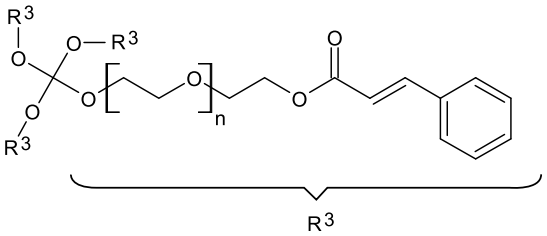

P4 (2000 g/mol)

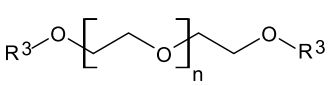

P2S (1000 g/mol)
P2L (4000 g/mol)

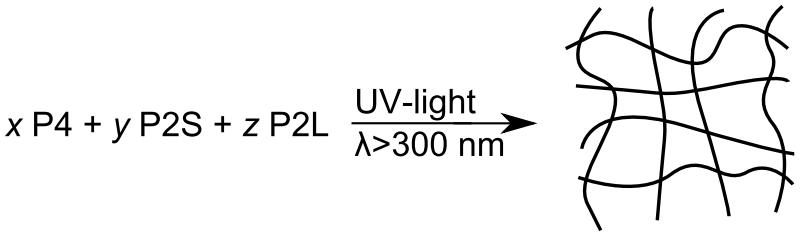

Network **A**: *x* is 100 w%.
Network **B**: *x* is 50 w%, *y* is 50 w%.
Network **C**: *x* is 23 w%, *z* is 77 w%.

Figure 3: Top: The molecular structure of the 4-armed star shaped P4 and the two linear polymers P2L and P2S. Bottom: The photo-active materials A, B and C consist of P4, P2S and P2L in different ratios. When the photo-active materials are irradiated with UV-light a four-functional network is formed.

The attachment of CA to the polymer was confirmed by NMR and SEC, and it was also observed using IR. In NMR the attachment of the CA-group to the polymer is confirmed by the occurrence of two multiplets at 4.35 and 3.76 ppm. The multiplets arise due to the protons in the first ethylene glycol group on the polymer chain. In SEC it was observed that the polymers after derivatisation showed a distinct UV-signal confirming the covalent attachment of the UV-absorbing CA end-groups. IR-data confirmed the disappearance of the OH end group as well as the appearance of an ester bond at 1710 cm^{-1}. Normally the absorption from ester bonds would be around 1735 cm^{-1} but the absorption is shifted due to the conjugation of the ester. The stimuli-responsive materials (**A**, **B** and **C**) were made by mixing P4, P2S and P2L in different ratios. The chosen ratios ensure that the relationship between the active end-groups on the polymers, referred to as χ, is kept at 1 for all samples. In Figure 3 the structure of P4, P2S and P2L can be seen, along with a schematic

representation of the four-functional network that **A**, **B** and **C** forms upon irradiation with UV-light, is shown.

The change in rheological properties (the storage modulus, G', and the loss modulus, G'') of the photoactive materials (**A**, **B** and **C**) after UV-irradiation for one hour (=315-400 nm) was investigated. The results are shown in Figure 4.

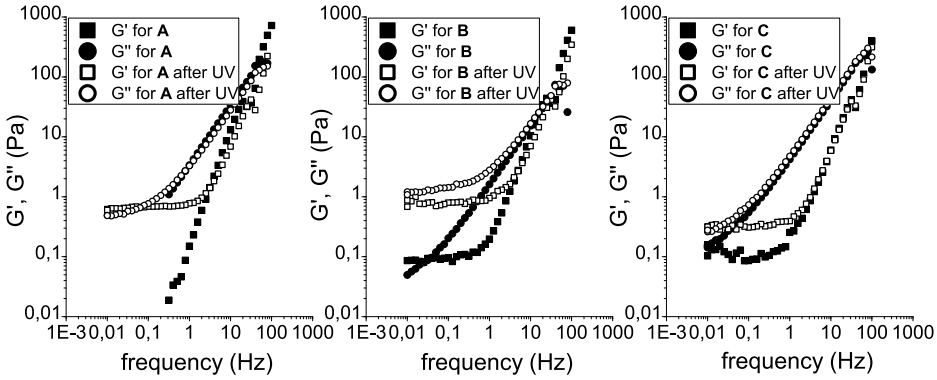

Figure 4: Rheological properties of **A**, **B** and **C** before (black symbols) and after (open symbols) irradiation with UV-light (=315-400 nm) for one hour. The measurements were carried out at 50 °C with a strain value of 10 %.

All data sets showed terminal relaxation before irradiation with UV-light indicating that the materials are liquids. The terminal relaxation is seen at frequencies (ν) below 50 Hz, where $G' > G''$ and G' is proportional to ν and G'' is proportional to ν^2. For sample **B** and **C** a plateau was observed for G' at low frequencies. This was ascribed to the detection limit of the rheometer. After irradiation all data sets showed a plateau at low frequencies. For **A** the observed elastic modulus is low ($G_0 \approx$ 0.8 Pa) but the presence of the plateau still clearly shows that a significant change in material properties has taken place. Similarly $G_0 \approx 0.8$ Pa for **B** and $G_0 \approx 0.3$ Pa for **C**. All samples show changes in rheological properties after irradiation with UV-light, but the change is most pronounced for **A**. It is expected that this observation is closely connected to the concentration of the photo-active CA-group (sample **A** and **B**: 1.59 mol CA/g sample; sample **C**: 0.727 mol CA/g sample) and the structure of the network formed. The distance between the cross-linking points is shorter in **A** than in **B** and therefore the formed network is stronger and the observed change is larger. It was assumed that P4 would act as a cross-linker for the linear polymers (P2S and P2L) in **B** and **C**, this is, however, not fully comprehensive. This would require that the reaction between the active groups on the cross-linker and on the linear chain should be very specific compared to reactions occurring "cross-linker to cross-linker" or "linear chain to linear chain". This is not the case for the dimerisation of CA. For the CA-system P4 could be regarded as a branched structure capable of creating complex branched structures. In Figure 5 a schematic representation of the structures formed in the network can be seen.

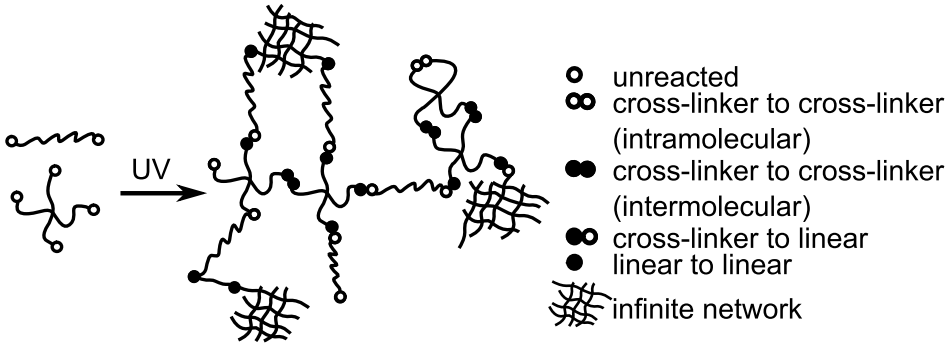

Figure 5: Schematic representation of the structures formed during nework formation between P4 (star, cross-linker) and P2S/P2L (linear chain). The CA-groups react with each other either star to star (intramolecular), star to star (intermolecular), star to linear or linear to linear. There is also a possibility that the group remains unreacted. Star-star-reactions give the possibility of loop formation, star-linear reaction gives the desired network structure while linear-linear combinations act as chain extenders.

A time dependence study was carried out with samples consisting solely of P4 (samples denoted $\mathbf{A_T}$). The development of the mechanical properties of this material is very dependent on the irradiation time and this was studied closely. A number of samples ($\mathbf{A_T}$) were made and irradiated with UV-light for up to 120 hours. Rheological data was collected for all the $\mathbf{A_T}$-samples and in Figure 6 a plot of G' and G'' at 0.01, 1 and 10 Hz as a function of the irradiation time (t) is shown.

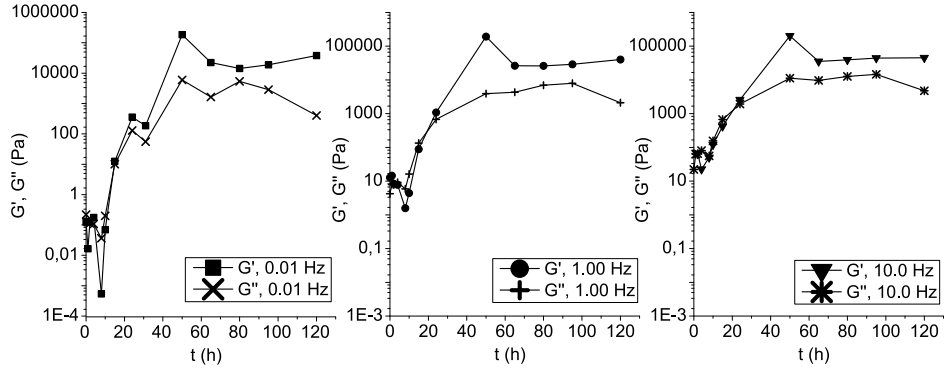

Figure 6: Development of G' and G'' over time. The plots show G' and G'' at v=0.01, 1.00 and 10 Hz for the $\mathbf{A_T}$-samples as a function of the UV-irradiation time (t). The gel point is observed at approx. 15 h irradiation time, where $G' > G''$. After app. 70 hours a plateau is reached at app. 0.01 MPa.

The data in Figure 6 shows the structural development of a network which is normally observed during network formation (curing). At low times the curve is steep because the limiting factor here

is the collision of the relatively free-moving polymer chains not yet hindered by the network. After approx. 15 hours of irradiation the gel point is observed ($G' > G''$). At longer timescales the curve flattens out because the limiting factor at this point is the spatial orientation of the active groups. If the active groups are far from each other and the network is reacted to an extent where the flexibility has decreased significantly the likelihood of "left over" active groups to get in close proximity and react is low. The time dependence of the reaction could also be observed simply by looking at the differences between the samples. In Figure 7 pictures of the material before and after UV-irradiation are shown.

Figure 7: Film formation of P1 after UV-irradiation. A) P1 before UV-irradiation. The material is a liquid. B) P1 after 96 h of UV-irradiation. The material is cross-linked to a film.

For short irradiation times the samples are liquids, while for long irradiation times (more than 24 hours) they are solid films. It was observed that the sample which was irradiated for 120 hours was brittle and broke very easily. A plateau is reached with $G' \approx 35000$ Pa and $G'' \approx 10000$ Pa after approx. 70 hours and at larger timescales no profound change is expected. A control experiment showed that the four-armed PEG did not cross-link upon UV-irradiation (up to 96 h) at 60 °C, and that P4 did not spontaneously cross-link at 60 °C (up to 96 h). In other words the UV-active compound is responsible for the observed changes in material properties.

The aim was to develop a material where bulk changes could be achieved rapidly in a solid material. The primary focus was the cross-linking reaction of CA and by using a UV-lamp with wavelengths above 315 nm it was ensured that the cross-linking reaction is favoured. The results presented show that bulk changes are possible and that irradiation with UV-light induced detectable macroscopic changes in the samples, see Figure 7. However a long exposure time is needed. It was not possible to detect any distinct changes in the IR-spectrum as a result of exposing the sample to UV-light. It was expected that a small shift in the carbonyl peak from the ester would occur when the conjugation was broken but this was not observed. When carrying out end group analysis it can be difficult to clearly determine changes because the signal arising from the end groups is much weaker than from the polymer chain itself. The reaction was investigated by recording the UV-spectrum of a thin film of P4 before and after irradiation, see Figure 8.

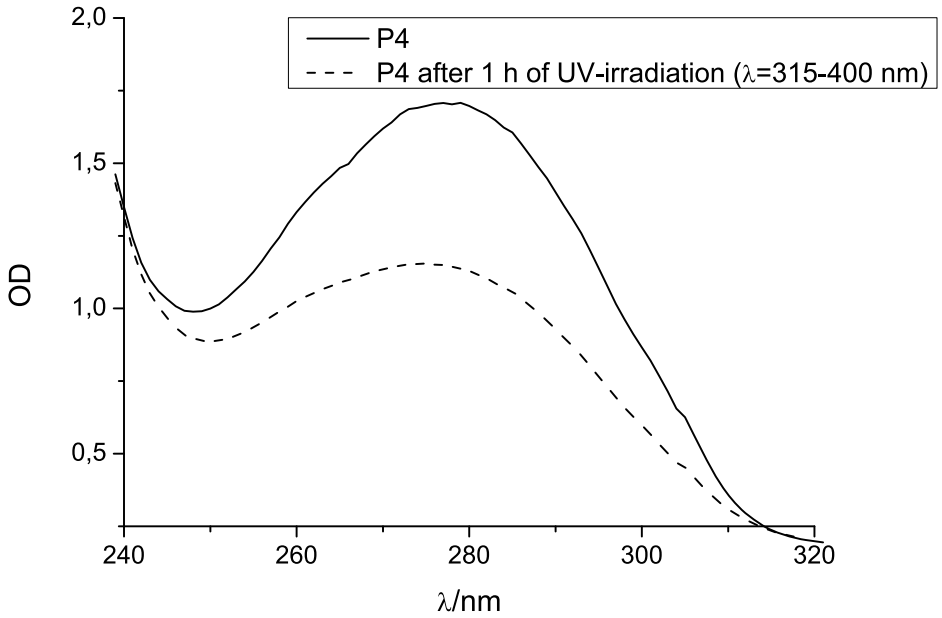

Figure 8: UV-spectrum of a thin film of P4 before (full line) and after (dashed line) one hour of irradiation with broad spectrum UV-light (> 300 nm). The maximum absorption at 278 nm is decreased with 39 %. OD is the optical density.

The data clearly showed a decrease in intensity of the absorption peak that arose from CA indicating a significant change in the system. This was interpreted as an indication of that the reaction between the UV-active groups takes place in a solid film of the UV-active polymer. It was observed that the samples which had been subjected to long UV-exposure times lost their ability to regain their original properties when exposed to UV-light with shorter wavelengths (irradiation with UV-light with =254 nm for up to 96 h). At shorter exposure times the change in rheological properties is smaller and the scattering of the data is larger, but the UV-absorption spectra of P4 showed that at short time scales the reversibility was possible. At the same time thorough investigation of UV-spectra of thin films of P4 (treated with UV-light with = 315-400 nm for 1 hour and then with =254 nm for 1 hour) showed reversibility similar to the 40 % reported by Lendlein *et al.* [3], who worked with a similar system.

The irradiated samples were insoluble and thus it was not possible to characterize the material with NMR or SEC. This was overcome by investigating a solution of P4 with NMR before and after UV-irradiation for 1 h, see Figure 9.

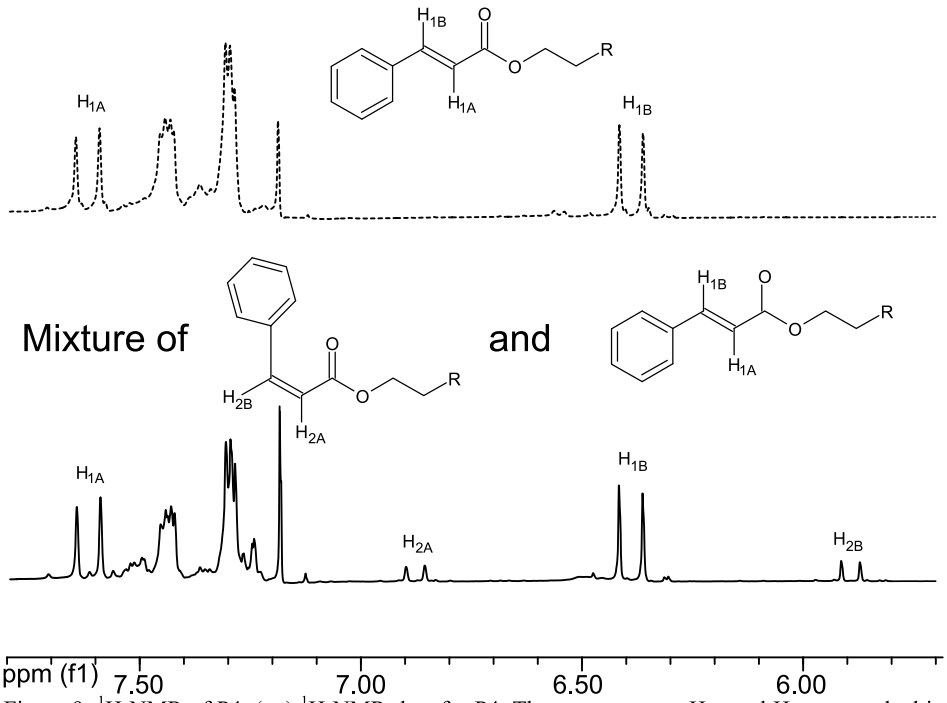

Figure 9: ^{1}H-NMR of P4. (---) ^{1}H-NMR-data for P4. The *trans*-protons H_{1A} and H_{1b} are marked in the spectrum (H_{1A} and H_{1B}, J= 16.0 Hz). (—)^{1}H-NMR-data for P4 after irradiation with UV-light for 1 hour. Irradiation was carried out in solution (DMF). The NMR-data shows occurrence of new proton stretches (H_{2A} and H_{2B}, J= 12.6 Hz) which indicate presence of the *cis*-isomer of the photo-active CA-group. The trans-isomer is also present (H_{1A} and H_{1B}, J= 16.0 Hz).

The NMR-data indicates the formation of the *cis*-isomer of P4 after UV-irradiation. As argued earlier, the spatial orientation is of great importance for cross-linking of P4. In polymer systems the end groups can be far from each other and the possibility of the end groups to meet is small. When some of the active CA-groups in addition have isomerised the possibility for dimerisation of two *trans*-isomers is further reduced since the *cis*-isomer is not reactive in dimerisation. Several studies report the possibility of forming the *cis*-isomer after irradiation with UV-light[15,16] and it is therefore a possible explanation for the long exposure times reported in this study. Lendlein *et al.* report exposure times of 60 minutes to obtain shape-memory results, but the system they present is significantly different by having a high concentration of photo-active groups fixed in the network. [3] The perspective of the work conducted is to incorporate polymers similar to those presented here in a polymer matrix and make an IPN-system rather than a single polymer system. It is our expectation that making an IPN system will improve the results. The reason for this is that a short polymer or a small star polymer will act as a lubricant in a polymer network and this effect will quickly be

eliminated when larger polymer structures are formed. Shorter exposure times should thus be needed and the reversibility will be intact.

Conclusions

As the presented work shows a first step towards the realisation of a bio-inspired material based on CA-derivatised PEG was taken. Three CA-derivatised PEG-polymers, P4, P2S and P2L, were synthesised and three photo-active materials, **A**, **B** and **C** were made. The latter were investigated for their rheological behaviour before and after irradiation with UV-light. It was observed that all samples displayed a change upon radiation but the change was most profound for sample **A**, characterised by the most significant change in rheological properties. This is due to the structure of the network formed as well as the concentration of the photo-active CA-group.

The observed time dependence of the reaction was studied closely and it was determined that after an exposure time of 24 h films were formed and that approx. 70 h was needed to get stable mechanical properties. This gave a pronounced increase in G' and G''. A control experiment was conducted and showed that it is the attachment of the photo-active CA-group that gives the possibility for the change in mechanical properties.

UV-absorption spectroscopy showed that the cross-linking of CA was reversible after shorter irradiation times (approx. 40% recovery), but after long exposure times the reversibility was obstructed.

NMR-data showed that isomerisation (from *trans* to *cis*) is a possible explanation when irradiated in solution. Isomerisation to *cis*-CA impacts the possibility of positive cross-linking reaction in a negative way.

It is expected that incorporating P4 in an IPN-system will lead to more rapid changes in rheological properties and thus retain the reversibility of the material.

References:

1: X. Yan, F. Wang, B. Zheng, F. Huang, *Chem. Soc. Rev*. **2012,** *41*, 2985.

2: R. J. Wojtecki, M. A. Meador, S. J. Rowan, *Nature mater.* **2010**, *10*, 14.

3: A. Lendlein, H. Jiang, O. Jünger, R. Langer, *Nature*. **2005**, *434*, 879.

4: Z. Ge, J. Hu, F. Huang, S. Liu, *Angew. Chem. Int. Ed*. **2009**, *48*, 1798.

5: D. Ratna, J. Karger-Kocsis, *J. Mater. Sci*. **2008**, *43*, 254.

6: M. Behl, A. Lendlein, *Mater. Today.* **2007**, *10*, 20.

7: J. R. Capadona, K. Shanmuganathan, D.J. Tyler, S.J. Rowan, C. Weder, *Science*. **2008**, *319*, 1370.

8: R. Bogue, *Assembly Automation*. **2011**, *31*, 207.

9: V. Engelmann, G. Wegner, K. Novak, K. B. Wagener, *J. Am. Chem. Soc.* **1993**, *115*, 10390.

10: H. Y. Jiang, S. Kelch, A. Lendlein, *Adv. Mater.* **2006**, *18*, 1471.

11: J. He, X. Tong, Y. Zhao, *Macromolecules*. **2009**, *42*, 4845.

12: K. M. Gattás-Asfura, E. Weisman, F. M. Andreopoulos, M. Micic, B. Muller, S. Sirpal, S. M. Pham, R. M. Leblanc, *Biomacromolecules*. **2005**, *6*, 1503.

13: X. Coqueret, *Macromol. Chem. Phys.* **1999**, *200*, 1567.

14: S. M. G Frankær, M. K. Jensen, A. G. Bejenariu, A. L. Skov, *Rheol Acta*. **2012**, *51*, 559.

15: P. L. Egerton, E. Pitts, A. Reiser, *Macromolecules*. **1981**, *14*, 95.

16: P. Gupta, S. R. Trenor, E. Timothy, G. L. Wilkes, *Macromolecules*. **2004**, *37*, 9211.

D.3 Article 3: Investigation of the properties of fully reacted unstoichiometric polydimethylsiloxane networks and their extracted network fractions

S.M.G Frankær, M.K. Jensen, A.G. Bejenariu & A.L. Skov.
Investigation of the properties of fully reacted unstoichiometric polydimethylsiloxane networks and their extracted network fractions.
Rheol. Acta, **2012** (51):559-567

Rheol Acta (2012) 51:559–567
DOI 10.1007/s00397-012-0624-z

ORIGINAL CONTRIBUTION

Investigation of the properties of fully reacted unstoichiometric polydimethylsiloxane networks and their extracted network fractions

Sarah Maria Grundahl Frankær · Mette Krog Jensen · Anca Gabriela Bejenariu · Anne Ladegaard Skov

Received: 9 August 2011 / Revised: 14 December 2011 / Accepted: 17 February 2012 / Published online: 11 March 2012

Abstract We investigated the linear dynamic response of a series of fully reacted unstoichiometric polydimethylsiloxane networks and of the two corresponding network fractions namely the sol and the washed network. The sol and the washed network were separated by a simple extraction process. This way, it was possible to obtain rheological data from the washed network without interference from the sol fraction and furthermore from the sol fraction without interference from the elastic washed network. When the stoichiometry increased towards perfectly reacted networks and beyond, we observed harder networks both qualitatively and by rheology, and the properties of the two fractions became more and more different. At the gel point, the sol fraction and the washed networks have more or less identical properties which our data also show. The storage and loss moduli, G' and G'', were analysed with the gel equation as proposed by Winter and Chambon (J Rheol 30:367–382, 1986) and Chambon and Winther (J Rheol 31:683–697, 1987). We observed that one of the investigated samples which before the swelling experiment did not show any elastic response gave an elastic washed network after swelling; this was verified by analysis with the gel equation. We also calculated the weight fraction of the sol fraction by using the theory by Villar et al. (Macromolecules 29(11):4072–4080, 1996) and compared this with experimentally found values.

Keywords Polymer networks · Gel · Soluble structures · Rheology · Linear viscoelastic properties

S. M. G. Frankær · M. K. Jensen · A. G. Bejenariu · A. L. Skov (B)
Department of Chemical and Biochemical Engineering, DTU, Danish Polymer Center, Søltofts Plads, Building 229, 2800 Kgs. Lyngby, Denmark
e-mail: al@kt.dtu.dk

Introduction

Polymer networks are widely used as 'damping materials' to suppress vibrations and noise and in other materials where a high loss tangent (i.e. large dissipation of energy) at a given frequency range is desirable. Urayama et al. (2004) investigated the damping properties of irregular polydimethylsiloxane (PDMS) networks and showed that rather than relying on the glass transition as the energy dissipation, one could utilise the temperature- and frequency-independent dissipation of deformation energy via the viscoelastic relaxation of irregular networks. By washing the networks, they removed the sol fraction which is responsible for the energy dissipation, and thereby, it was possible to get a response from the 'pure' washed network without the interference of the sol fraction. This behaviour is difficult to predict but as Urayama et al. (2004) showed, the individual contributions can be found experimentally.

Winter and Chambon (1986) and Chambon and Winther (1987) performed several studies on addition curing silicones where they investigated the structural development of the networks by means of rheological characterization by dynamical measurement analysis.

They showed that it was possible to cool down the silicone samples and stop the curing reaction completely. Thereby, they investigated perfect networks (i.e. networks where the stoichiometric imbalance, r, equals 1) as a function of the extent of reaction.

In this study, a number of fully reacted PDMS samples with stoichiometric imbalances between 0.73 and 1.07 were investigated by rheology before and after removal of the sol fraction. This approach is significantly different from the studies by Winter and Chambon (1986) and Chambon and Winther (1987) since we did not need to control the extent of reaction for the curing process.

We were interested in the dynamics of the initial network as well as the dynamics of the sol fraction and the pure washed network. We used a simple extraction procedure to remove the sol fraction; the networks were swelled in solvent. After 48 h, the solvent and the swelled sample were separated, and the solvent was allowed to evaporate. This way, we could recover the washed network and the sol fraction, respectively (Nandi and Winter 2005). If any volatiles were present in the system, they would also be removed with the solvent. The frequency dependence of the storage and loss moduli, G' and G'' respectively, for all samples was determined. Thereby, we could investigate the dynamics of each of the network fractions without interference from the other.

Networks

The networks were made by endlinking PDMS chains with a trifunctional cross-linker in an addition curing process (Bejenariu et al. 2010). During the process, the material changed from being a large number of individual and finite molecules into, in theory, one large infinite molecule (Chambon and Winther 1987). This abrupt change is denoted as the gel point and has been investigated to a large extent for networks of different types and with different stoichiometries. The stoichiometric imbalance of the network, r, is defined as:

$$r = \frac{[\text{hydride}]}{[\text{vinyl}]} = \frac{f\,[\text{cross-linker}]}{2\,[\text{PDMS}]} \tag{1}$$

where f is the functionality of the cross-linker, and [cross-linker] and [PDMS] are the concentrations of the cross-linker and the PDMS, respectively. r expresses the relationship between the active functional groups. For $r < 1$, there is excess PDMS, and some chains will not be part of the cross-linking process; for $r \geq 1$, the opposite situation is present, and all PDMS molecules should be linked to a cross-linker molecule. Another important definition is that of the critical stoichiometric imbalance r_c:

$$r_c = \frac{1}{f-1} \tag{2}$$

Values of r below r_c will not result in the formation of networks. For an ideal network, the system should contain only one great molecule, where all coupling points are connected to the networks. However, practice shows that cross-linking of finite polymers to form a network gives a system with at least two phases, the washed polymer network and the sol fraction (Nandi and Winter 2005).

We expect that the structure of the molecules in the sol depends highly upon the extent of reaction. In general, the formed networks have excess of PDMS chains to cross-linker, meaning that closely above the gel point, the sol fraction will consist of many different types of structures namely unreacted chains, inreactive species, chains with only one active site, fully reacted cross-linker molecules and larger more complex structures. Moving towards fully reacted networks, the structure of the molecules in the sol will be more uniform. In general, the sol will consist of unreacted and inreactive chains, chains with one active site and fully reacted cross-linker molecules. The washed network consists of elastically active network chains, i.e. PDMS chains connected in both ends to the network and reacted with a cross-linker. So in the washed network, we would expect to see dynamics caused by the elastically active network and the dangling chains and substructures (Hild 1998). For $r < 1$, the washed network will have a higher value of r compared to the initial network, while the sol fraction will have a lower value since we primarily are looking into cross-linker-deficient networks.

In the close vicinity of the gel point, we should be able to part our solution into two fractions and obtain almost identical dynamics of these two fractions. As we proceed beyond the gel point, it should not be (in theory) possible to separate the mixture into two parts. It is therefore clear that in a close range around the gel point, we will obtain similar properties of both the sol fraction and the washed network. However, the gel is very soft and may break, so a separation may be very difficult.

According to Flory's theory of an ideal cross-linking reaction, the PDMS system should become a network for stoichiometric imbalances in the range of $r = 0.5-2$. Slightly higher values of r are however anticipated

here to compensate for the non-ideal behaviour of the reaction (Flory 1941a, b, 1953).

Experimental

Sample preparation

A series of networks of PDMS were prepared by endlinking of divinyl-terminated PDMS (DMS-V31, $M_n = 28,000$ g/mol, Gelest Inc.) with a three-functional cross-linker, phenyltris(dimethylsilyloxy) silane (HMS, Gelest Inc.). A platinum–cyclovinylmethylsiloxane complex (511, Hanse Chemie) was used as a catalyst. The chemicals were used as received. The networks were prepared in two rounds with the use of two different batches of PDMS. In the first round of experiments, networks with $r = 0.73, 0.75, 0.85, 0.95$ and 1.07 were made, and in the second round of experiments, networks with $r = 0.80, 0.84, 0.91$ and 1.00 were made.

The networks were made in simple weight-based ratios from two ready-made mixtures of PDMS and cross-linker (mixture A) and PDMS and catalyst (mixture B), see Table 1. The A and B mixtures were made beforehand by mixing the components and stirring until complete mixing was obtained. More details about the mixing procedure can be found in Larsen et al. (2003).

The networks were made by mixing predetermined amounts of mixtures A and B thoroughly and leave the mixture to cure for 12 h. Mixtures A and B were combined in different ratios resulting in networks with different r values.

Swelling of networks

The networks were swelled in heptane (10–15 times excess, i.e. app. 35–50 mL solvent to a sample of 3.5 g; in all experiments, we made sure that the PDMS networks were fully covered in solvent) for 48 h. After the 48 h, the networks were separated from the heptane solution. The heptane was removed by evaporation over 48 h under atmospheric conditions. The procedure resulted in two samples which were analysed, the washed network and the corresponding sol fraction.

Table 1 Preparation of the applied mixtures A and B

Mix	PDMS/g	Catalyst/g	Cross-linker/g
A	50	–	0.66
B	50	0.035	–

Small amplitude oscillatory shear measurements

The samples were measured in small amplitude oscillatory shear (SAOS). The measurements were made with a TA 2000 Rheometer from TA Instruments set to a controlled strain mode; the strain was set to 2% which was ensured to be within the linear viscoelastic regime. The measurements were done with parallel plate geometry of 25 mm in the frequency range of 100–0.01 Hz and at temperatures between 0 and 200°C. After the measurements were done, the data were shifted to 25°C using the time–temperature superposition principle (TTS).

Results and discussion

The initial PDMS samples with low r values were liquid-like and very soft both before and after swelling. The samples with r values above 0.90 were rubbery but slightly greasy to the touch before swelling. The greasy feel disappeared after the washing procedure.

From the experimentally determined weight fraction of sol, W_{sol} (Table 2 and Fig. 1), it is obvious that an ideal network with no sol fraction is not obtained. It rather seems that for values of r around and above 1, we obtain a value between 5 and 10% sol fraction, which gives a clear indication of the inreactive species within the polymer and of the imperfections in the formed network. Furthermore, for values of r approaching 0.7, it seems that there is a large variation in W_{sol} which corresponds well when r is approaching r_c, and hence, the mixing is critical for reproducibility. For slow mixing procedures, we observed heterogeneity in the mixes, so a fast and immediate mixing procedure had to be applied. From Eq. 2, it is obvious that when $f = 3$ then $r_c = \frac{1}{2}$. This value indicates the gel point with respect to the stoichiometry. The high value of the stoichiometric imbalance at the experimentally determined gel point may be due to steric hindrance of the cross-linker. In order to clarify if steric hindrance was a kinetic problem, we investigated the curing profiles obtained in the rheometer at a constant frequency of 1 Hz where we followed the structural development of the networks for several hours. Post-curing processes could not be detected within 5 h after a constant level in G' and G'' had been reached, and we therefore conclude that our procedure ensured complete reaction. In Fig. 1, the theoretical weight fraction of the sol fraction, $W_{sol\ theoretical}$, is plotted along with the experimentally found $W_{sol\ experimental}$. The experimental data show the same tendency as the theory; however,

Table 2 r values, weight percentages (wt%) and $W_{sol\ experimental}$ for the networks

r	wt% PDMS	wt% cross-linker	wt% catalyst	$W_{sol\ experimental}$
0.73 ± 0.02	99.3 ± 0.017	0.667 ± 0.018	0.034 ± 0.001	0.489 ± 0.141
0.75	99.3	0.684	0.033	0.068
0.80 ± 0.02	99.2 ± 0.016	0.736 ± 0.016	0.031 ± 0.001	0.077 ± 0.045
0.84 ± 0.02	99.2 ± 0.019	0.771 ± 0.021	0.046 ± 0.002	0.086 ± 0.034
0.85 ± 0.00	99.2 ± 0.002	0.782 ± 0.002	0.028 ± 0.000	0.108 ± 0.043
0.91 ± 0.01	99.1 ± 0.012	0.834 ± 0.013	0.026 ± 0.000	0.171 ± 0.034
0.95 ± 0.00	99.1 ± 0.002	0.869 ± 0.002	0.023 ± 0.000	0.088 ± 0.047
1.00 ± 0.02	99.1 ± 0.017	0.910 ± 0.017	0.021 ± 0.001	0.103 ± 0.002
1.07 ± 0.00	99.0 ± 0.003	0.979 ± 0.003	0.017 ± 0.000	0.064 ± 0.019

The measurements are averages of data from 2–6 samples, except for $r = 0.71$ where only one sample was available

W_{sol} is more constant and higher around $r = 1$ than expected.

SAOS data

Figures 2, 3 and 4 show the dynamics for the initial networks, the sol fractions and washed network, respectively. If we look at the data for the initial samples (Fig. 2), it is observed that samples with r above 0.84 act as viscoelastic solids indicated by the plateau seen for G at low frequencies. The networks with $r = 0.73$ and $r = 0.75$ behave as viscous materials, while the sample with $r = 0.80$ must be close to the gel point since $G \approx G$ in the entire frequency range.

For the sol fraction (Fig. 3) for $r = 0.73$, the data show indications of the presence of a physical network of long entangled PDMS chains. For $r = 0.75$, the sol fraction is viscous. The sol fraction from the sample with $r = 0.80$ again shows indications of being close to the gel point. For the samples with higher stoichiometric imbalances, the results show no general tendency. In some of the samples (mainly $r = 0.84$, $r = 0.85$, $r = 0.95$ and $r = 1.00$), a tendency towards elastic properties is indicated by a plateau at low frequencies. However, it is observed that the value for the G plateau does not consistently increase with increasing stoichiometry as is observed for the initial networks. We expect that this is related to the structure of the molecules in the sol. We expect that the largest structures in the sol are found for r values above the gel point (0.5) but not too close to 1. Close to $r = 1$, we expect the sol to consist mainly of inactive chains and chains with only one active site due to imperfections in the PDMS polymer.

All the washed networks (Fig. 4) with $r \geq 0.85$ show viscoelastic properties, and the value for the G plateau is increasing steadily with increasing r as expected. The data for the washed network with $r = 0.73$ indicate that the sample is close to the gel point by having $G \approx G$ in the entire frequency range. Furthermore, it is interesting that the washed network with $r = 0.80$ has $G > G$ in the entire frequency range indicating that the sample is more elastic than viscous, while both the initial network and the sol fraction showed gel point characteristics. For the sample with $r = 0.75$, we observed that at low frequencies, G is larger than G

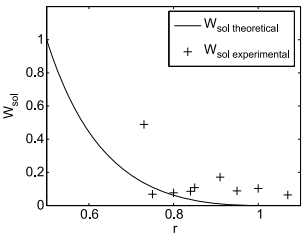

Fig. 1 Comparison of experimentally found and theoretical values of W_{sol}

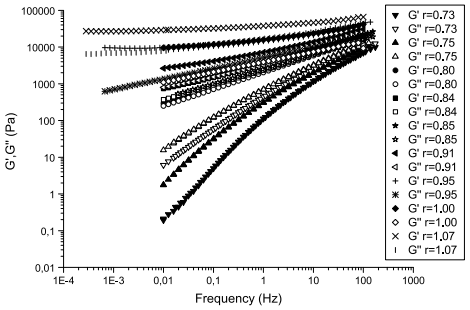

Fig. 2 The dynamics of the initial networks. The stoichiometric imbalance is given in the figure. The higher the stoichiometric imbalance, the more elastic the network. The data were shifted to 25°C by TTS, and the strain was set to 2%

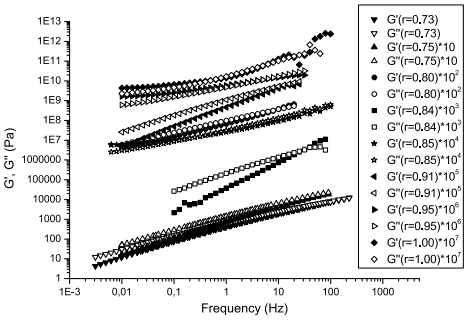

Fig. 3 The dynamics of the sol fractions. The stoichiometric imbalance of the initial network is given in the figure. The data were shifted to 25°C by TTS, and the strain was set to 2%

again indicating elastic response in the sample. For the initial sample with $r = 0.75$, no elastic response could be detected. In other words, it is possible to extract an elastic washed network from a sample which initially shows no elastic response. The sol fraction of this sample was able to smear the elastic response out, so it was undetectable.

Fitting the experimental data to the gel equation

The viscoelastic properties were measured in SAOS experiments, and the measured G' and G'' were analysed. In the cases where the PDMS samples have formed networks beyond the gel point, they will behave as viscoelastic solids. This means that a plateau is reached for G' at the low frequency regime, and it will often be orders of magnitudes higher than the loss modulus, G''. At higher frequencies, G' and G'' will be of the same order of magnitude; however, the plateau regime will increase as the cross-link density increases, hence as r increases. For gels, G' is following a power law behaviour over the whole frequency range and is thus proportional to ω (Bird et al. 1987; Hild 1998; Morrison 2001; Jensen et al. 2009). One way to analyse G' and G'' is to use the gel equation proposed by Winter and Chambon (1986) and Chambon and Winther (1987):

$$G(t) = St^{-n} \tag{3}$$

From the relaxation modulus, it is possible to derive corresponding expressions for G' and G'', and the relation between G' and G'' is very simple and can be derived from Eq. 3:

$$G'(\omega) = \omega \int_0^\infty G(s)\sin(\omega s)ds = \frac{S\Gamma\omega^n}{2\Gamma(n)\cos\frac{n\pi}{2}} \tag{4}$$

$$G''(\omega) = \omega \int_0^\infty G(s)\cos(\omega s)ds = \frac{S\Gamma\omega^n}{2\Gamma(n)\sin\frac{n\pi}{2}} \tag{5}$$

$$G'' = \frac{G'}{\tan(\frac{n\pi}{2})} \tag{6}$$

Equation 3 is a simple model for the relaxation modulus of a critical gel as a function of time. By critical gel is meant a sample at the gel point where the viscosity is infinite, while the equilibrium modulus is zero. S, in Eq. 3, is a measure for the gel stiffness with respect to the number of entanglements of the precursor chains (PDMS chains), while n is a relaxation exponent, and it is thus the slope of G' in a double logarithmic plot. Winter and Chambon (1986) and Chambon and Winther (1987) made a thorough investigation of the size of n at the gel point, and they found that for a stoichiometric balanced gel ($r = 1$), n was equal to $1/2$ and that G' and G'' would be congruent over the entire frequency range, $0 < \omega < \infty$. For stoichiometric imbalanced ($r = 1$) gels, n would increase and lie in the range $1/2 < n < 1$. Hild (1998) found a similar result for $r < 1$, while for $r > 1$, n was found to be equal to $1/2$ at the gel point.

A more general indication of the size of n can be found in Eq. 6, which predicts that if $n > 1/2$ then $G'' > G'$, while $G'' < G'$ if $n < 1/2$. It is important to notice that this analysis has been performed on gels at the gel point. In this study, the network is beyond the gel point. When analysing data beyond the gel point,

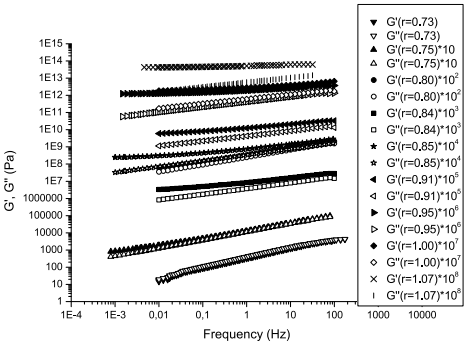

Fig. 4 The dynamics of the washed networks. The stoichiometric imbalance of the initial network is given in the figure. The tendency towards more elastic networks with higher stoichiometric imbalances is also seen here. The data were shifted to 25°C by TTS, and the strain was set to 2%

it is necessary to modify the gel equation, such that it accounts for the plateau obtained for G'. This was done by Jensen et al. (2009). They analysed stoichiometric-imbalanced polypropylene oxide networks, $r < 1$, cured to complete reaction, by adding an additional term to Eq. 3:

$$G(t) = St^{-n} + G_0 H(t) \quad (7)$$

where $H(t)$ is the Heaviside step function, while G_0 is the equilibrium modulus or plateau modulus obtained for G' at low frequencies. The study by Jensen et al. (2009) showed that even for gel beyond the gel point, n can change significantly. n would be high, $> 1/2$, for very soft gels, while for $r \to 1$, harder gels are obtained and n could drop to about 0.35. Hence, n is a measure for the softness of the gel (Jensen et al. 2009). A similar analysis of n will be made in this study with imbalanced PDMS networks that are also cured to complete reaction.

The modified gel equation given in Eq. 7 was used to fit the linear viscoelastic data of the samples at or beyond the gel point. Figure 5 shows the viscoelastic data measured for the initial network with $r = 0.95$ together with the curves corresponding to Eqs. 4 and 5. The parameters S and n were determined with a least square routine, while G_0 was determined by the plateau given by the experimental data.

The parameters, G_0, S and n for all the gels are listed in Tables 3, 4 and 5. It is seen that the parameters cannot be determined for the initial networks with $r = 0.73$, 0.75 and 1.07 and the sol fractions with $r = 0.73$, 0.75, 0.80, 0.85 and 1.07. The reason for this is that many of the mentioned samples are simply not gels, and fitting the gel equation to data on samples which are not gels gives problems. We present the fits here because they underline the large differences in the networks' fractions. This is however not the case for the initial network with $r = 1.07$; this will be discussed in details later. Interestingly, it is possible to determine the parameters for the washed network at $r = 0.73$ and 0.75. The result shows that the samples with $r = 0.75$ is in fact beyond the gel point, since G' levels are indicated by a plateau at low frequencies. This shows that it is possible to extract a network beyond the gel point from a sample that appears not to exhibit any elastic characteristics, which was also mentioned earlier, but this is due to change of time scales for relaxation. The initial sample with $r = 0.80$ showed gel point characteristics in the SAOS data, and the fit to the Eqs. 4 and 5 underlines this since n is 0.49.

The parameters for the initial network with $r = 1.07$ could as mentioned earlier not be determined. The reason for this is not clear; however, it was not possible to fit both Eqs. 4 and 5 to G' and G'' at the same time. This indicates that there is no consistency between the data as there should be according to the Kramers–Kronig relation (Bird et al. 1987). The data measured for this sample, along with that for the sample with $r = 0.73$ where the gel parameters could not be found for any of the parts, will therefore not be used in the

Table 3 Gel parameters, G_0, S and n, obtained by fitting Eqs. 4 and 5 to the linear viscoelastic data for the initial networks

	Initial network		
r	G_0 [Pa]	S [Pa·s^{-1}]	n
0.73	–	–	–
0.75	–	–	–
0.80	140	1,700	0.49
0.84	310	2,700	0.41
0.85	200	2,800	0.39
0.91	2,100	4,000	0.38
0.95	7,900	7,600	0.32
1.00	8,400	6,000	0.31
1.07	–	–	–

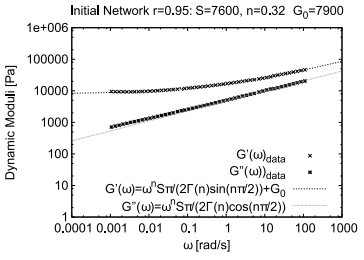

Fig. 5 The dynamic moduli of the initial network with $r = 0.95$. The curves are fits of G' and G'' with Eqs. 4 and 5

Table 4 Gel parameters, G_0, S and n, obtained by fitting Eqs. 4 and 5 to the linear viscoelastic data for the sol fractions

	Sol fractions		
r	G_0 [Pa]	S [Pa·s^{-1}]	n
0.73	–	–	–
0.75	–	–	–
0.80	(9)	(500)	(0.6)
0.84	53	150	0.64
0.85	(0.1)	(15)	(0.94)
0.91	2.5	200	0.9
0.95	65	440	0.42
1.00	54	40	0.82
1.07	–	–	–

Values in parenthesis are from a fit with high deviation

Table 5 Gel parameters, G_0, S and n, obtained by fitting Eqs. 4 and 5 to the linear viscoelastic data for the washed networks

	Washed network		
r	G_0 [Pa]	S [Pa·s^{-1}]	n
0.73	1	500	0.55
0.75	30	1,020	0.46
0.80	70	2,800	0.41
0.84	2,000	5,000	0.35
0.85	1,500	6,000	0.3
0.91	2,700	8,600	0.26
0.95	10,000	10,000	0.26
1.00	16,000	10,000	0.31
1.07	40,000	10,500	0.27

discussion given below. Moreover, linear viscoelastic data were not obtained for the sol fraction at $r = 1.07$ because the amount of sol fraction was too small for rheological characterization.

All the data in Tables 3, 4 and 5 are plotted vs. r in Figs. 6, 7 and 8. It is seen that both G_0 and S increase with r while n decreases. This is expected since G_0 is a measure for the elasticity of the network, and therefore as r increases, the more network strands are connected to the elastic active network. S is a measure for the stiffness with respect to the number of trapped entanglements which also will increase as r increases. Finally, the more dynamic the network, the higher is n. Similar to Jensen et al. (2009), we observed that $n > 1/2$ for very soft networks, and when r is increase to 1 and beyond, n decreases to around 0.30. It is also obvious from the determined values of n that n for the initial networks and the washed networks differs the most at low values of r where the large sol fraction really softens the initial network.

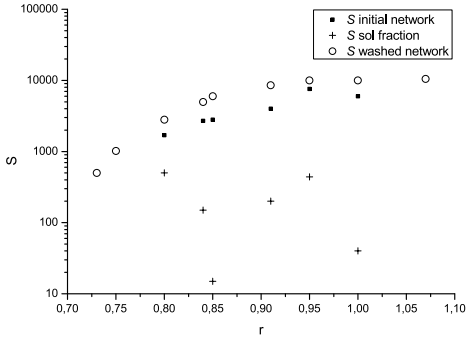

Fig. 7 The gel stiffness, S, determined from the fits of Eqs. 4 and 5 to the dynamic moduli as a function of r

G_0 for the networks, see Fig. 6, showed that they were very soft compared to traditional silicone networks which are prepared with cross-linkers of higher functionality ($f > 3$) (Mark and Llorente 1980). The moduli of the investigated initial networks are in the order of 10^2–10^4 Pa. This is easily explained by the properties of the three-functional cross-linker which requires that *all* the reaction sites on the cross-linker have reacted and that all the polymers are reacted with the infinite network in both ends in order to be elastically active. If only two chains are connected to the cross-linker, the cross-linker will in fact only act as a chain extender and therefore not act as a cross-linking point. The introduction of chain extenders will hence lead to rapid decrease in the resulting modulus compared to a fully cross-linked network.

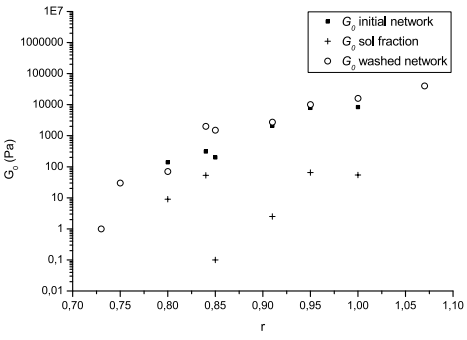

Fig. 6 G_0 determined from the fits of Eqs. 4 and 5 to the dynamic moduli as a function of r

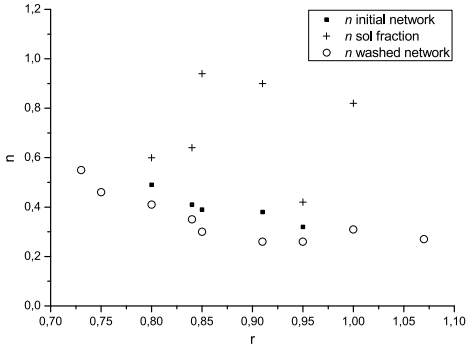

Fig. 8 The relaxation exponent, n, obtained from fitting Eqs. 4 and 5 to G and G

Calculating the weight fraction of elastic chains and sol and M_n for the sol fraction

Villar et al. (1996) published results where the molecular structure of a network (network, pendant chains and sol) was investigated. They developed a model to determine the amount of sol. This technique has been applied to the work presented here to check if the investigated system followed the theory. Villar et al. (1996) considered a system of monofunctional and bifunctional polymers with elastic chains, pendant chains and soluble material (sol). The set of equations used here is simpler since there is only bifunctional polymers (PDMS with two vinyl end groups), and only the network (elastic and pendant chains) and the sol will be considered as there is no way to separate dangling ends and network into two fractions. Thus, our network is formed by mixing PDMS with functional end groups (B) and a trifunctional cross-linker (A_3). Using the terminology of Villar et al. (1996), we obtain that the probability that looking out from an A group the reaction leads to a finite or dangling chain rather than to the infinite network, $P(F_A^{out})$, is given by:

$$P(F_A^{out}) = \frac{1 - rp^2}{rp^2} \tag{8}$$

where p is the extent of reaction with respect to either A or B groups and $p = p_A = \frac{p_B}{r}$. For the PDMS system, it is assumed that the reaction goes to completion, and hence $p_A = 1$ as long as $r \leq 1$. For $r > 1$, then $p_B = 1$.

The probability that looking out from a B group the reaction leads to a finite or dangling chain rather than to the infinite network, $P(F_B^{out})$, is given by:

$$P(F_B^{out}) = 1 + rp(P(F_A^{out})^2 - 1) \tag{9}$$

We define the network fraction, (W_{net}), as:

$$W_{net} = W_e + W_p \tag{10}$$

where W_e is the elastically active weight fraction, and W_p is the pendant chain fraction.

The elastically active fraction can be calculated from:

$$W_e = W_{A_3}\,(1 - P(F_A^{out}))^3 + 2P(F_A^{out})) \cdot (1 - P(F_A^{out}))^2 + W_{B_2}(1 - P(F_B^{out}))^2 \tag{11}$$

where W_{A_3} is the initial weight fraction of A_3 and W_{B_2} is the initial weight fraction of B. W_{A_3} is given by:

$$W_{A_3} = \frac{M_{nA_3}}{M_{nA_3} + \frac{3}{2r}M_{nB_2}} \tag{12}$$

Table 6 The calculated and experimentally determined sol fractions

r	$W_{sol\ calculated}$	$W_{sol\ experimental}$
0.73	0.1363	0.489
0.75	0.1107	0.068
0.80	0.0622	0.077
0.84	0.0361	0.086
0.85	0.0310	0.108
0.91	0.0097	0.171
0.95	0.0028	0.088
1.00	0	0.103
1.07	0	0.064

The sol fraction is calculated by use of Eq. 15. In the performed calculations, $M_{nA_3} = 28,000$ g/mol and $M_{nB_2} = 330$ g/mol

And W_{B_2} is given by:

$$W_{B_2} = \frac{M_{nB_2}}{M_{nB_2} + \frac{2r}{3}M_{nA_3}} \tag{13}$$

The pendant chain fraction can be calculated from:

$$W_p = W_{A_3}3P(F_A^{out})^2(1 - P(F_A^{out})) + W_{B_2}2P(F_B^{out})(1 - P(F_B^{out})) \tag{14}$$

And finally, the sol fraction can be calculated from:

$$W_{sol\ calculated} = W_{A_3}P(F_A^{out})^3 + W_{B_2}P(F_B^{out})^2 \tag{15}$$

In Table 6, the calculated weight fractions of sol can be found along with those found experimentally. The values for $W_{sol\ experimental}$ decrease but seem to find a steady level of 5–10% when r approaches 1. The values for $W_{sol\ calculated}$ decrease steadily to 0 (when $r = 1$) and thus do not describe the experimental observations. The reason for this can be that either the theory does not fully describe what is observed or that there are some problems with the used polymers—such as inreactive chains, chains with only one active site, etc. as mentioned earlier.

Conclusion

We observed that it was possible to extract an elastic network from a sample which initially showed viscous properties. The sol fraction of the specific sample was able to totally smear out the elastic response from the formed network. We also were able to isolate samples close to the gel point. These observations were verified by fitting the data to the modified gel equation. In general, the gel equation could be fitted to the data, and the obtained variables S, n and G_0 depend on r in the expected ways, so G_0 and S increase with increasing r while n decreases. G_0 is related to the elasticity and S to the trapped entanglements in the network, and both

of these will increase with r since more and more chains are attached to the network and the complexity of the network structure is more developed. n is related to the dynamics of the network and therefore decreases when r increases because the mobility of the chains is hindered. All in all, we observed that $n > 1/2$ for very soft networks, and for harder networks, n decreases to around 0.30, which correlates with values from the literature (Jensen et al. 2009).

We calculated the amount of sol and compare this with experimental results. However, we observed that the theory could not describe what we observed in the lab, and in general, $W_{\text{sol experimental}}$ is larger than $W_{\text{sol calculated}}$. We expect that the primary reason for this is impurities in the PDMS polymer (such as inreactive species, chains with only one active site, etc.). The amount of impurities should be 1%, but we estimate that it is significantly higher.

References

Bejenariu AG, Rasmussen HK, Skov AL, Hassager O, Frankaer SM (2010) Large amplitude oscillatory extension of soft polymeric networks. Rheol Acta 49:807–814

Bird RB, Armstrong RC, Hassager O (1987) Dynamics of polymeric liquids, vol 1. Fluid dynamics. Wiley, New York

Chambon F, Winther HH (1987) Linear viscoelasticity at the gel point of a crosslinking PDMS with imbalanced stoichiometry. J Rheol 31:683–697

Flory PJ (1941) Molecular size distribution in three dimensional polymers. I. Gelation. J Am Chem Soc 63(11):3083–3090

Flory PJ (1941) Molecular size distribution in three dimensional polymers. II. Trifunctional branching units. J Am Chem Soc 63:3091

Flory PJ (1953) Principles of polymer chemistry. Cornell University Press, Ithaca

Hild G (1998) Model networks based on 'endlinking' process: synthesis, structure and properties. Prog Polym Sci 23:1019–1149

Jensen MK, Bach A, Hassager O, Skov AL (2009) Linear rheology of cross-linked polypropylene oxide as a pressure sensitive adhesive. Int J Adhes Adhes 29:687–693

Larsen AL, Hansen K, Sommer-Larsen P, Hassager O, Bach A, Ndoni S, Jørgensen M (2003) Elastic properties of non-stoichiometric reacted PDMS networks. Macromolecules 36(26):10063–10070

Mark JE, Llorente MA (1980) Model networks of end-linked polydimethylsiloxane chains. 5. Depenence of the elastomeric properties on the functionality of the network junctions. J Am Chem Soc 102(2):632–636

Morrison FA (2001) Understanding rheology. Oxford University Press, New York

Nandi S, Winter HH (2005) Swelling behavior of partially cross-linked polymers: a ternary system. Macromolecules 38(10):4447–4455

Urayama K, Miki T, Takigawa T, Kohjiya S (2004) Damping elastomer based on model irregular networks of end-linked poly(dimethylsiloxane). Chem Mater 16(1):173–178

Villar MA, Bibbo MA, Valles EM (1996) Influence of pendant chains on mechanical properties of model poly(dimethylsiloxane) networks. 1. Analysis of the molecular structure of the network. Macromolecules 29(11):4072–4080

Winter HH, Chambon F (1986) Analysis of linear viscoelasticity of a crosslinking polymer at the gel point. J Rheol 30:367–382

The Danish Polymer Centre
Department of Chemical and Biochemical Engineering
Technical University of Denmark
Søltofts Plads, Building 227
DK-2800 Kgs. Lyngby
Denmark

Phone: +45 4525 6801
Web: www.dpc.kt.dtu.dk

ISBN : 978-87-93054-00-4